TAMPEREEN TEKNILLINEN YLIOPISTO
TAMPERE UNIVERSITY OF TECHNOLOGY
Julkaisu 553 • Publication 553

Teemu Hartikainen

Environmental Impacts of Superconducting Power Applications

Tampere 2005

Tampereen teknillinen yliopisto. Julkaisu 553
Tampere University of Technology. Publication 553

Teemu Hartikainen

Environmental Impacts of Superconducting Power Applications

Thesis for the degree of Doctor of Technology to be presented with due permission for public examination and criticism in Sähkötalo Building, Auditorium S1, at Tampere University of Technology, on the 2nd of December 2005, at 12 noon.

Tampereen teknillinen yliopisto - Tampere University of Technology
Tampere 2005

ISBN 952-15-1459-0 (printed)
ISBN 952-15-1549-X (PDF)
ISSN 1459-2045

Abstract

Superconducting power applications boast several properties that can prove them environmentally advantageous over conventional electric power applications. Such are, for example, up to 50% lower losses, which means savings in electricity and thus savings in greenhouse gas (GHG) emissions from electricity production, and less raw materials required to construct devices resulting in lower environmental impact of manufacturing. This thesis reviews the superconducting power applications, namely generators, transformers, electric motors, cables, superconducting magnetic energy storages (SMES), fault current limiters (FCL) by introducing first their theoretical background and then each application from the point of view of advantages they pose. By starting from the mining of materials, a life cycle assessment (LCA) is conducted for commercial NbTi superconductor. Comparison between conventional copper wire and NbTi/Cu wire is made and magnets made of both materials are also examined from LCA-perspective. Detailed calculation of GHG emissions reduction potential of Finnish and European electrical networks is presented in view of the Kyoto Protocol, which requires the EU countries to reduce their GHG emissions by 8% from 1990 levels between 2008–2012. The proposed distributed generation (DG) networks are considered as one solution to introduce new renewable energy sources to the network and lower the environmental impact of energy production. Here this issue is studied by examining the environmental advantages that superconducting devices could bring to a DG-network. Finally, magnetic separation as a way to reduce heavy metal emissions from steel mill wastewaters is studied by a novel prototype of an open-gradient magnetic separator. Results showed that above certain break-even power, superconducting machinery can save electrical energy and thereof emissions from electricity generation. When considering the complete life-cycle of electrical machines, superconducting devices become even more preferable from environmental point of view. In DG-networks the advantages of superconductivity are quite modest and are concentrated on the issue of electricity storage. With magnetic separators it is possible to efficiently separate heavy metals from fluid streams. Magnetic separation is thus seen as a promising alternative to conventional filtration techniques.

"There is no narrowing so deadly as the narrowing of man's horizon of spiritual things. No worse evil could befall him in his course on earth than to lose sight of Heaven. And it is not civilization that can prevent this; it is not civilization that can compensate for it. No widening of science, no possession of abstract truth, can indemnify for an enfeebled hold on the highest and central truths of humanity. "What shall a man give in exchange for his soul?" [Mark 8:37]"

–Carved inscription in Stanford Memorial Church at the heart of the Stanford University Campus in Silicon Valley, California, U.S.A. Collected by Jane L. Stanford, co-founder of the University.

Preface

This thesis marks the culmination of my research work at the Tampere University of Technology between 2002 and 2005. First and foremost, I would like to thank Dr. Jorma Lehtonen, the main instructor of my work, who dedicated untold hours to teaching me how to do scientific research. Indeed, I have learned much from him, and not least the attitude that the classic Finnish commonsense is "pretty tough word against the world", helping crack the hardest nut in just about anything, sciences included!

I wish to express my gratitude to Risto Mikkonen, the advisor of my work. His work ethics and leadership skills serve as examples for all of us in the superconductivity research group. I thank Maija-Liisa Paasonen and Lasse Söderlund for their minimum bureaucracy management style and their willingness to help in all administrative matters. I also thank the Director of the Laboratory of Electromagnetics, Professor Lauri Kettunen, for providing the facilities for my work. I gratefully acknowledge the financial support of my work by the National Technology Agency of Finland (TEKES), PrizzTech Ltd., Outokumpu Superconductors, and TVO.

My sincere thanks go to Dr. Timo Lepistö for proofreading this thesis and to Heidi Koskela for the various drawings there. I also thank (in alphabetical order) the people I have worked with in the past few years: Iiro Hiltunen, Aki Korpela, Mika Masti, Lauri Rostila, and Juha Tuisku. You guys keep up the good work! Special thanks go to our chemistry wizard, Juha-Pekka Nikkanen, for solving the challenges posed by wastewaters in the magnetic separation project.

Finally, my beloved wife Suvi has been a great source of encouragement and good cheer. Thank you for being there!

In my opinion, reading contemporary scientific literature can get humdrum and boring at times. In those moments, I yearn for something written in a more timeless manner. With awe and inspiration I then turn to what the Apostle John wrote in the 1st century: "In the beginning was the Word. The Word was with God, and the Word was God. In him was life, and that life was the light of men. The Word became flesh and made his dwelling among us. We have seen his glory, the glory of the One and Only who came from the Father, full of grace and truth. No one has ever seen God. The only Son, who is truly God and is closest to the Father, has shown us what God is like".

List of publications

Publication **I**
T. Hartikainen, J. Lehtonen and R. Mikkonen
"Role of HTS Devices in Greenhouse Gas Emissions Reduction"
Superconductor Science & Technology, **16**, pp. 963-969, 2003.

Publication **II**
T. Hartikainen, J. Lehtonen and R. Mikkonen
"Reduction of Greenhouse-gas Emissions by Utilization of Superconductivity in Electric-power Generation"
Applied Energy, **78**, pp. 151-158, 2004.

Publication **III**
T. Hartikainen, A. Korpela, J. Lehtonen and R. Mikkonen
"A Comparative Life-Cycle Assessment Between NbTi and Copper Magnets"
IEEE Transactions on Applied Superconductivity, **14**, pp. 1882-1885, 2004.

Publication **IV**
T. Hartikainen, J. Lehtonen and R. Mikkonen
"Environmental Advantages of Superconducting Devices in a Distributed Generation Network"
submitted to *Applied Energy*

Publication **V**
T. Hartikainen, J.-P. Nikkanen and R. Mikkonen
"Magnetic Separation of Industrial Waste Waters as an Environmental Application of Superconductivity"
IEEE Transactions on Applied Superconductivity, **15**, pp. 2336-2339, 2005.

Publication **VI**
T. Hartikainen and R. Mikkonen
"Open-gradient Magnetic Separator with Racetrack Coils Suitable for Cleaning Aqueous Solutions"
IEEE Transactions on Applied Superconductivity, **16**, 2006. *In press.*

Contents of the thesis

List of symbols

a	ratio of the losses in HTS-device to the losses in corresponding conventional one
A_A	cross-sectional area of NbTi wire used in separation magnet coil A
A_B	cross-sectional area of NbTi wire used in separation magnet coil B
$\mathbf{B}$	magnetic flux density
B_0	magnetic flux density at the center of the coil (Chapter 4)
B_c	critical magnetic flux density
B_{c1}	lower critical magnetic flux density in type II superconductors
B_{c2}	upper critical magnetic flux density in type II superconductors
B^*	irreversibility field, where J_c comes close to zero
D	y-directional distance between center points of separation magnet coils
e_b	full reduction potential in emissions due to device replacements
e_{kWh}	average value of emissions per kilowatt-hour
e_{rpl}	expectation value for achieved emission reduction
e_{tot}	total greenhouse gas emissions saved
$\mathbf{E}$	electric field
E	energy
E_G	generated electrical energy
E_k	kinetic energy
E_S	combined energy savings potential
E_S^{tr}	energy savings potential in transformers
f	frequency
F	market share in certain year
F_1	probability that devices are still operating
$\mathbf{F}_m$	magnetic force
h_A	height of separation magnet coil A
h_B	height of separation magnet coil B
i	index number
I	current
I_1	incoming current in fault current limiter
I_c	critical current
I_{op}	operating current

j	index number
$\mathbf{J}$	current density
J_c	critical current density
k	load factor
k^{TR}	load factor of transformers
l_A	length of separation magnet coil A
l_B	length of separation magnet coil B
L_c	characteristic length of a transformer
n_l	number of devices installed l years ago
m	mass
M	moment of inertia
N	total number of devices operating in the network
N_b	number of devices to be written off
N_r	number of installed HTS devices
$N_{r,tot}$	total number of HTS devices in operation
p	market increase percentage
P	power
P_{be}	break-even power
P_n	nominal power
P_{ave}	average power
Q	volumetric average of energy loss density per cycle
r_A	inner radius of separation magnet coil A
r_B	inner radius of separation magnet coil B
R_N	resistance of superconductor in fault current limiter
R_S	shunt resistance in fault current limiter
S^{etot}	sensitivity of total greenhouse gas emissions saved
t	time
T	temperature
T_{ave}	average lifetime of a device
T_c	critical temperature
T_p	period of study
V	volume
w_A	thickness of separation magnet coil A
w_B	thickness of separation magnet coil B

α	fitting parameter of market share equation
β	fitting parameter of market share equation
γ	fitting parameter of market share equation
η_c	efficiency of conventional devices
η_{sc}	efficiency of superconducting devices
η_{sm}	efficiency of synchronous motors
κ	Ginzburg-Landau parameter
λ	London penetration depth
μ_0	permeability of vacuum
ξ	superconducting coherence length
σ_t	standard deviation of the lifetime of a device
ϕ_0	magnetic flux quantum
χ	magnetic susceptibility
ω	angular velocity

List of abbreviations

2G	second generation coated conductor technology
AAS	atomic absorption spectrophotometry
AC	alternating current
Bi-2223	bismuth-based high temperature superconductor $(Bi,Pb)_2Sr_2Ca_2Cu_3O_x$
CAES	compressed air energy storage
CAS	compressed air storage
CCGT	combined cycle gas turbine
CD	cryogenic dielectric design of superconducting cable
CFC	chlorofluorocarbon
$CO_{2\text{-eq}}$/kWh	carbon dioxide equivalent per kilowatt-hour
DC	direct current
DG	distributed generation
DOD	depth of discharge in electrochemical batteries
DOE	United States Department of Energy
EU	European Union
EuP	energy using product

FCL	fault current limiter
FEM	finite element method
FU	functional unit in life-cycle assessment
GHG	greenhouse gas
GSD	goal and scope definition of life-cycle assessment
HTS	high temperature superconductor
ITER	International Thermonuclear Experimental Reactor
LCA	life-cycle assessment
LCI	inventory of life-cycle assessment
LCIA	life-cycle impact assessment
LHe	liquid helium at 4.22 K
LN_2	liquid nitrogen at 77 K
LTS	low temperature superconductor
MHD	magnetohydrodynamics
MRI	magnetic resonance imaging
NMR	nuclear magnetic resonance
OGMS	open-gradient magnetic separation
OK42	NbTi superconductor with 42 filaments by Outokumpu Superconductors
PIT	powder-in-tube
PQI	power quality issues
RTD	room temperature dielectric design of superconducting cable
SMES	superconducting magnetic energy storage
SQP	sequential quadratic programming
SQUID	superconducting quantum interference device
USA	United States of America
YBCO	yttrium-based high temperature superconductor $YBa_2Cu_3O_x$

Chapter 1

INTRODUCTION

The history of superconductivity has witnessed two revolutionary moments. The first was the discovery of the phenomenon in metals by Kamerlingh-Onnes in 1911 [57], and the second was ceramic high temperature superconductors (HTS) discovered in 1986 by Müller and Bednorz [74]. Instantly, metallic superconductors were renamed as low temperature superconductors (LTS). The epoch of HTS reintroduced old ideas about applying these materials in the real world. Superconductivity had attained only scientific interest up to 1962, when Westinghouse Corporation commercialized LTS wire with a compound of niobium and titanium (NbTi) in a copper matrix. Now it became the *de facto* superconductor for practical applications because it could be wound like conventional copper wire. Until today, NbTi has been the only superconductor used in truly commercial electric appliances, a topic addressed in section 2.3. However, new manufacturing technologies are being developed for HTS materials [61], and hopefully by the end of the decade the stage is set for a competition.

The 1960s and '70s with their overall technological optimism were decades of vigorous dreaming, and a wide variety of applications utilizing superconductivity were proposed. One of the wildest ideas was a thought-driven spacecraft with ramjet engines [91]. In reality, superconductivity offers three distinct features for applications: zero resistivity, transition between normal state and

superconducting state, and Josephson junctions. The first two properties, enabling lossless conductors and strong electromagnets, are exploited in power applications, namely generators, transformers, electric motors, cables, superconducting magnetic energy storages (SMES), fault current limiters (FCL), and magnetic separation [52], and they are the main focus of this thesis. Josephson junctions make it possible to manufacture fast-acting and non-heating electronic components, such as SQUIDs, which are the most sensitive magnetometers known [89]. However, with them one cannot foresee any such environmental implications as viewed in this thesis.

Meanwhile, the industrialized societies have been facing environmental problems because of pollutants emitted to air, water and soil. Since the early days of industrialization, technological advances have greatly eased our daily life, but we have paid the price with our environment, which is being depleted of natural resources and rife with health hazards for people and ecosystems. From the late 1970s, these issues have been gaining general interest with action thereof being accepted as necessary. International commitments, begun in the '80s, have led the way towards more sustainable societies, and these commitments serve as inspiration and driving forces behind this thesis.

1.1 The driving forces

Four themes, all involving the environment, constitute the driving forces for this thesis, which examines in detail the impacts of superconducting applications in the context of each theme.

1. *The Eco-design directive for energy-using products*. In August 2004, The European Commission adopted a proposal for a framework directive on Eco-Design for Energy-using Products (also known as the EuP-directive). The eco-design requirements stipulate that manufacturers consider the entire life cycle of their product groups and make ecological assessments. Complying with the requirements involves life cycle analysis of equipment with attention paid to the raw materials used, acquisition, manufacturing, packaging, transport and distribution, installation and maintenance, use, and, finally, the end of product life. In each phase, manufacturers are required to assess consumption of materials and energy, emissions to the environment, pollution, expected waste, and ways of recycling and re-use. The proposal defines Energy-using Products as "equipment which, once placed on the market and/or put into service, is dependant on energy input (electricity, fossil and renewable fuels) to work as intended and a product for the generation, transfer and measurement of such energy" [29]. The directive is expected to become law in the European Union (EU) member states by 31st of December 2005, and manufacturers are obligated to comply from 1st of July 2006.

Consequently, it is now high time to research the impacts of superconductors for the environment from life cycle perspective as compared to conventional copper conductors.

2. *The Kyoto protocol*. The reduction of greenhouse gas (GHG) emissions is becoming a topical issue because of the Kyoto Protocol, which requires that the EU reduce its emissions by 8% from 1990 levels by the beginning of the 5-year period of 2008–2012. Signed in 1997 and effective since 16th of February 2005, the Kyoto Protocol is the first legally binding contract that links emissions, energy production, and economic growth. The main source of GHG emissions is energy production, and the Protocol states, among other things, that an enhancement in energy efficiency should be exploited [119]. Therefore, all means of improving energy efficiency must be clarified. Compared with conventional devices, superconducting windings in electrical machinery can cut energy losses by half. Their higher efficiency saves electrical energy and thereby reduces GHG-emissions as well. Hence, it is imperative to examine the possible savings potential of superconducting machinery.

3. *Distributed electricity generation*. Not only do the threat of terrorist attacks against power stations or the current investment climate hindering large governmental projects, but also environmental considerations promote the idea of de-centralized, small-scale energy production often called distributed generation (DG). The goal here is to pursue sustainability with an emission-free system where hydrogen and electricity would be the main interchangeable energy carriers with fuel cells transforming one into the other. In addition, the system would make many of us owners of generators and thus both producers and consumers of electricity. "This revolution will require … advanced energy storage technology, power electronics and superconducting devices", writes Philippe Busquin, the European Commissioner for Research [17]. But for this "revolution" to be desirable, we must first show whether certain technologies are environmentally better than others.

4. *Eco-efficient factory*. In the long run, pursuit of sustainability and eco-efficiency aims to make factories self-sufficient in such a way that their process waters are circulated internally without neither influents nor effluents [27]. Such circulation would require effective means of removing concentrated materials from fluid streams. Among many other industries, steel making produces wastewaters that contain dissolved heavy metals that are difficult to remove by conventional means. With superconducting magnetic separators and by the help of magnetic carriers, it is possible to separate fine and weakly magnetic substances directly from water flows. Such a system was designed and constructed at our laboratory and tested with wastewaters of genuine steel mill and synthetically made solution.

1.2 Organization of the thesis

The second chapter gives an overview of superconducting systems with special emphasis on the benefits obtained by HTS power applications. After that, the four driving forces give rise to four consecutive chapters in the following way. Starting with the manufacture of superconductors, chapter 3 focuses on the life-cycle assessment of commercial NbTi superconductor and compares it with traditional copper wire and magnets made of both materials. Chapter 4 deals with the emissions reduction potential of superconducting machinery in the present electrical network of the EU, and Finland in particular. Then looking into the future, chapter 5 examines the environmental benefits of superconducting devices in a prospective distributed generation network, in which energy storage becomes an important issue. Comparisons are made between battery-based and superconducting storage solutions. After applying superconductivity in a passive way for the benefit of the environment, chapter 6 focuses on active treatment of industrial wastewaters, that is, magnetic separation. In this chapter, I present the work done on a superconducting, open-gradient magnetic separator constructed during a recent four-year project. Finally, conclusions will be drawn in chapter 7.

1.3 The author's contribution

I am the corresponding author of all the six original papers comprising this thesis. Publications **I** and **II** were written in close collaboration with Dr. J. Lehtonen. The magnet design in Publication **III** is made by Dr. A. Korpela, who also wrote that part of the paper. The chemical method to attach dissolved metals into magnetic carriers presented in Publication **V** was engineered by Mr. J.-P. Nikkanen. Mr. R. Mikkonen contributed to all the papers by supervising the research. Furthermore, many valuable ideas emerged during discussions with the co-authors.

Chapter 2

SUPERCONDUCTING SYSTEMS

Any discussion of superconducting systems must begin with a review of the theory of superconductivity to clarify the differences between LTS and HTS materials in applications. The theory serves as a basis for introducing the specialities of superconducting power applications, grouped here under electrical machinery, network applications, and other power applications. Bypassing any elaborations on superconductivity, this chapter provides a background for more comprehensive analyses in later chapters.

2.1 Theoretical background of superconductors

Engineering applications of superconductivity come with a long list of benefits but also with a number of challenges posed by unique superconducting materials. First, to ensure smooth operation, a superconductor must be maintained under its critical temperature, T_c, at all times. This requirement is typically fulfilled by the use of cooling fluids in a special insulation vessel called a cryostat; liquid helium (LHe) for LTSs at 4.2 K and liquid nitrogen (LN_2) for HTSs at 77 K. With a mechanical cryocooler, we can operate between these temperatures, but we must keep in mind that under ideal conditions, removing 1 W at 4.2 K requires 69 W at room temperature whereas for 1 W at 77 K we

need only 3 W at 293 K. Second, a superconducting wire or tape has a critical current density, J_c, defined by its material properties and manufacturing technology. Finally, we have a critical magnetic flux density, B_c, explained more closely below. All these three are necessary conditions for superconductivity and are interrelated as seen in Fig. 2.1.

Superconductors are divided in two groups according to their behavior in the presence of a magnetic field. In type I superconductors, the current flows only on the surface and superconductivity vanishes already in a magnetic field as weak as a few tens of mT. Most superconducting materials are of this type. However, some materials withstand magnetic fields up to tens of Teslas, forming a group of type II superconductors. With type I, the external magnetic field is expelled from the interior by the so-called Meissner-effect while $B(T) < B_c(T)$. However, in type II superconductors, B_c is two-fold. Below $B_{c1}(T)$, the Meissner-state dominates, but when $B(T) > B_{c1}(T)$, a lattice of quantized magnetic flux lines, also known as fluxons, begins to penetrate the material. These fluxons—each carrying a flux quantum of $\phi_0 = 2 \cdot 10^{-15}$ Wb—stick to so-called pinning centers, introduced into the material as point defects during manufacturing. Each fluxon forms a normal conducting tube of radius $\xi(T)$, which is the superconducting coherence length, surrounded by a superconducting current vortex of radius $\lambda(T)$, which is the London penetration depth. The number of fluxons in the material per unit area is equal to $B(T)$; thus at $B_{c2}(T) = \phi_0/2\pi\xi(T)^2$, the normal conducting cores overlap and superconductivity finally vanishes [110]. Now, applications are limited by a lower characteristic field called the irreversibility field, $B^*(T)$, where J_c approaches zero [61], [54].

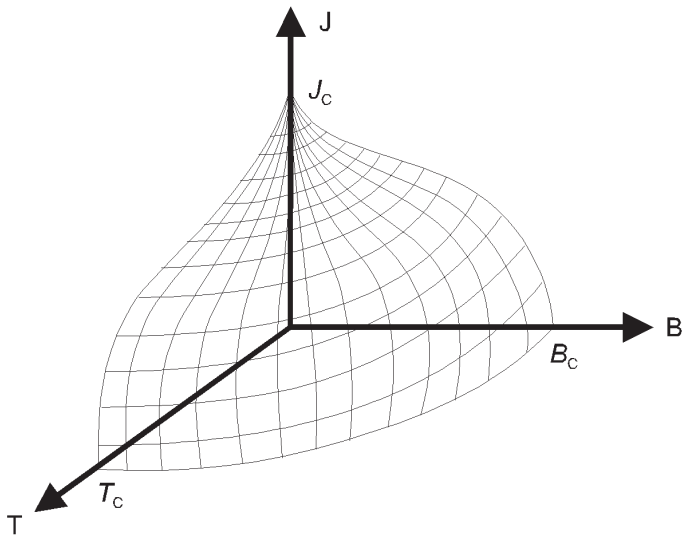

Fig. 2.1. The *J-B-T* surface is the top limit for superconductivity. If one parameter value is varied, the values of the other two change as well. For example, a higher operating temperature requires a lower current and magnetic flux density.

The two LTS-superconductors, NbTi and Nb_3Sn, are isotropic materials and their $B^*(T)$ is about $0.85 \cdot B_{c2}(T)$. For example, $B^*(4.2\ \mathrm{K}) = 10.5$ T for NbTi and 24 T for Nb_3Sn [107], [14]. But the two commonly used HTS materials, $(Bi,Pb)_2Sr_2Ca_2Cu_3O_x$ (Bi-2223) and $YBa_2Cu_3O_x$ (YBCO) have an an-isotropic layered structure, which results in lower $B_{c2}(T)$, if the external field is applied perpendicular to the conductor's longitudinal plane. For Bi-2223, $B^*(77\ \mathrm{K}) \sim 0.2$ T [94] whereas for YBCO $B^*(77\ \mathrm{K}) \sim 7$ T [61]. Therefore, the only useful HTS conductor for applications (except power cables) operating at LN_2 temperature is YBCO, manufactured as a coated conductor to avoid brittle grain boundaries, which also limit J_c. The wire made by coated conductor technology is often called Second Generation (2G) wire, as opposed to First Generation powder-in-tube (PIT) process of making HTS-conductors [67].

Fig. 2.2 shows the conductor cross-section of the practical superconducting wires, NbTi, Nb_3Sn and YBCO. These are the type of wires used in most applications, though HTS magnets are still made with Bi-2223, which YBCO is expected to replace in the near future. A new superconductor, MgB_2, was found in 2001 and is now produced with PIT technology in kilometer-lengths [22]. However, the current-carrying characteristics of MgB_2 ($T_c \approx 40$ K) fall short those of both Nb-based and YBCO conductors as seen in Fig. 2.3. But Mg and B are both cheap and abundant elements, and easy processing technology makes this new material an attracting option for price-conscious customers.

Significant issues are connected with the AC drive of contemporary electric appliances. A 50/60 Hz AC creates so-called AC-losses that are problematic with superconductors. A time-varying magnetic field generates electric fields inside the conductor, and when there are an electric field, **E**, and current density, **J**, present in the conductor, the created losses can be expressed by the general equation

$$Q = \oint_{1/f} \frac{1}{V} \int_V \mathbf{E} \cdot \mathbf{J}\, dV dt\,,$$

where Q is the volumetric average of energy loss density per cycle, f the frequency and V the total volume of the superconductor. The total AC-loss of the conductor is the sum of the three loss components. In the superconducting filaments, they are called hysteretic losses, between the filaments they are called coupling losses, and in the normal conducting matrix metal surrounding the filaments they are called eddy-current losses [63]. Thus, development of materials having low AC-losses is of major importance for superconductivity to make a real breakthrough in the electric power sector.

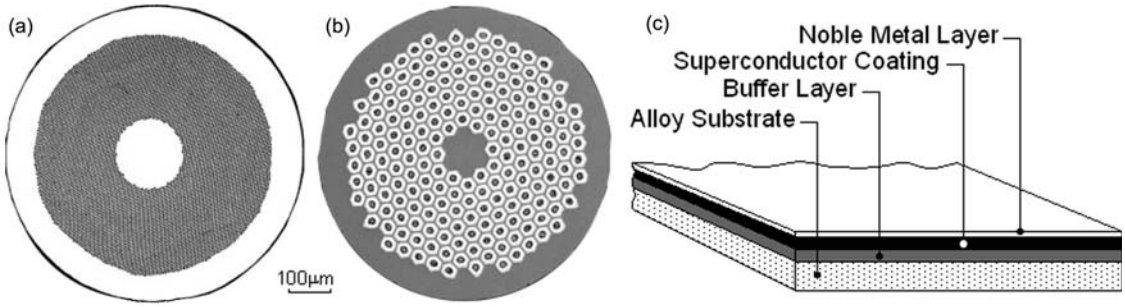

Fig. 2.2 Conductor cross-sections of practical superconductors. **a**) Conductor (∅ = 0.8 mm) containing about 3000 NbTi filaments embedded in a copper matrix, which protects the conductor during transition to normal state. **b**) Nb_3Sn conductor (∅ = 1 mm) produced by powder-in-tube (PIT) technology with 192 filaments. **c**) Structure of an YBCO second generation (2G) coated conductor. The layer thickness of the superconductor is typically about a micrometer. Nickel or steel can be used as a substrate material whereas silver is often used in noble metal layer.

According to the current notion, HTS wires would have to show performance similar to LTS wires but at LN_2 temperatures if HTS devices were truly to challenge their conventional counterparts [96], [114], [70]. On the other hand, in certain applications superconductivity is enabling technology because the saturation point of iron, B ~ 2 T, limits conventional electromagnets. Therefore, superconducting magnets are necessary in applications requiring higher magnetic fields [129]. Next I will review the benefits of both enabling and substitutive superconducting systems. Substitutive systems compete with established systems, which are often well developed and highly reliable. The section will also refer to several sources about the performance of demonstrational systems.

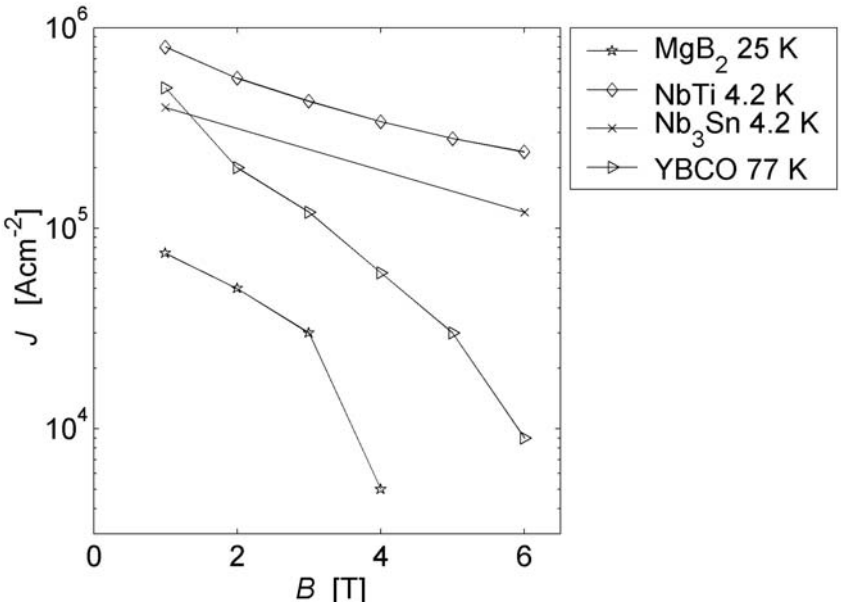

Fig. 2.3. Short-sample critical current densities versus magnetic flux density for state-of-the-art MgB_2 [38], NbTi [79], Nb_3Sn [19], and YBCO [135] wires. Nb_3Sn wires are best suited for high-field applications, where they exceed the J_c values of NbTi.

2.2 Overview of applications

Besides the mentioned power applications and certain special research applications, superconducting magnets are used in particle accelerators to bend and focus the beam and in devices based on nuclear magnetic resonance (NMR). For example, Fermilab and Brookhaven National Laboratories in the USA, DESY in Germany, and CERN in Switzerland/France all have several kilometers of tunnels encircled by LTS magnets. NMR devices are used to determine the structure of chemical compounds and also the commercial magnetic resonance imaging (MRI) is based on NMR phenomenon. MRI is an established diagnostics tool used by hospitals worldwide and a growing business worth over 3 billion USD annually [61]. However, since this thesis is about superconducting power applications, I will henceforth concentrate solely on them. In the rest of this section, I will briefly review each power application with emphasis on benefits of superconductivity.

2.2.1 Electrical machinery

This category covers economically the most interesting HTS applications: generators, transformers and synchronous motors. In the EU alone, approximately 30,000 generators and 4.5 million transformers are in operation in its electrical networks [35], [104], and though it is not reasonable to replace all of them with superconducting machinery, the potential savings obtained via higher efficiency and lower capital costs are significant. For example, a single 500 MVA base-load generator has losses of 1.5 TWh over its lifetime [6], [36]. If half of this energy could be sold as electricity (which would be the case with a HTS generator), priced at € 0.12/kWh [43], it would be worth € 86 million. Furthermore, considering that the retail price of a 500 MVA generator is estimated at € 12–13 million [109], it is no wonder device manufacturers find this sector in which to promote superconducting applications. Note that in reality, future savings need to be discounted to get present value. However, from environmental point of view great expectations are placed on the savings potential of electrical machinery.

Generators

Superconducting generators have three potential benefits over conventional types. Without an iron core, they can operate at higher magnetic fields (up to 5–6 T) and thus have 50% less size and weight [121]. This translates into reduced material requirements, capital costs, and manufacture-induced impact on the environment. Second, superconducting generators offer greater system stability against

frequency and load variations in the grid. Their smaller size leads to smaller synchronous reactance, thereby enhancing the critical clearing time after a fault condition [60]. Finally, because of their higher efficiency, their losses are expected to drop by 50%, resulting in less fuel needed to generate electricity and thus fewer emissions per generated kWh. However, the cryogenics of superconducting generators are challenging. Though it is possible to construct a rotating cryostat for the rotor, preferably with fiberglass composite, problems arise with maintaining a sufficient vacuum and thus the low temperature [111]. Such operation requires, for example, special sensors, which have not been used in other experiments. Therefore, operational reliability remains the paramount issue undermining the triumph of superconducting generators. The electrical protection of these devices can be accomplished by a HTS fault current limiter, as shown in [123]. Demonstrations of superconducting generator appear in [134], [3].

Synchronous motors

Synchronous AC and DC machines are well suited to apply superconductivity because DC drives the excitation winding, which is also not exposed to time-varying magnetic fields. The benefits of superconductivity here are essentially the same as with the generators already mentioned. However, compared to generators, the greater complexity in case of motors makes them less attractive in this regard. In addition, the use of synchronous motors is also limited to special low-speed high-power drives, such as paper and steel mills. A typical industrial machine, the AC induction motor, is not suited to apply superconductivity because the rotor needs resistance to produce torque, and asynchronous operation exposes current-carrying wires to an alternating magnetic field. Small-scale demonstrations of HTS synchronous machines are discussed in [55], [34] and [39]. The American Superconductor Corporation is developing HTS-based motors, especially for ship propulsion [56].

Transformers

The rated nominal power, P_n, of a transformer is proportional to current density J in conductors, characteristic length L_c and mass m of the transformer, thus [62]

$$P_n \propto JL_c m \, .$$

Now with superconductors, the value of J can be greatly increased, thus decreasing the size and weight of the transformer of similar rating by up to 50%. Interestingly, a superconducting transformer can be built with or without an iron-core, but either way the weight of the system remains unchanged [62]. As with generators, the total electrical losses can be halved also with transformers. A typical utility transformer of 50 MVA has lifetime losses of 27 GWh [73], which

would yield a saving of 1.6 M€ over 40 years of use with a superconducting transformer. Yet with the savings of a superconducting transformer, we could buy up to three conventional transformers at a retail price of 0.5 M€ apiece. Moreover, a transformer is typically cooled and insulated with oil or, in the case of devices exceeding 100 kV, with SF_6 gas [1]. SF_6 is the most potent greenhouse gas ever evaluated with a global warming potential of up to 36,500 times that of CO_2 [47]. In HTS transformers, chemically inert and environmentally benign LN_2 replaces this hazardous substance, though with the drawback that LN_2 must be pressurized to prevent bubble formation, which could weaken the insulation. In a severe transient fault condition, a superconducting transformer can automatically limit the current and thereby protect the rest of the network cell from collapsing [69]. Several research groups have built and tested HTS transformers [95], [59], [41].

2.2.2 Network applications

This category comprises the equipment for power transmission and energy storage. Typically, electricity is transmitted along high-voltage overhead lines that are very economical in AC use. However, in cities cables are preferred to overhead lines, and here superconductivity can show benefits in transmission capacity and environmental concerns. Superconducting fault current limiters can stabilize networks by limiting fault currents and enabling lower switchgear ratings. Energy storage is not widely exploited in contemporary networks, but prospective distributed generation networks will depend heavily on storage systems.

Power cables

The transmitting power of an underground cable is limited by the amount of heat generated in the conductor inside the cable. Between 1945 and 1965, the growth in electric power demand quadrupled in the developed countries; therefore, in the early 1970s high-amperage superconducting cables were seen as the only way to feed expanding cities if such growth continued [121], [46]. But then the growth stabilized, and oil prices dropped along with the funding for LTS cable programs. HTS renewed interest in cables, and today they are seen as the most promising HTS application with their commercialization expected to get underway by the end of the present decade [73], [67]. This issue with two proposed cable designs is discussed in detail in section 6.2. Compared with conventional cables, YBCO-based cables offer 60–70% lower losses at full load with 3–5 times the current carrying capacity. In addition, HTS cables boast the important advantages of eliminating electromagnetic stray fields and being easily recyclable after active duty [42]. Use of HTS cables has been recently successfully demonstrated in the USA [106], Japan [116], and Europe [64], [128].

Fault current limiters (FCLs)

Faults in electrical networks cause short-circuit currents of 10–20 times the rated current. All components connected to the grid must withstand these heavy overloads and must therefore be designed accordingly. As the networks expand, effective impedances decrease, in turn increasing the fault currents. Thus all devices, present and new, must be able to handle stronger and stronger currents. FCLs can limit the short-circuit currents, and thereby lower the required ratings the devices, an advantage that would add up to considerable savings in material requirements per device. An FCL is, in principle, variable impedance installed in series with a circuit breaker [70]. When a fault occurs, the impedance of FCL jumps such that the current is lowered to a safe level for the circuit breaker to operate. Superconductors, with their specific I_c, can exploit the transition between the normal and superconducting state in FCLs, and are therefore especially suited for limiting fault currents. There are two main types of superconducting FCLs, resistive and inductive, as shown in Fig. 2.4. For example, the inductive design has been used to protect a generator [123]. Because today no conventional device can limit short-circuit currents at voltages above 110 kV [46], superconductivity becomes here an enabling technology by enhancing reliability, flexibility and overall system stability of high voltage networks (for more about these advantages and references to demonstrational units, see [102] and [46]). Environmentally, superconducting FCLs enable lower switchgear ratings, thus limiting the need for SF_6 as dielectric. It is estimated that full deployment of superconducting technology might reduce SF_6 use by 10–20%, which is equivalent to an annual 44–131 Mt of CO_2, if ultimately all of the manufactured SF_6 were to escape into the atmosphere [130]. However, the number of emissions is open to dispute because the electric utilities have effective programs for SF_6 capture, and disposal or recycling [7], [120], [51].

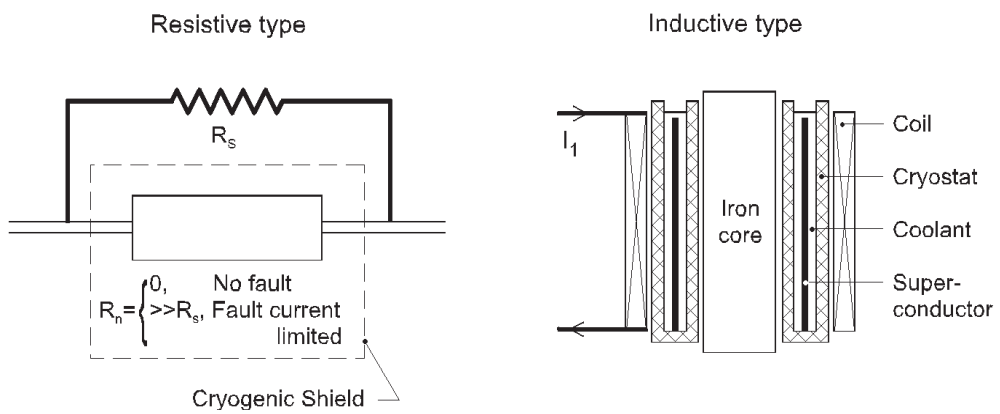

Fig. 2.3 Schematic presentation of resistive and inductive type FCLs. The resistive FCL has superconducting (R_n) and shunt (R_s) resistors, for the current to flow during normal operation and during fault, respectively. The inductive FCL is coupled to a busbar and operates basically like a transformer; if the incoming current I_1 exceeds a rated value, the superconducting secondary coil ceases to compensate the flux of primary coil and thus the impedance of the FCL jumps.

Superconducting magnetic energy storages (SMESs)

In a SMES system, electrical energy is stored as DC in the static magnetic field of a superconducting magnet. Here, superconductivity is truly enabling technology, for such storage is impossible by conventional means. Power conditioning systems convert the current between SMES and the grid, in turn charging and discharging the magnet. SMES has a high power density, that is, it can deliver all of its energy within seconds when needed. This ability has attracted the U.S. military because ballistic missile defense by ground-based lasers calls for large quantities of pulsed power [121]. In electrical networks, SMES is applied commercially to power quality control. For example, for 5 years now, seven NbTi-based units of the American Superconductor 3 MW D-SMES system have been operating in the Wisconsin Public Service 115 kV grid, where they were "selected as the most cost-effective solution for a network instability problem" [8]. Large SMESs (over 1 GWh) would be suitable for diurnal storage and load leveling, and, in fact, concepts of such systems were designed in the 1970s [45] but later abandoned because of their huge investment costs and questionable reliability. Today, SMES is seen as a candidate for storing energy in DG networks (for details, see chapter 5). A variety of SMES applications together with recent projects are discussed in [113]. SMES has also been studied at our institute [71], [81].

Flywheels with HTS bearings

The essential components of a modern flywheel are rotor made of fiber composite, magnetic bearings, power conversion system, and containment vessel. The rotor stores energy as the kinetic energy of a rotating body

$$E_k = \tfrac{1}{2} M \omega^2 ,$$

where M is the moment of inertia and ω is the angular velocity of rotation. Power density of a flywheel can exceed 500 W/kg with a specific energy of 10–50 Wh/kg, the same as lead-acid batteries [48]. Because HTS bearings exploit the Meissner effect of superconductivity, a flywheel with such bearings operating in LN_2 has up to 100 times lower losses than a similar flywheel with conventional magnetic bearings [131]. By blocking the magnetic field from its interior, a piece of superconducting material possesses complete diamagnetic properties and thus provides frictionless and stable levitating bearing [23]. Fig. 2.4 shows the common HTS bearing concepts of flywheels [70]. The containment vessel should maintain vacuum for the flywheel rotor and provide safety in case of failure. A rotor weighing 100 kg and running at a rim velocity of 1500 m/s can be pretty dreadful if it breaks free from its containment. Flywheels are considered for many locations where currently chemical batteries are used, for example, the International Space Station and hybrid electric

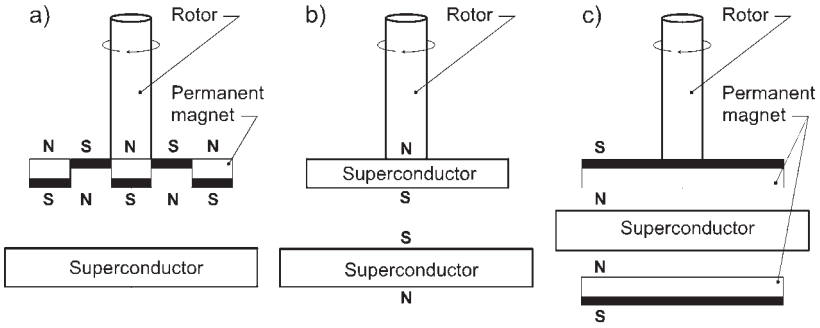

Fig. 2.4 Three concepts for HTS bearings used in flywheels. In **a**) stationary HTS part aims to simple refrigeration, whereas **b**) enhances the magnetic field but complicates the cooling system. The hybrid solution **c**) prevents air gap drift.

vehicles [48]. As with SMES, DG networks are also one potential site for flywheel deployment. Connecting a flywheel to a network requires a motor/generator unit to be installed to the shaft of the rotor, for example, by using an ingenious disk-type unit [122]. A detailed list of research groups and firms concentrating on flywheels is given in [131].

2.2.3 Other power applications

Other power applications in this context consist of magnetic separation, nuclear fusion, and magnetohydrodynamics (MHD). LTS separators are commercial devices used to purify kaolin clay [12], and nuclear fusion and MHD are novel methods to produce energy.

Magnetic separators

Magnetic separation, a method to separate particles according to their magnetic properties, has been exploited by the mining industry since the 1840s to concentrate magnetic ore and to remove magnetizable particles from slurries. The advent in the 1960s of high field superconducting magnets gave rise to superconducting separators that were first used to refine kaolin clay. In the next decade, high-field superconducting magnets along with high-gradient magnetic separation process made it possible to separate fine, weakly magnetic particles [108]. Lately, environmental applications have come to the fore, and several superconducting separators have been built for various water purification processes. For example, viruses, algae, phosphate and dissolved pollutants have been removed by magnetic seeding technique, which enhances the magnetic properties of the materials to be removed [21], [44], [92], [40]. Additional applications have been sulphur removal from combustible coal and the treatment of nuclear power station cooling fluids [25], [84], [65]. Magnetic purification accelerates considerably the separation of sludge from liquid, thus speeding up the process compared to conventional decantation and mechanical filtration used by many industries.

Nuclear fusion

To reach the 100 million degrees required for nuclear fusion in a Tokamak-type fusion reactor, the deuterium-tritium plasma must be confined with a magnetic flux density of over 10 T provided by superconducting magnets [13]. The International Thermonuclear Experimental Reactor (ITER) project has adopted the Tokamak-design with Nb_3Sn magnets for toroidal coils and NbTi magnets for poloidal and correction coils [66]. ITER needs approximately 1500 tons of conductor with forced LHe-flow [31], making the magnet system thus the costliest part of the project. However, even if the ITER construction get underway in this decade, the plant will not be operational until 2020s, and a commercial fusion reactor is estimated to be at least 40 years hence in the future [66]. Therefore, this thesis is not the place to speculate on the possible environmental benefits of nuclear fusion. We need to know first whether it is even possible to have controlled fusion for economical energy production.

Magnetohydrodynamics (MHD)

Electrically conducting fluids (for example, salt water) can be moved in the presence of a magnetic field by the Lorentz force. This enables a propulsion engine for maritime vessels without any moving parts. Unfortunately, neither the power-to-weight ratio nor the capital costs have been attractive enough for MHD to be of more than scientific interest [132]. But the principle works also the other way around: electricity is generated when a conducting fluid is moved in a magnetic field. Such a device is called the MHD generator, initially intended to be applied in series of a conventional thermal power station. By routing the exhaust gases of thermal power plant through an MHD generator, the conversion efficiency of fossil fuels into electricity can go up to 65% as opposed to the present 38%. Again, the device has not been cost-effective so far; besides other challenges have surfaced with the materials involved. For example, at high temperatures the electrodes tend to oxidize rapidly, thus necessitating special materials such as tungsten and zirconium [88]. Consequently, MHD is not examined in this thesis though advanced HTS conductors might ease on the economic side of these applications.

2.3 Concluding remarks

So far, we have learned about enabling and substitutive superconducting systems, and seen that all commercial devices—MRI, SMES and magnetic separator— are based on the NbTi superconductor. HTS offers promising advantages for cables, FCLs and flywheels, but the commercialization of HTS conductors requires current densities of 10^5 A/cm^2 @ 77 K [61], along with low AC-losses. The development work enhances these, and aims to price target of US $10–25 per kA-m [67].

Chapter 3

LIFE-CYCLE ASSESSMENT OF A SUPERCONDUCTOR

I start the environmental analysis of superconducting applications by first examining the manufacture of superconductors. Because electromagnets are wound from copper or superconducting wire, we must first compare the production of copper and superconductors from the environmental point of view by assessing their material requirements, energy use, wastes, and emissions. This chapter draws on Publication **III** by first introducing the concept of life-cycle assessment, then comparing magnet designs, and finally discussing the assessment process itself.

3.1 Background for life-cycle approach

The concepts of sustainable development and eco-efficiency were introduced to the general public in the 1992 Earth Summit in Rio de Janeiro. They are defined, respectively, as "development that meets the needs of the current generation without undermining future generations' ability to meet their own needs" and as "strategy to improve the environmental performance of a company or a nation by the use of performance indicators" [27]. Life-cycle assessment (LCA) is one such indicator to deal with the complex interaction between a product and the environment. It is a *from-cradle-to-grave*

approach, where all environmental impacts from the extraction of raw materials and energy to the final disposal of the product are assessed [118].

Formal LCA study is divided into four main categories: goal and scope definition (GSD), life-cycle inventory analysis (LCI), impact assessment (LCIA), and interpretation [53]. GSD determines the intended application and the reason for carrying out the study, whereas setting the goal defines the scope of the study. LCI is divided into four substeps. First, all processes involved in the life-cycle of the product must be identified. Ultimately, every process starts with the extraction of raw materials and energy from the nature and ends with inputs to the environment in the form of emissions to air, water, and soil. A process flow chart is prepared to clarify the path of materials. In the second step, quantitative data are collected. The third step is to define the system boundaries to manage the size of the LCA study. Finally, the inputs and outputs from all processes are adjusted with regard to the functional unit [118]. LCIA and its interpretation are explained later in the text.

During the last decade, companies adopted environmental management as one of their basic functions. Outokumpu, the largest Finnish copper producer and the world's leading manufacturer of superconductors, had its LCA of copper products made in 2000 as part of a larger study of the Finnish metals industry [97]. The Outokumpu 42-filament NbTi/Cu –wire, OK42, is widely used in MRI magnets. Since the latter are wound from both copper and NbTi/Cu wire, MRI is a suitable application to carry out a comparative LCA study. It is also one of the few truly commercial uses of superconductors. Consequently, MRI is the only possible target for a reasonable LCA study.

3.2 Magnet design

For us to be able to compare copper and NbTi magnets, they must show similar performance. Therefore, a numerical optimization study, based on Sequential Quadratic Programming (SQP) and Finite Element Method (FEM), was made to design both magnets. A magnet's volume is minimized when the maximum achievable magnetic flux density and the bore diameter are taken as constraints [125]. The properties of the optimized copper and NbTi magnets in this study corresponded roughly to the main coils in MRI systems [75]. Then the minimum lengths of copper and NbTi/Cu wires were computed as a function of the required field in the magnet's open bore. Once the optimal magnet geometries were known results from the LCA were applied.

The optimization of NbTi coil converged to a feasible solution of an inner radius of 502.1 mm [24], an outer radius of 520.2 mm, and an axial length of 412.3 mm. This solution had operating current I_{op} of 263.8 A [101] and a magnetic flux density at the center of the coil B_0 of 1.50 T [10]. With 55% filling factor [72], the optimized NbTi coil geometry resulted in a volume of 8.25 dm^3 with a total wire length of about 7,993 m. The density of the copper wire is 8.9 kg/dm^3 while the density of OK42 is 8.36 kg/dm^3 [79], [129]. Thus the NbTi magnet's total mass amounted to 38 kg.

The optimization of copper coil converged to a feasible solution of an inner radius of 500.1 mm [24], an outer radius of 644.1 mm, and an axial length of 366.6 mm. With an I_{op} of 7.85 A and a B_0 of 0.20 T [10], the volume and the total wire length of the optimized copper coil were 150.8 dm^3 and 105,600 m, respectively. The copper coil's total mass was 738 kg.

This preliminary study indicates the reason for the interest towards superconductivity in MRI applications. When a copper coil is replaced with an NbTi coil, multifold magnetic flux densities are gained with considerable reduction in size and mass.

3.3 Results and discussion

When LCA is applied in a process technology, product use, recycling, and waste disposal are normally excluded from the system boundaries. Such a modified method is often referred to as *cradle-to-gate* [124] assessment and was applied also in this study. The system boundaries are presented with a process flow chart in Fig. 3.1. Since this was a comparative analysis, I needed to address only the differences in the production of copper and NbTi/Cu wire. One ton of NbTi/Cu wire at the factory gate (the same as in [97]) was chosen as the functional unit in this study.

The product systems comprised the extraction of elements Nb, Ti, and Cu, and their processing into wire, as well as fuels, energy production, and various transports. The processing of NbTi requires several more stages than that of copper, besides production wire from NbTi is far more complex and therefore energy consuming. Table 3.1 shows LCI for the mining, concentration, and processing of cathode copper and NbTi-ingots [15], [18], [26], [28], the materials used in copper and NbTi/Cu wire production.

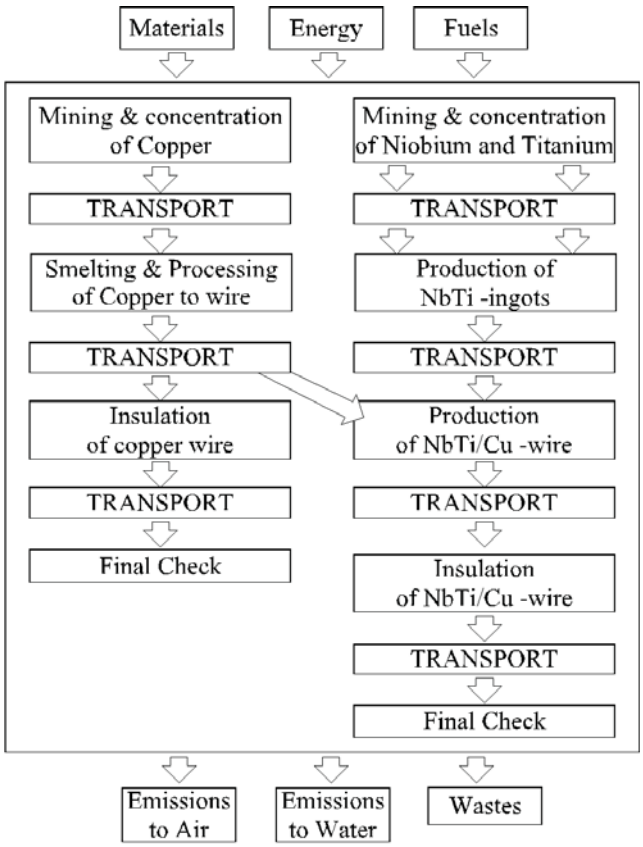

Fig. 3.1. The process flow chart and LCA system boundaries of copper and NbTi.

The LCI data shown in Table 3.1 is not complete, for it does not include the use of chemicals in processing Nb and Ti. Furthermore, niobium processing companies consider their energy use as proprietary information [127], [20]. Therefore, LCI data on titanium was used for niobium also in the calculation that 2 tons of niobium raw material, FeNb, are needed to concentrate 1 ton of pure niobium [15]. The composition of a superconductor grade NbTi ingot is 53% Nb and 47% Ti [127].

The next step is the production of wire and the insulation of the finished product. Table 3.2 presents the LCI for these stages [15], [80]. The net energy use of 10.2 GJ and the emissions of all the

TABLE 3.1
LCI FOR MINING, CONCENTRATION AND PROCESSING OF COPPER AND NBTI

	Copper	NbTi
Vector	1 ton cathode-Cu	1 ton NbTi-ingots
Net energy use	48.5 GJ	376 GJ
Mine tailings	28.8 tons	905 tons
Water usage	4,000 litres	1,303,800 litres (*)
SO_2	23 kg	not available
CO	4.45 kg	42.4 kg
NO_x	11.43 kg	20.6 kg
CO_2	3.69 tons	20.4 tons

(*) Data not available on water used for titanium processing.

TABLE 3.2
LCI FOR PRODUCTION AND INSULATION OF COPPER AND NBTI/CU -WIRE

	Copper wire	NbTi/Cu wire
Vector	1 ton of product	1 ton of product
Net energy use	55.4 GJ	151.4 GJ
Water usage	1,000 litres	527,053 litres
SO_2	7.5 kg	11.3 kg
CO	2.85 kg	3.90 kg
NO_x	8.32 kg	25.25 kg
CO_2	3.31 tons	9.06 tons
HNO_3	-	280 kg
HF	-	5 kg
C_3H_7OH (propanol)	-	30 kg

transports shown in Fig. 3.1 are included in table 3.2 [79], [15]. The ratio of copper to NbTi in the finished wire, OK42, is 4 to 1. Total materials intake is included in the calculations but not released.

According to LCA practice, the inventory table drawn during LCI is used as input to LCIA where formal evaluation is made for classification. However, the impact categories to be included in this classification are not fully agreed on [118], and even tougher problems arise with the valuation and weighing of the impact. For example, is the increasing greenhouse effect a more serious problem than acidification, and if so, how serious [9]? Consequently, LCIA was not carried out here; instead the results from LCI were used as such.

When copper wire was compared with superconducting NbTi/Cu wire, the addenda copper data from Tables 3.1 and 3.2 were compared with the combined NbTi and copper data from Tables 3.1 and 3.2. The material shares in the NbTi/Cu wire were taken into account. Table 3.3 shows the results of this calculation.

TABLE 3.3
COMPLETE LCI FOR COPPER AND NBTI/CU -WIRE

	Copper wire	NbTi/Cu wire
Vector	1 ton of end-product	
Net energy use	103.9 GJ	284.6 GJ
Mine tailings	28.8 tons	905 tons
Water usage	5,000 litres	856,235 litres
SO_2	30.5 kg	29.88 kg (*)
CO	7.3 kg	18.10 kg
NO_x	19.75 kg	39.64 kg
CO_2	7.0 tons	17.14 tons
HNO_3	-	280 kg
HF	-	5 kg
C_3H_7OH (propanol)	-	30 kg

(*) The share of NbTi mining, concentration and processing is not available.

Results show that while the net energy used in NbTi/Cu production is almost three times that in copper wire production, the difference in water use is 170-fold. Differences in air emissions are about 2–3-fold. However, a fair comparison between the conventional and superconducting technology, as far as environmental issues are considered, can be made only by comparing the applications of these technologies. Therefore, by taking into account the different weights of the magnets studied here, I obtained for the most interesting vectors completely different results, as seen in table 3.4.

Compared to a copper magnet, nine times the water is consumed to manufacture an NbTi magnet but only a fraction of the energy with minimal emissions. Note though that this comparison applies only to the magnets designed here. Thus, though the results in table 3.3 are generally applicable, the coils of, for example, electrical machines must be studied individually.

TABLE 3.4
LCI FOR COPPER AND NBTI MAGNETS

	Copper magnet	NbTi magnet
Net energy use	76.8 GJ	10.81 GJ
Mine tailings	21.3 tons	34.4 tons
Water usage	3 690 litres	32 537 litres
CO_2	5.17 tons	0.65 tons

4.4 Concluding remarks

To obtain information about the environmental impacts of superconducting technology, I carried out a comparative life cycle assessment of copper and NbTi/Cu wires. First, using numerical optimization, a resistive and a superconducting magnet for MRI operation were designed. The optimization results showed that the copper coil weighed 738 kg whereas the NbTi coil weighed 38 kg. I then conducted a life cycle assessment (LCA) of NbTi/Cu wire and compared the results with previous LCA data on copper wire. Finally, the LCA data was adjusted to enable comparison between the copper and NbTi magnet. Results showed that, environmentally, the NbTi magnet was the more preferable because the energy consumption and CO_2-emissions of its manufacture are 14% and 13% respectively, of those of the copper magnet. However, compared to a copper magnet, the manufacture of an NbTi magnet consumes 8.8 times more water and produces 1.6 times more mine tailings.

Chapter 4

REDUCTION POTENTIAL IN EMISSIONS BY HTS MACHINERY

The preceding chapter covered the manufacture of superconductors. Now we move on and observe what environmental impact these materials could have within the framework of present electrical networks. The driving force in the previous chapter was the EuP-directive; now it is the Kyoto Protocol. In this chapter, I examine high-temperature superconductivity (HTS) as a way to improve the efficiency of energy production. Energy will be saved by utilization of HTS-based generators, transformers, and synchronous motors in power stations and heavy industry facilities. This chapter makes a detailed survey of the replacement of existing devices with HTS units to determine the efficiency level and power range where HTS becomes reasonable. The original study appears in Publications **I** and **II**.

So far, nothing definite is known about the efficiency of future commercial HTS-machinery because the efficiency depends on various issues, such as material properties, tape geometry, and the cooling system. Also in many cases, it is not practicable to optimize the machine only for the lowest possible losses [112], [100]. Therefore, one aim of this chapter is to examine what efficiency these HTS machines should reach so as to save energy and thus lower the GHG emissions.

Today it is unquestionable that the burning of fossil fuels increases GHG-content of the atmosphere. In order of importance, the major greenhouse gases from human activity are carbon dioxide (CO_2), methane (CH_4), nitrous oxide (NO_2) and halocarbons (CFC's). Annually, over 20 gigatons of CO_2 are released into the atmosphere through human activity, yet that is only about 3% of the natural flow through the air–ground interface [16]. However, some developed countries have committed themselves to reducing their emissions as agreed in the Kyoto Protocol. In the following, I will show what impact the superconducting electrical machinery could have in this regard.

4.1 Computational model

The efficiencies for conventional machinery, η_c, can be given accurately as a function of their rated nominal power. The efficiencies for transformers and generators are shown as a function of their power in table 1 of Publication **I**. The efficiency of synchronous motors, η_{sm}, rises linearly from 96% for a 3 MW device to 98% for a 15 MW device [2]. To study the achievable reduction in GHG emissions, we can use the ratio of losses in HTS devices to losses in corresponding conventional devices, a, as a variable to express the efficiency of the former,

$$\eta_{sc} = 1 - a(1 - \eta_c). \qquad (4.1)$$

HTS-based machinery is most competitive in systems with high nominal power. The break-even power, P_{be}, is defined so that it is reasonable to replace a conventional device i having nominal power of $P^i_n \geq P_{be}$ with a superconducting one. However, P_{be} is not defined uniquely but depends strongly on the optimization criteria. In general, P_{be} is different for transformers, generators, and synchronous motors and also dependent on the application. For example, in transportation systems, P_{be} is much lower than in stationary applications, because the weight of the device plays a crucial role in moving systems [112]. In addition to the efficiency, P_{be} contributes strongly to the achievable reduction of GHG emissions. When the number of HTS devices replacing conventional ones in the power grid increases, total savings in electrical energy rise as well.

Next, savings in electricity are translated into reduced GHG emissions. Electricity generation from fossil fuels is a significant source of GHG emissions. For example, in 1999, the generation of electricity created 24.6 Mt of CO_2-eq. (megatons of CO_2-equivalent) or 35% of Finland's total 71 Mt of CO_2-eq. GHG emissions [104]. When electricity is used more efficiently, less energy needs to be produced. Furthermore, eliminating the most polluting power plants would maximally reduce GHG emissions. Hard coal burning produces highest life-cycle emissions per generated kWh as can be

seen in table 4.1. Coal-fired power stations worldwide consume over 2,500 million tons of coal each year to produce 38% of the total generated electricity [103]. In Finland, the share of hard coal was 8.4 TWh or 10.6% [104]. Therefore, clearly the proportion of hard coal in electricity generation can and should be reduced. In this analysis, the energy savings were attributed to reductions in the use of hard coal and then converted to grams of CO_2-equivalent per kWh, which is a common way to report GHG emissions. For hard coal, an average value of emissions per kilowatt-hour, e_{kWh}, is 1 kg of CO_2-eq/kWh [103].

The total of GHG emissions saved, e_{tot}, when all conventional devices having $P^i_n \geq P_{be}$, where P^i_n is the nominal power of device i, are replaced with superconducting ones are obtained from

$$e_{tot} = e_{kWh} T_p \sum_{i=1}^{N} P^i_{ave} \left(\eta^i_{sc}(a) - \eta^i_c \right) \ , \quad (4.2)$$

where η^i_{sc} and η^i_c are the efficiencies of superconducting and the conventional device i, respectively, P^i_{ave} the average power delivered to the device i during the period of study T_p, and N the number of devices having $P^i_n \geq P_{be}$. Here generators, transformers and motors are arranged in decreasing order (that is, $P^i_n \geq P^{i+1}_n$) and T is one year. However, the components of the electric power grid are not loaded with nominal power all the time. The average power delivered to the device i on the scale of one year, P^i_{ave}, is usually given as

$$P^i_{ave} = k^i P^i_n, \qquad (4.3)$$

where k^i is the load factor of the device i. Together equations (4.2) and (4.3) yield

$$e_{tot}(P_{be}, a) = e_{kWh} T_p \sum_{i=1}^{N} k^i P^i_n (\eta^i_{sc}(a) - \eta^i_c) \ . \qquad (4.4)$$

The estimate of k^i for transformers is 0.4–0.6 and for synchronous motors 0.75. Generators of nuclear, hydroelectric, and thermal power have an average k^i of 0.94, 0.59 and 0.36, respectively [104]. Here, the dependence of the average efficiency on the load factor is neglected.

TABLE 4.1
GHG-EMISSIONS FROM ELECTRICITY PRODUCTION

Energy vector	e_{kWh} (Direct)	e_{kWh} (In-direct)
Hard coal or peat	790–1017	176–289
Natural gas	362–575	77–113
Hydro	0	4–236
Solar (photovoltaic)	0	100–280
Wind	0	10–48
Nuclear	0	9–21

The range of GHG emissions from electricity production in grams of CO_2 equivalent per kilowatt-hour. The first values are direct emissions from burning whereas the second values indicate indirect emissions during life-cycle. The exact value depends on the state of technology [103].

To study the effect of variations in a and P_{be} on total saved GHG emissions, we must introduce the concept of sensitivity. The sensitivity of e_{tot} with respect to a variable x is defined as [126]

$$S_x^{e_{tot}} = \frac{de_{tot} / e_{tot}}{dx / x}$$

In this case x is either a or P_{be}. $S_{Pbe}^{e_{tot}}$ is computed with finite differencing whereas $S_a^{e_{tot}}$ can be calculated analytically from eq. (4.4). When we apply equation (4.4), we must know in detail the nominal power distribution of transformers and electrical machines before we can accurately analyze the effect of P_{be} and a on the reduction in GHG emissions.

Finally, I studied the time-scale within which the HTS devices could replace conventional ones. To be exact, I studied only the replacement of existing devices, omitting any future market growth of electrical devices. The replacement rate of devices can be computed as a function of time. The number of devices, N_b, written off during year j (here j equals zero at the moment) is given as

$$N_b(j) \approx \sum_{l=1}^{\infty} n_l \int_{l+j-1}^{l+j} f(T_{ave}, \sigma_t)\,\mathrm{d}t \qquad (4.5),$$

where n_l is the number of devices installed l years ago, $\int_t^{t+\Delta t} f\,\mathrm{d}t$ is the probability that a device is written off in the time interval $[t,t+\Delta t]$, T_{ave} and σ_t are the average value and the standard deviation of the lifetime. $N_b(j)$ can be calculated after an equation is found for n_l. The total number of devices operating in the network at the moment, N, can be given as

$$N = \sum_{l=1}^{\infty} n_l F_l(T_{ave}, \sigma_t), \qquad (4.6)$$

where F_l is the probability that these devices are still operating. When the market increases $p(l)$ % during year l

$$n_l = \frac{n_1}{\prod_{l'=1}^{l}\left(1 + p(l')/100\right)}, \qquad (4.7)$$

where $\prod_{l'=1}^{l}\left(1 + p(l')/100\right)$ reduces to $\left(1 + p(l')/100\right)^l$ if $p(l)$ is constant over time. Now equation (4.6) becomes

$$N = \sum_{l=1}^{\infty} n_1 \frac{1 - \int_{-\infty}^{l} f(T_{ave}, \sigma_t)\,\mathrm{d}t}{\prod_{l'=1}^{l}\left(1 + p(l')/100\right)}. \qquad (4.8)$$

The terms in the summation decrease rapidly as l increases. Therefore, only first $T_{ave} + 2\sigma_t$ terms are taken into account and

$$N \approx n_1 \sum_{l=1}^{T_{ave}+2\sigma_t} \frac{1-\int_{-\infty}^{l} f\left(T_{ave},\sigma_t\right)\mathrm{d}t}{\prod_{l'=1}^{l}\left(1+p\left(l'\right)/100\right)} \qquad (4.9)$$

gives a good enough approximation for the original infinite sum in equation (4.8). Now, the number of devices installed l years ago can be solved from equations (4.7) and (4.9).

$$n_l \approx \frac{N}{\prod_{l'=1}^{l}\left(1+p\left(l'\right)/100\right)} \left\{ \sum_{l=1}^{T_{ave}+2\sigma_t} \frac{1-\int_{-\infty}^{l} f\left(T_{ave},\sigma_t\right)\mathrm{d}t}{\prod_{l'=1}^{l}\left(1+p\left(l'\right)/100\right)} \right\}^{-1} \qquad (4.10).$$

When we substitute equation (4.10) for equation (4.5), we obtain

$$N_b\left(j\right) \approx N \left\{ \sum_{l=1}^{T_{ave}+2\sigma_t} \frac{1-\int_{-\infty}^{l} f\left(T_{ave},\sigma_t\right)\mathrm{d}t}{\prod_{l'=1}^{l}\left(1+p\left(l'\right)/100\right)} \right\}^{-1} \left\{ \sum_{l=1}^{T_{ave}+2\sigma_t} \frac{\int_{l+j-1}^{l+j} f\left(T_{ave},\sigma_t\right)\mathrm{d}t}{\prod_{l'=1}^{l}\left(1+p\left(l'\right)/100\right)} \right\}.$$

Note that all the devices written off are not replaced by HTS ones, for new conventional devices are still being installed. Therefore, a market penetration model is used to account for the fact that HTS devices, like any new technology applications, will gradually take over from their old competitors on the market. The empirical equation describing the market share of a new product as a function of time is

$$F\left(j\right) = \frac{\beta}{1+\mathrm{e}^{2(\gamma-j)/\alpha}} \qquad (4.11),$$

where F gives the market share in year j, and α, β, and γ are the fitting parameters [73]. Now, this yields the number of installed HTS devices during year j,

$$N_r(j) = F\left(j\right)N_b(j)$$

Thus, the total number of HTS devices operating in year j is

$$N_{\mathrm{r,tot}}\left(j\right) = \sum_{j'=1}^{j} N_{\mathrm{r}}\left(j'\right).$$

Note that $N_{\mathrm{r,tot}}$ is only the statistical expectation value. The expectation value, $e_{\mathrm{rpl}}(j)$ for reductions in GHG emission is gained by

$$e_{\mathrm{rpl}}\left(j\right) \approx \frac{e_{tot}}{N} N_{\mathrm{r,tot}}\left(j\right).$$

Correspondingly, the full emission reduction potential upon device replacements is

$$e_{\mathrm{b}}\left(j\right) \approx \frac{e_{tot}}{N} \sum_{j'=1}^{j} N_{\mathrm{b}}\left(j'\right).$$

4.2 The case of Finland

To take an EU country as an example, I have provided accurate GHG emission reduction potential figures for Finland because detailed statistical and emission data were freely available of her large electrical machinery. In Finland, electricity is generated by 875 power generators with their rated nominal capacity totaling 17.2 GW. The transformer ratings in electric power plants follow closely the generator ratings so that the peak power of a transformer is fixed slightly over the corresponding generator. Because of many voltage levels needed in the transmission grid, the total capacity of transformers is over five times higher than that of generators. This implies that many more devices exist at the lower end of the power scale. In total, Finland has 132,282 transformers in her power grid, the largest being 1,000 MVA, with a total capacity of 94,428 MVA [4]. Fig. 4.1 shows the distribution of nominal power of the generators and transformers operating in Finnish power stations.

Industry consumes 53% of the country's total electricity supply, and from the point of view of this study, possible savings can be attributed to synchronous industrial motors. In the class over 1 MW, about 450 synchronous motors are in operation in Finnish industry with a combined power of 2.85 GW, this large number of powerful synchronous motors being due to the dominant position of the Finnish paper industry. Furthermore, large-scale wood processing requires lots of power at a steady pace [2].

Fig. 4.2 shows the reduction potential in GHG emissions for generators as a function of P_{be} and a according to equation (4.4). The achievable emission reduction is a linear function of a. On the other hand, it is estimated that the utilization of HTS windings in power devices can reduce losses by about half, compared with conventional devices [73], [130]. Therefore, we gain the most interesting information when we examine emission reduction as a function of P_{be} near a = 50%. Fig. 4.3 presents three curves corresponding to the different efficiencies of HTS devices, computed with a = 40%, 50% and 60%. Naturally, when we know $e_{tot}(P_{be}; a = 0.5)$, we can compute the reduction potential in GHG emissions for a given efficiency of a superconducting devices as

$$e_{tot}(P_{be}; a) = \frac{(1-a)}{0.5} \cdot e_{tot}(P_{be}; 0.5).$$

Different institutes have used slightly different criteria to determine the technological and economical limitations for choosing the P_{be}s. The American Superconductor Corporation has used P_{be} = 750 kW for synchronous motors and P_{be} = 100 MVA for transformers and generators to calculate possible energy savings potential [8]. Applying these P_{be}s, we can obtain 0.21–0.32 Mt of

CO_2-eq. savings with HTS synchronous motors (all units replaced, also henceforth), 0.21–0.31 Mt with HTS generators (40 units replaced), and 0.15–0.34 Mt with HTS transformers (100 units replaced). In total, this means 0.57–0.97 Mt of CO_2-eq. reductions annually, as attributed for hard coal. The range depends on varying values of a and the load factor of transformers, k^{TR}.

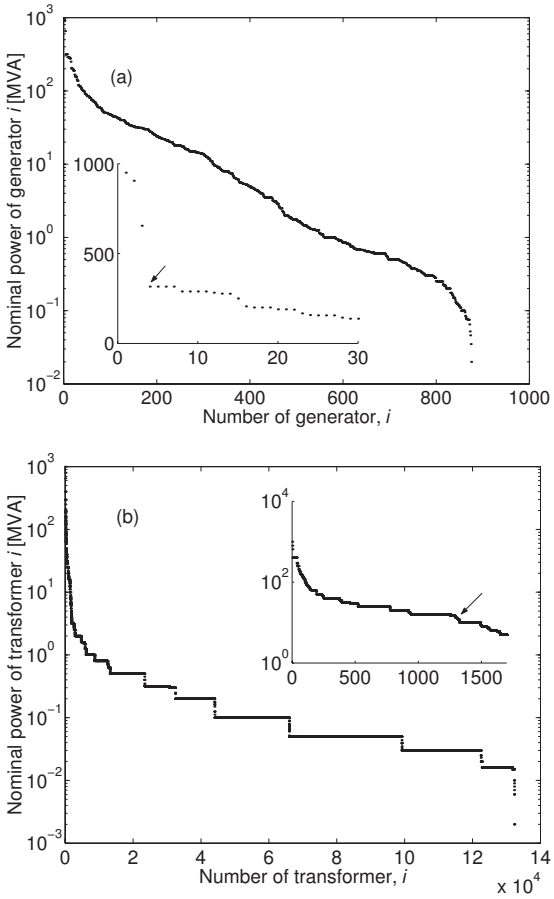

Fig. 4.1. The nominal power of each a) generator and b) transformer operating in the Finnish power grid. The inset is a close-up of the first values of the curve with the arrow pointing to the most sensitive power level.

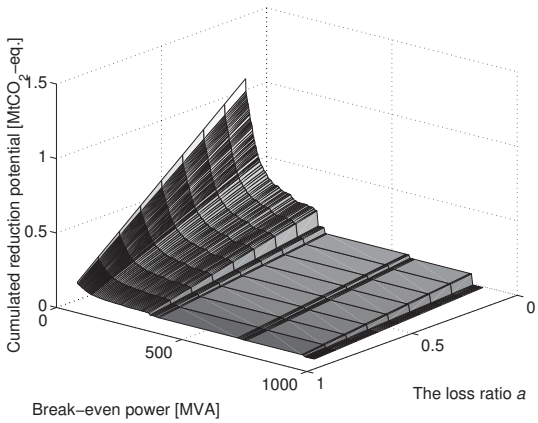

Fig. 4.2. Saved emissions as a function of break-even power and efficiency (in terms of loss ratio a) for HTS generators.

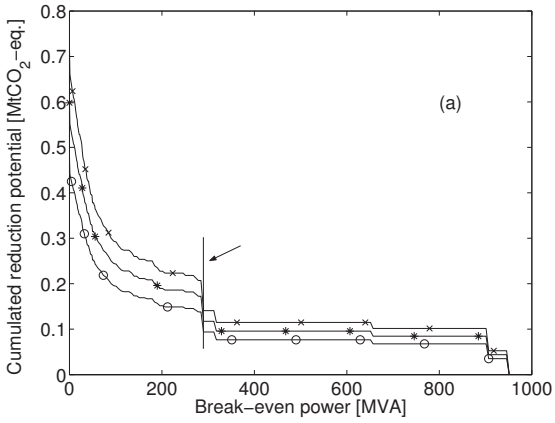

Fig. 4.3. Saved GHG emissions as a function of break-even power for generators. The symbols x, *, and o correspond to a = 40%, 50% and 60%, respectively. The variable a is the loss ratio between HTS and corresponding conventional ones.

However, since a 30 MVA HTS transformer with η = 99.97% has been designed by a French group [90] (though not including the energy loss for cooling) we are justified in setting P_{be} for transformers below that. The U.S. Department of Energy (DOE) suggested a P_{be} of 20 MVA, 100 MVA, and 375 kW for transformers, generators, and synchronous motors, respectively. These values would give 0.21–0.32 Mt with HTS synchronous motors, 0.21–0.31 Mt with HTS generators (40 units replaced) and 0.36–0.80 Mt with HTS transformers (774 units replaced). Combined, a reduction of 0.78–1.43 Mt could thus be obtained.

In terms of emissions, we can see in Fig. 4.3 that above a certain power level, savings accumulate much more than below the level. These "steps" are for transformers at 12.5 MVA, for generators at 300 MVA and for synchronous motors at 1 MW (shown here only for generators; for transformers and motors, see Publication **I**). The steps arise simply from the power distribution of the devices, as can be seen in the insets of Fig. 4.1. These P_{be}s would mean 0.21–0.32 Mt with HTS synchronous motors, 0.15–0.22 Mt with HTS generators (7 units replaced), and 0.44–0.99 Mt with HTS transformers (1,303 units to be replaced). In total, this makes 0.8–1.53 Mt of CO_2-eq. or 3–6% of total GHG emissions from electricity production. A close estimate would be 1.14 Mt of CO_2-eq., at which superconductivity would cut losses by half, that is, when a = 50% and k^{TR} = 0.5.

With the P_{be}s used by the American Superconductor, 3.1±0.8% of GHG emissions from electricity generation could be avoided. The DOE's P_{be}s give 4.4±1.4% reduction. When the P_{be}s are optimized with respect to GHG emissions in Finnish power grid, they agree well with the DOE estimates. For generators below 300 MVA the achievable reduction in GHG emissions increases smoothly with decreasing P_{be}. However, it is not economically viable to lower the P_{be} below the "step" because

more devices need to be built without a notable decrease in emissions. Consequently, P_{be}s of 300 MVA for generators and 12.5 MVA for transformers are suggested as worth pursuing.

The sensitivities $S_{Pbe}^{e_{tot}}$ and $S_{a}^{e_{tot}}$ for generators are presented in Fig. 4.4. The importance of sensitivity can be illustrated as follows. If we use a = 40% with P_{be} = 300 MVA, we can obtain 0.22 Mt of CO_2-eq. reduction by replacing 7 generators. To achieve the same reduction potential with a = 50%, we must lower P_{be} to 170 MVA and replace 14 generators; that is, e_{tot} is more sensitive to changes in a than in P_{be}. The average $S_{Pbe}^{e_{tot}}$ between 170 MVA and 300 MVA is –0.38 whereas $S_{a}^{e_{tot}}$ between a = 40% and a = 50% is –4.38, that is, over tenfold. In general, above 300 MVA e_{tot} is more sensitive to rise in a than to drop in P_{be}, except at 900 MVA where a variation in P_{be} results in major change in saved GHG emissions. Thus, emissions are reduced rather by boosting the efficiency of the devices than by increasing their manufacturing volume. Fig. 4.4a shows only one curve, because sensitivity with respect to P_{be} is independent of the value of a. Sensitivities are not shown for transformers and motors because the curve for transformers is similar to that for generators, except a hundred times higher. The curve is not relevant in the case of synchronous motors because all conventional motors are above 1 MW and therefore replaced with HTS ones when any of the above P_{be} criteria are used.

The lifetimes of electrical machines are considered normally distributed and are an average of 31, 35 and 40 years for motors, generators, and transformers, respectively. The market of electrical power devices has been growing about 4.7% per year during the 1960s and '70s, 2.7% per year during 1980s, and 1.7% per year since 1990 [73]. Based on this data, the market penetration of HTS machinery is estimated and the achieved GHG-emission reductions are presented in Fig. 4.5.

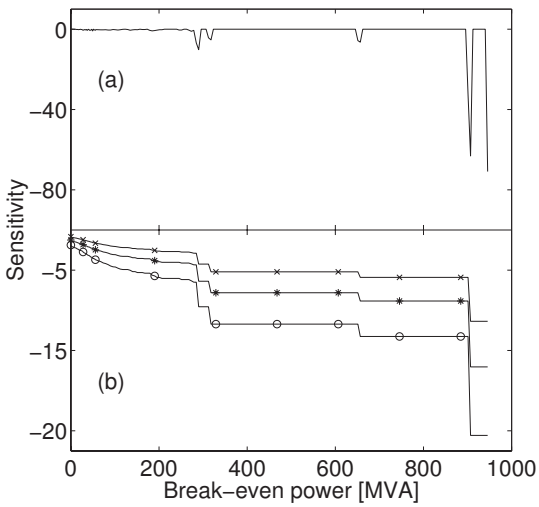

Fig. 4.4. Sensitivity of saved GHG emissions to variables a) P_{be} and b) a. The symbols x, *, and o correspond to a = 40%, 50% and 60%, respectively.

Because the standard deviation of a lifetime, σ_t, is unknown, the range of the number of replaced devices is obtained by assuming $5\ \mathrm{y} \le \sigma_t \le 20\ \mathrm{y}$. The theoretical maximum of GHG emissions reduction is achieved by assuming that all new units are HTS devices. In the near future, only a few of the devices are to be replaced, but the write-off rate will reach its maximum in 25–30 years. Hence, it will take at least 20 years to realize 50% of the full GHG emissions reduction potential. However, in reality even a longer time is needed because market penetration of HTS-devices is not ideal. Mulholland et al. have estimated the coefficients of the market penetration model for HTS devices (table 4.2) [73]. According to their estimates, in 25 years only 13% of generators, 17% of transformers, and 30% of synchronous motors are replaced with HTS equivalents. These estimates are pessimistic because included in the coefficients is the fact that small devices will not replaced, a fact I already took into account with the concept P_{be}. Furthermore, the authors did not consider the new advantages of HTS machinery, for example, positive environmental impacts, when they determined their coefficients. Instead, they determined the coefficients based on contemporary technological viewpoints, such as insensitivity to load variations, higher HTS generator stability, absence of fire hazards, overload capability, and lower noise of HTS transformers.

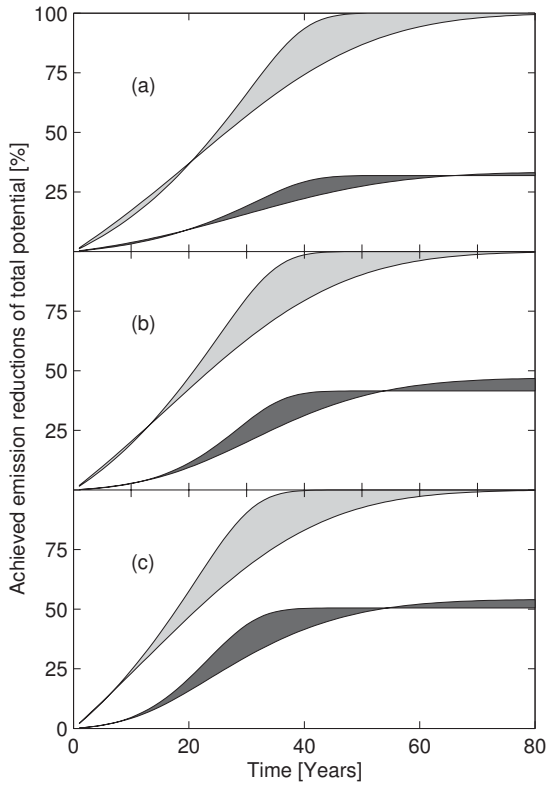

Fig. 4.5. Total GHG emissions as a function of time according to the market-penetration model: (a) generators, (b) transformers, and (c) synchronous motors. Light gray correspond to e_b/e_{tot} and dark gray to e_{rpl}/e_{tot}. The range is due to the variation $5\ \mathrm{y} \le \sigma_t \le 20\ \mathrm{y}$.

TABLE 4.2
THE COEFFICIENTS OF THE MARKET PENETRATION MODEL

Machine	α [years]	β	γ [years]
Generators	44.39	0.50	11
Transformers	17.76	0.80	10
Synch. motors	10.68	0.75	12

4.3 The case of the European Union

The scenario is somewhat different in the case of the EU as a whole. The biggest difference is in the use of combined heat and power, which in Finland is widespread. In addition, in the EU, the load factors of nuclear and hydroelectric power are lower than in Finland, but their k^i is higher for thermal power. Put together, these facts mean that relative emissions per generated kWh are higher in the EU than in Finland. The share of synchronous motors in other EU countries is roughly half that in Finland.

Electricity generation is the single largest contributor to GHG emissions in the EU. In 1999, CO_2-emissions from electricity generation were 913.6 Mt while total CO_2-emissions from fuel combustion were 3,085 Mt. This is approximately 80% of all the GHG emissions in the EU [104]. According to table 4.1, an average European GHG emissions value in electricity generation is estimated at 475 g of CO_2-eq/kWh.

In 1999, the EU generated 2,531 TWh of electricity with a maximum net generating capacity of 575 GW [104]. The current annual growth in production is 1.7%. Typically, electricity is generated at 10–20 kV and stepped up by transformers to 275–400 kV for transmission via overhead lines. Three more transformation points are required for fully functional electrical network, a pattern standardized throughout the EU. Transformers are responsible of approximately one third of total network losses, which are, on average, 6% of the generated electricity. The remaining 4% is consumed mainly in overhead transmission lines [35]. The power distribution of transformers in the EU was constructed from Finnish statistics based on the facts that there are 30 times more transformers in the EU than in Finland, the networks are identical, and that the electricity consumption is 30 times higher in EU [35]. The transformers were arranged so that $P^i_n \geq P^{i+1}_n$, where P^i_n is the nominal power of transformer i.

By applying equation (4.3), we can calculate the energy savings potential for transformers, E^{tr}_S, from

$$E_S^{tr} = T_p \sum_{i=1}^{N} P_{ave}^i (\eta_{sc}^i - \eta_c^i), \qquad (4.12)$$

where N is the total number of transformers, and T_p is the period of study, here one year. Equation (4.11) gives E^{tr}_S = 20.67 TWh with k = 0.5. Fig. 4.6 shows the dependence of the savings potential on P_{be}. However, EU generators cannot be analyzed in this fashion because the contributions of the various electricity producing sources differ between Finland and the EU average. In 1999, the contributing power sources in the EU were as follows: conventional thermal power 52% (of which 55% by coal/peat-fired power plants), nuclear power 34%, hydro power 13% and wind power 1%.

As we have seen, it is reasonable to use superconductivity in generators only above 100 MVA, which means those in nuclear power, coal/peat-fired thermal power, and combined cycle gas turbine (CCGT) power plants. However, this is a pessimistic simplification because there may be, in the absence of exact statistics, a few other thermal power plants with over 100 MVA generators. Possible savings in generators were thus calculated from electricity production statistics with

$$E_S^j = \frac{E_G^j}{\eta_c^j} \eta_{sc}^j - E_G^j, \qquad (4.13)$$

where j refers to the source (i.e nuclear, coal/peat-fired thermal, CCGT), E_G is generated electricity (TWh) and E_S is the savings potential (TWh). η_{sc} is calculated from equation (4.1). Results for the 15 EU countries that obtained their membership before May 2004 are shown in table 4.3 [117].

Despite some simplification, the results calculated for Finland with equation (4.13) agree relatively well with the results in section 4.2. The difference, which is only -5% compared to calculations from generator statistics on conventional steam turbines of over 100 MVA, is due to the fact that Finland has some gas turbines with over 100 MVA generators. One additional note on table 4.3 is that in

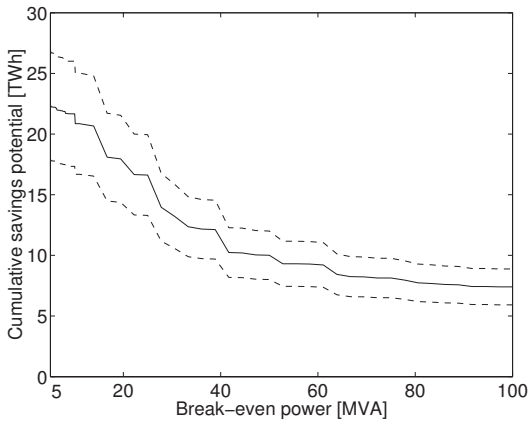

Fig. 4.6. The annual energy savings potential of transformers with respect to P_{be}. The solid line indicates the savings potential when a = 0.5 and k = 0.5; the dashed lines show the range when 0.4 < k < 0.6.

TABLE 4.3
ANNUAL SAVINGS POTENTIAL IN GENERATORS IN DIFFERENT EU COUNTRIES

Country	Savings potential in TWh
Austria	0.02429
Belgium	0.42024
Germany	2.52389
Denmark	0.09838
Spain	0.87929
Finland	0.21255
France	2.44008
United Kingdom	1.86923
Greece	0.17733
Ireland	0.05466
Italy	0.81595
Luxembourgh	0
Netherlands	0.22227
Portugal	0.18170
Sweden	0.43785
EU-15	**10.3577**

EU-15 means the total savings potential of all the 15 EU countries.

Spain and Italy, boiler oil is widely used for large-scale electricity generation. According to their electricity companies, about 90% in Spain [33] and 80% in Italy [32] of the electricity generated with boiler oil is produced with generators over 100 MVA.

When it comes to the combined annual savings potential of generators and transformers, E_S, which depends linearly on a, we can easily calculate the savings with different a-values from

$$E_S(a) = \frac{(1-a)}{0.5} E_S(0.5)$$

This way, we can draw a graph similar to Fig. 4.2 if we must vary P_{be}s from their present values. The energy savings can be converted to GHG emissions by multiplying E_S by e_{kWh}. If in electricity generation, the total savings potential is to be gained from cutting down on the use of hard coal/peat, this multiplication gives e_{tot} = 35.25 Mt of CO_2-eq., which, according to the Kyoto Protocol, makes 48% of the needed reduction in CO_2-emissions from electricity generation. However, it would be more relevant here to use the average European value, e_{kWh} = 475 g-CO_2-eq/kWh. Accordingly, the savings potential becomes e_{tot} = 14.74 Mt of CO_2-eq., or 20% of the Kyoto Protocol requirement.

In the case of Finland, I examined GHG emission reductions by way of the write-off rate of conventional devices based on their normal life span. The maximum achievable reduction is given here because several other issues besides device lifetime, such as political decisions on commitment to the Kyoto Protocol, affect the write-off rate.

4.4 Concluding remarks

I made a detailed study of the replacements of existing conventional transformers, generators, and synchronous motors with HTS equivalents to ascertain the levels of efficiency and nominal power that make HTS devices environmentally competitive. The study concentrated on the potential to reduce greenhouse gas (GHG) emissions in the Finnish electrical power grid by taking comprehensively into account the production and consumption of electricity and the causes of GHG emissions. I determined the break-even power limits of superconductivity, P_{be}, on the basis of previous economical and technological estimates combined with GHG emission analysis. The suggested P_{be} = 1 MW, 300 MVA, and 12.5 MVA for motors, generators, and transformers, respectively, can in Finland lead to an annual emissions reduction of 0.8–1.53 Mt of CO_2-eq. The range reflects uncertainty about the efficiencies of future commercial devices.

By widespread use of HTS, the EU could save an annual 31 TWh of electricity, which is 1.2% of her total generation. In terms of GHG emissions, this means 14.7 Mt of CO_2-eq. at average European values, which is about 20% of the emissions to be reduced in electricity generation required by the Kyoto Protocol. Thus, environmentally, HTS devices are ahead of their conventional counterparts. However, according to the market penetration model based on the write-off rate of present electrical machinery, the time estimated to reach 50% of the reduction potential is 20 years. We should also note that since the use of electricity is increasing by an annual 1.7%, the growth in consumption overtakes any savings in less than a year, if average European e_{kWh} stays constant. Finally, according to sensitivity analysis, it is better to improve the efficiency of HTS devices than to aim at manufacturing large volumes.

On 1st of January 2005, stock exchanges across Europe began trading in CO_2-emissions. International trading in emissions constitutes one of the flexibility mechanisms defined by the Kyoto Protocol. Currently, the price of a ton of CO_2 is € 23 [78], but its volatility is now high before the commitment period (2008–2012). However, at that price, potential annual savings with HTS machinery would amount to € 18–35 million in Finland and € 338–811 million in the EU as a whole. Without speculating about the future prices of superconducting machinery, we can calculate that if a 500 MVA superconducting generator were to cost the same as a conventional one today, the annual savings in Finland would buy us only two units. However, it is too soon to make such calculations because the price of a CO_2 ton has not been fixed to a definite figure.

Interesting results occur when the annual savings potential in emissions due to device replacement is compared to fuel consumption of automobiles. How much would the average fuel consumption of road vehicles have to drop to obtain the same impact in emissions as with HTS devices? In 2003, total number of kilometers driven on public roads of Finland was 50,600 million and these vehicles consumed 4,610 million liters of fuel [76]. In total, GHG emissions from road traffic were 12.27 Mt of CO_2-eq. These numbers yield to an average fuel consumption of 9.1 liters per 100 km. Now, to obtain the same 0.8–1.53 Mt of CO_2-eq. reduction in emissions as with HTS devices, the average consumption would have to drop to 8.5–8.0 liters per 100 km, respectively. Since all the heavy traffic trucks and buses, consuming tens of liters per 100 km, are included in these numbers, much engine development is needed to obtain similar savings as with HTSs.

Chapter 5

CENTRALIZED VERSUS DISTRIBUTED ELECTRICITY GENERATION

Distribute generation (DG) is emerging as an alternative to centralized electricity generation system. DG can be defined as electricity generation connected to a distribution network or a customer site with less than 10 MW of power delivered [85], [50]. Traditionally, electricity is generated in large power stations, located near resources or at logistical optimums, and delivered through a high voltage transmission grid and locally through medium voltage distribution grids. DG aims to add versatility of energy sources and reliability of supply and to reduce emissions and dependence on fossil fuels. In addition, DG can contribute to the reduction of transmission losses and help introduce new developments such as fuel cells and superconducting devices [17]. Fig. 5.1 illustrates the differences between a central plant and a DG model.

The goals of DG include the minimization of the environmental impacts of energy production. Superconducting devices are proposed for DG because of their high efficiency, small size, and more stable operation during peak loads. This chapter concentrates on the environmental benefits of superconducting machinery by comparing suitable devices with their competitors in DG-network. Superconducting devices that could be exploited in DG consist of superconducting magnetic energy

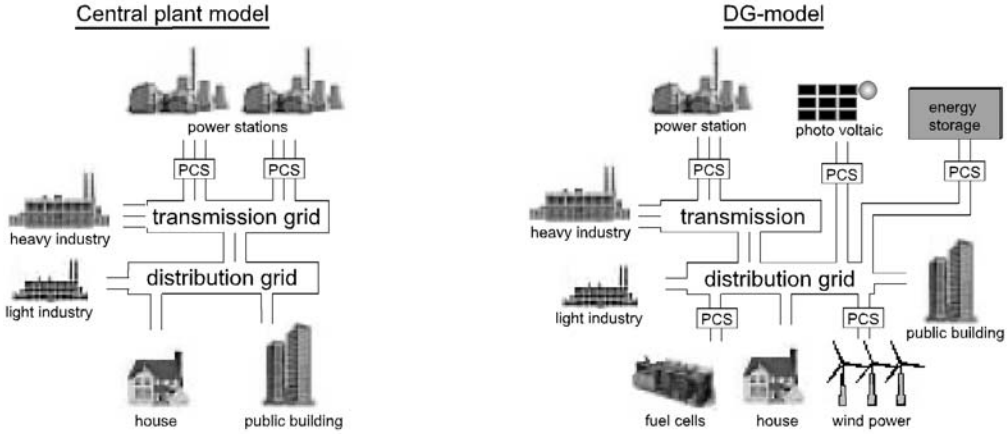

Fig. 5.1. Schematic diagram of a traditional central plant model and a DG-model. PCS stands for power-conditioning system.

storages (SMES), flywheels, and cable systems. However, according to the P_{be}s found in chapter 4, HTS machinery is not applicable to DG because of the 10 MW limit. Large MW-class motors are used only in heavy industry, which cannot be located under a DG-network. Life-cycle assessment (LCA) is used as a tool in comparisons of energy storage devices suitable for DG, that is, SMESs, flywheels and batteries.

5.1 Comparative analysis of energy storage solutions

Energy storage is becoming increasingly important in electrical networks because the energy sources considered for DG are typically less reliable steady-power suppliers than traditional power stations. Therefore, we need storage unless we are ready to accept intermittent electricity supply and operation at lower, that is, non-optimal efficiency. Suitable storage technologies for DG are based on either electrical (batteries, SMES) or mechanical (flywheels, compressed air, pumped water storage) devices [93].

The recent blackouts in Europe and the USA have raised questions about the reliability of electricity transmission network. In addition, power quality issues (PQI) have come to the fore, especially because of the varying nature of these new maturing energy technologies and their increased need of power converters. Harmonic distortion in current and voltage challenges equipment manufacturers. Superconducting FCLs and SMESs offer certain benefits here, but PQIs are beyond the scope of this thesis. Instead, I compared FCLs with traditional circuit breakers, and SMESs and flywheels with HTS bearings with other proposed energy storage solutions only in terms of their environmental impacts. In my environmental analysis of energy storage devices, I used the already established tool

of LCA, and took a more common approach with cables. The idea is to first phase out the irrelevant storage methods, and then compare the relevant ones with superconducting counterparts.

Storage methods that use air-compression can be divided in two types: compressed air energy storage (CAES), and compressed air storage (CAS). The main component in both concepts is a natural-gas-driven turbine generator. A compressor is used during off-peak hours to compress air into underground caves (CAES) or vessels (CAS), from where it is then released to combustion chamber during hours of usage. Since the power required by the compressor in not taken from the turbine, the output is increased by a factor of two [93]. CAES plants have been built since the 1970s, but because their minimum feasible power is tens or even hundreds of MWs, they are too large for DG systems [99]. The CAS concept, in turn, would be feasible at DG ratings, but CAS is still in its infancy and does not lend itself to LCA yet. However, since the turbine generator uses natural gas for fuel, we can roughly estimate the GHG emissions of this "storage method" from the data in table 4.1, while keeping in mind that the plant's efficiency is twice that of a conventional gas turbine plant. Consequently, its emissions are halved and fall into a range of 220–344 g of CO_2-eq. per kWh.

Pumped water storage can be reduced to a simple hydropower plant, in which case environmental damage is limited mostly to the construction of the dam and auxiliary structures. Estimably, the higher emission number of hydropower in table 4.1, 236 g(CO_2-eq)/kWh, applies as well to pumped water storages, which have a low utilization rate and are typically constructed in artificial rather than natural formations. They release about the same amount of emissions per kWh as photovoltaic solar cells but five times more than wind power and eleven times more than nuclear power. Comparison with CAS reveals that in terms of emissions these storage methods are equal if we use state-of-the-art turbine generators. Unfortunately, LCA for pumped water storages is not available.

The energy storage methods that remained under comparison here by LCA were SMES, flywheel, and batteries. A good environmental assessment between conventional lead-acid batteries and their likely replacements, vanadium-redox batteries, was carried out in [90], and the results were exploited in this analysis. Lead-acid batteries are commercial whereas vanadium-redox batteries are prototypes being developed, as are the flywheel systems. The SMES system I studied was a theoretical design. The functional unit (FU) of [90], *an electricity storage system with a power rating of 50 kW, a storage capacity for 450 kWh and an average delivery of 150 kWh electrical energy per day for 20 years*, was applied also in this study. This FU enables two possible systems with a maximum capacity of 450 kWh. The first possibility is a system for diurnal use with a daily energy storage of

150 kWh, which is suitable, for example, for leveling peak-hour loads in a DG-network. A second possibility is an autonomous system for three-day power back-up with 450 kWh of stored energy, equivalent to the electricity requirements of several remote houses for 10–70 persons for three days. Selection between these systems affects the depth-of-discharge (DOD) in lead-acid batteries and the number of flywheels in operation, which again bear on the durability of stack membranes in batteries and the refrigeration requirements of flywheels. Therefore, two different cases are studied, and a range between the results is given in table 5.1. Vanadium-redox batteries allow deep DODs without adverse effects on the lifetime of stack membranes whereas the SMES system is one complete unit whose refrigeration is independent of the energy stored.

The SMES was designed as an LTS, NbTi-based system with liquid helium cooling and *in situ* liquefier. NbTi system was chosen because HTSs are not yet advanced enough to hold competitive current densities with LTSs in SMES magnets. According to the design principles in [77] and [87], a 450 kWh SMES system needs 856 kg of NbTi wire, 5,933 kg of stabilizing copper, and 52.3 tons of reinforcing material (stainless steel) per FU. The results of LCA in chapter 3 can be employed also for the present concept. Thus the production statistics of the SMES in table 5.1 include wire production data from there. Under normal operating conditions, a SMES does not lose any of its stored energy but achieves 100% electrical efficiency. However, heat leaks through the cryostat create losses that must be eliminated with proper cooling. Necessary power conditioning systems naturally dissipate energy, but because the amount is considered equal in all applications, it was ignored. From [87] I could estimate the cooling requirements and rate the liquefier's capacity at 45 l/h. I chose a Linde TCF50 liquefier of weight 8.5 tons and of energy consumption 132 kW.

The flywheel system design consist of 45 units of 10 kWh Boeing flywheels with superconducting YBCO bearings [131], [98]. The flywheels themselves are made of carbon fiber, which is materially and energywise demanding to produce, and which has only partly been subjected to LCA [105]. Because only a 9.6 kg per FU of YBCO material is needed for the bearings, the amount was ignored in this LCA. The YBCO bearings can be cooled by either liquid nitrogen or a mechanical cryocooler. Depending on the use (diurnal or three-day back-up), either 15 or all the 45 flywheel units are running, resulting in varying refrigeration power and thus losses.

The stack membranes of the battery systems must be changed four to six times during the functional unit of 20 years, because average lifetime of a membrane is 3–5 years, depending on DOD. The first values in the lead-acid battery column are for 5-year stack membranes whereas the second values are

for 3-year membranes. The more often the membranes are replaced, the more material is needed and emissions accumulate. However, both vanadium and lead are recyclable materials. The impact of recycling and re-assembling of the batteries was scrutinized with results therein included in table 5.1. Unlike the membranes, the flywheel system has a designed lifetime of 25 years and the SMES system that of 30 years, figures that were taken into account in the production parameters [90], [98].

The very first impression from table 5.1 is that the SMES system designed here is an absurd energy storage application because it stores about one GWh but needs over 23 GWh for refrigeration over 20 years of operation. However, this analysis only confirms the fact that an LTS SMES is not economically sound. In an HTS SMES with similar performance and liquid nitrogen cooling, dissipation would be only 6 kW and thus losses over a 20-year period 1051 MWh [86]. Therefore, fully developed HTS wires would also considerably increase interest in SMES devices. Another peculiarity of the SMES is that while its electrical efficiency is 100%, losses from refrigeration account for total efficiency of 5% over 20 years. A similar sized HTS SMES would achieve 50% total efficiency. By economical or environmental standards, such a system falls slightly behind flywheels and batteries; on the other hand, SMES is the only storage method to deliver uniform, high quality electricity and is therefore the foremost choice in terms of PQIs.

TABLE 5.1
LCA BETWEEN SMES, FLYWHEEL AND BATTERIES OVER 20 YEARS OF USE

		SMES	Flywheel	Lead-Acid battery	Vanadium battery
Dimensions	Mass [kg]	98,000	27,035	47,974	23,601
	Volume [m3]	800	260	4.3	9.6
Production	Water [m3]	4,718	7,200	6.4–9.6	11.3
	Energy [GJ]	2,669	1,225	1,062–1,593	281
	Lead [kg]	0	0	29,400–44,100	0
	Vanadium [kg]	0	0	0	2,309
	Superconductor [kg]	856	9.6	0	0
	Copper [kg]	5 933	0	130–195	184
	Carbon fiber [kg]	0	2,988	0	0
	Steel [kg]	52,333	18,640	0	2,516
	Sulphuric Acid [kg]	356	N/A	4,600–6,900	6,103
	Nitric Acid [kg]	1,900	N/A	0	0
Electricity	Net delivery [MWh]	1,095	1,095	1,095	1,095
	Electrical efficiency	100 %	88–92 %	75 %	72–88 %
	Refrigeration [W]	132,000	450–1,350	~0	~0
	Losses [MWh]	23,126	200–358	365	150–425
	Total efficiency	5 %	75–85 %	75 %	72–88 %
Emissions	Nox [kg]	563	36	242–363	45
	SO2 [kg]	404	57	215–323	28
	CO [kg]	133	N/A	57–86	5
	CO2 [tons]	433	173	148–222	46
	[g(CO2-eq) / kWh]	416	159	145–217	44

Denotation N/A stands for data not available. Emissions from electricity production to charge the storages are not included. Emissions for flywheel are only from production of required steel and energy.

Environmentally, the flywheel seems a lucrative choice with moderate energy needed for production and low losses. Unfortunately, emission data is still incomplete on the flywheel because LCAs are not yet available on carbon fiber and YBCO production. One disadvantage of the flywheel system is its volume: for the same energy storage capacity, it needs 37 times the space of an average battery installation. On the other hand, the absence in flywheels of sulphuric acid and toxic lead—30–44 tons of them are needed in a lead-acid battery system—are important advantages over battery systems. The average electricity losses of flywheels, including cooling needs, equal those of prospective vanadium batteries whereas their losses are about 75% of those of lead-acid batteries.

All the above energy storage devices—CAS, pumped water storage, SMES, flywheel, and batteries—share one common factor: their GHG emissions in g(CO_2-eq)/kWh. This number gives the emissions generated in discharging 1 kWh of electricity from storage, without the emissions from charging a storage. Depending on the electricity source, emissions from generation must thus be added to the indirect emissions shown in table 5.1 and the chapter on CAS and pumped water storage. Simply comparing the figures, we can see that vanadium-redox batteries show the best performance with flywheels coming a good second.

5.2 The case of cables and FCLs

The cable system, which connects the network's production and consumption sites, consists of wires, switchgear, and controlgear assemblies. In DG networks, cables are preferred to overhead lines because transmission distances are short and losses low. Overhead lines are often seen as blot in the landscape, and the recent devastating storms around the world have increased interest towards underground transmission cables as well. From the emissions point of view, the biggest problem lies in circuit breakers that use SF_6 gas as insulator to prevent electric arcs. However, in DG-networks, the usage of SF_6 in circuit breakers is minimum because these breakers are best suited for high voltages (110 kV and over) and little would be gained environmentally by replacing them with lower switchgear ratings, enabled by superconducting FCLs. DG-networks are supposed to operate at medium voltage, that is, 20 kV and below.

Nowadays, a typical conventional cable for DG networks is a 10–20 kV, 3-phase AC ground cable with aluminum conductors and polyethylene PEX plastic as electrical insulator. In the range of 1.5–8.5 MW at nominal current ratings, the losses of these cables remain within 50–65 W/m [83]. Superconducting HTS cables come in two competing designs, called the room temperature dielectric

(RTD) and the cryogenic dielectric (CD) (for their differences, see Fig. 5.2). The RTD design has the advantages of common materials used for insulation and smaller total cable diameter whereas the CD design boasts higher overall current density and lower losses. The development of HTS cables is now focused on the CD design [133]. By computations based on [68], the losses of future HTS AC cables incorporating YBCO material would lie within 15–25 W/m, including LN_2 cooling requirements. For true comparison of these cables, we should design a complete DG network with power sources and PCS systems. However, the network would involve such a myriad of choices to be made about power ratings, devices, and geographical issues concerning the cables that each case would have to be examined separately.

A DC transmission system incorporating underground cables has been suggested as the best alternative to interconnect different DG-networks [11]. Superconducting cables would be ideal for this purpose because they can be designed to automatically limit over-currents [64]. Yet power engineers should also study the possibility of distributing electricity in a DG-network by DC. A common DC voltage in the whole system would make the system simpler and thus more durable—and would require power converters only at generation and consumption sites. The AC/DC conversion is of course not ideal, but conversion efficiencies of 99% can be obtained. Since a DG-network could contain energy sources generating DC (for example, fuel cells, solar panels, batteries and SMESs) or variable quality AC (for example, wind farms), it would thus be a good idea to promote DC transmissions for enhanced quality and negligible transmission losses.

In the following, I present a commercialization schedule together with a market penetration model for HTS cables. It is estimated that 2G wires will become commercial in 2007 and that the first

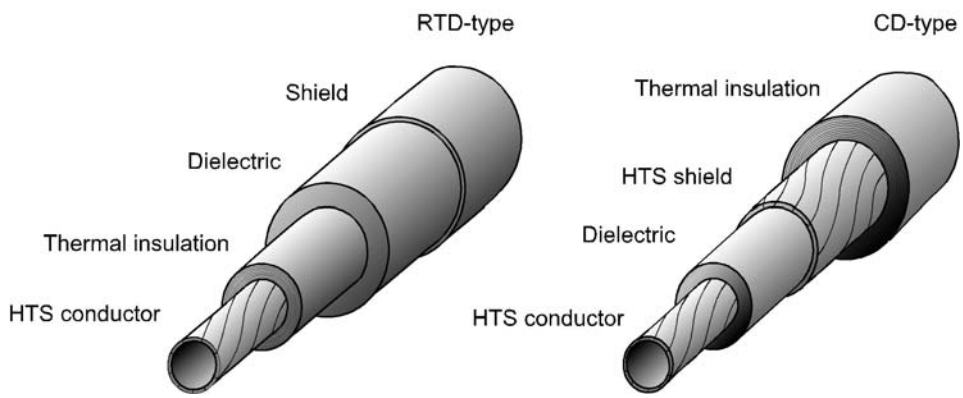

Fig. 5.2. Schematic presentation of the two designs for superconducting cable: room temperature dielectric (RTD) and cryogenic dielectric (CD) design.

profitable market year for HTS cables will be 2010 [73], [67]. Therefore the first superconducting application to be exploited in DG-networks is HTS cables, and their future role is of interest here. Fig. 5.3 shows estimated market penetration curves for HTS cables in DG-networks calculated with equation 4.11. In an electricity network, HTS cables could reach a 45% asymptotic market share and penetrate the market quickly [73].

Because DG networks are an emerging market and intended as platforms for modern technology, we can expect the share of superconducting cables in DG to pass the 45% mark in the whole network. For example, superconducting transformers and synchronous motors with powers above their P_{be}s could reach 80% and 75% shares in the entire network, respectively [73]. Because future DG networks can be designed to make full use of the advantages imbedded in superconducting cables, the market share of superconducting cables in the network can be expected to reach or even exceed that of transformers. Consequently, I estimated the cables' upper market share at 85%. Their market penetration was estimated to be rather deep because HTS cables are unlike to replace conventional cables but instead saturate DG networks from the start.

With the lowest 45% market share, average losses in DG network cables at nominal current would fall within 39–53.5 W/m, which means about 20% less loss in electricity and in GHG emissions in all transmission losses. The higher 85% market share brings along average energy losses of 20–31 W/m, which in turn reduce both losses and emissions by 56%.

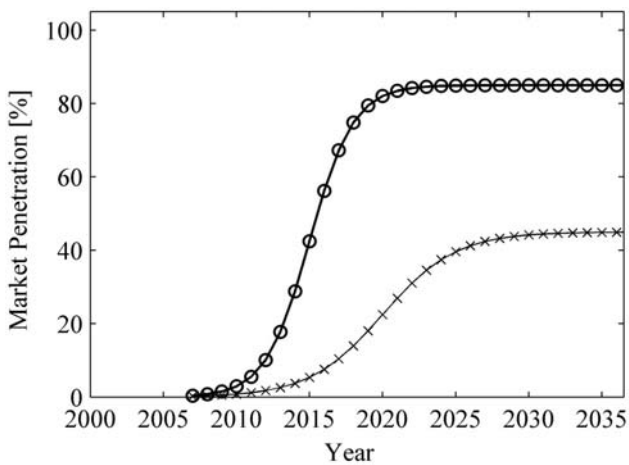

Fig. 5.3. Estimated market penetration of HTS cables over the next 30 years. Symbols o and x denote the upper and lower limits for market share in DG networks, respectively.

5.3 Concluding remarks

This chapter focused on the environmental impacts of using superconductivity in DG networks. Three suitable superconducting applications emerged for DG: HTS SMES, flywheels incorporating superconducting bearings, and cable systems. LCA used as a tool to compare conventional batteries and superconducting alternatives in energy storage devices. Environmentally, flywheels outperform conventional lead-acid batteries and compete favorably with prospective vanadium-redox batteries. The designed SMES do not show such competence, but a SMES incorporating high temperature superconductors offers far better performance. Superconducting cables have 60–70% less losses than conventional cables and are capable of preventing over-currents. Finally, a commercialization schedule of HTS cables in DG networks was examined. According to the model, HTS cables can make a significant market penetration during the next decade.

Chapter 6

MAGNETIC SEPARATION AND THE ENVIRONMENT

The previous chapters dealt more or less indirectly with how to apply superconductivity in reducing the environmental load of human activity. This chapter discusses magnetic separation as a direct method to treat wastewaters containing heavy metals. The study focused on a magnetic separator designed and built at our laboratory over the past four years. The driving force behind the study was the pursuit of eco-efficient factory with internal circulation of process waters.

Two types of wastewater were tested with the separator: synthetic wastewater made at the Department of Chemistry and genuine steel mill wastewater from Outokumpu Stainless, the world's largest steel mill in Tornio, Finland. Synthetic solutions each contained 25 mg of dissolved Cr, Fe, and Ni whereas the genuine steel mill wastewater contained Cr, Fe, Ni, and Mo in both dissolved and particle form. With the aid of magnetic carriers, ions were attracted to larger magnetic particles, and the solution was then run through the separator. The device was designed, not only to treat wastewaters, but also to determine the separation parameters, and to gain experience with the technology. Publications **V** and **VI** report the original work.

6.1 Test with isodynamic open-gradient magnetic separator

The force, $\mathbf{F}_m$, needed to separate materials in a magnetic separator is proportional to magnetic flux density, **B**, its gradient, magnetic susceptibility of the particle to be separated, χ, and the volume, V, of the particle, as expressed by the following formula [108]:

$$\mathbf{F}_m = \frac{\chi}{\mu_0} V \|\mathbf{B}\| \nabla \|\mathbf{B}\| = \frac{\chi}{2\mu_0} V \nabla(\mathbf{B} \cdot \mathbf{B}),$$

where μ_0 is the permeability of vacuum. There are two ways of creating the needed $\nabla\mathbf{B}$, namely by the aid of a ferromagnetic matrix or by so-called open-gradient magnetic separation (OGMS). By installing a ferromagnetic material, typically iron, in the volume where **B** is present, gradient of **B** is created, and thus particles with positive χ move towards the ferromagnetic matrix. In OGMS, $\nabla\mathbf{B}$ is created by magnet design, and particles are deflected in the separation volume. The direction and angle of deflection are defined by χ of each particle. An OGMS device can also be made isodynamic, which means that $\mathbf{F}_m$ is nearly constant throughout the working volume of the separator. This way we can study how varying the parameters affects separation. Next, the magnet system, the cryostat of the built separator, and the water-pumping unit are presented.

The magnet system had interchangeable pairs of NbTi and Nb_3Sn superconducting coils with applied **B** in the working volume up to 3 T. The water pump unit had stepless flow velocity control, enabling velocities of up to 7 liters per min (L/min) (the experimental set-up shown schematically in Fig. 6.1). The cryostat, a cylindrical vessel made of AISI 316 L stainless steel, was designed to minimize the evaporation of liquid helium, which was used to cool the coils and the lower end of the current leads. The outer vessel's total height and diameter were 2.2 m and 1.62 m, respectively. The vessel's outer wall thickness was 6 mm, and the thickness of its top and bottom plates was 20 mm. The top plate supported the coils and their bracket structure along with current leads and instrumentation. The space between the inner and outer walls was insulated with 40 layers of MLI superinsulation in a vacuum. Vaporized helium cooled the radiation shield, which reached the vacuum space. Two ion-pumps were attached between the vessels to maintain a sufficient vacuum regardless of possible leaks (Fig. 6.2 shows an exploded view of the cryostat) [115].

The current leads feeding the coils consisted of two parts, an upper part made of a brass tube of inner and outer diameters 20 mm and 32 mm, respectively, and a lower part with NbTi tape wound around the brass tube. A hollow structure with a large inner diameter was used to cool the current leads with

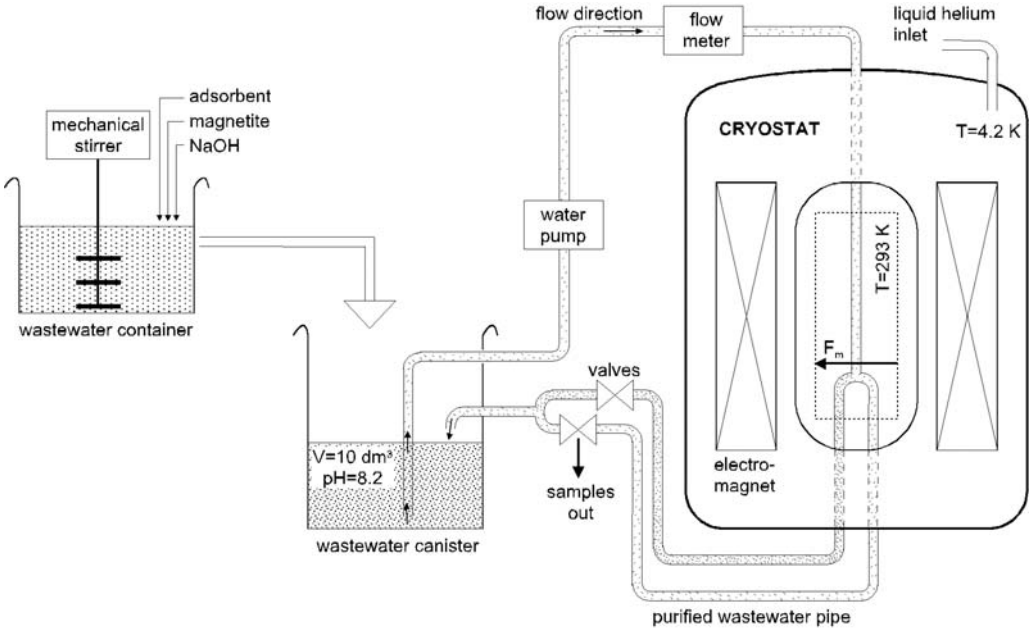

Fig. 6.1. Schematic view of the experimental set-up. The direction of the magnetic force, $\mathbf{F}_m$, is shown inside the separation volume.

vaporizing helium. In isodynamic open gradient magnetic separation, high and nearly constant magnetic force density is needed. Solenoid, racetrack, and saddle-shape coils were studied to establish suitable magnetic field distribution. The two last mentioned turned out to give the best results, and the racetrack geometry was chosen because of its easier manufacture. The coils and the separation zone are illustrated in coordinate system in Fig. 6.3 with model dimensions r_A, r_B, w_A, w_B, h_A, h_B, l_A, l_B. Numerical value for the y-directional distance between the center points of the coils, D, is given in table 6.1.

Because the magnetic force density distribution is sensitive to changes in the coil's operating current ratio, we can avoid fluctuations by connecting the coils in series and feeding the current from a single power source. The critical currents I_{cA} and I_{cB} are short-sample values of the NbTi wires with cross sections of A_A and A_B. The dimensions, wire specifications, magnetic force density and its uniformity of the NbTi magnets are shown in table 6.1 [5].

The wastewaters were pumped from a canister into the separation zone through a pipe divided into two at the end of the homogenous force density distribution area, that is, at the end of the separation volume with cleaned wastewater flowing in the lower pipe. Two pipe constructions were used, one which divided the incoming flow 50/50 and another 25/75; that is, cleaned wastewater flowed through the smaller diameter pipe. A water flow meter by IFM Electronic was attached to the pipe,

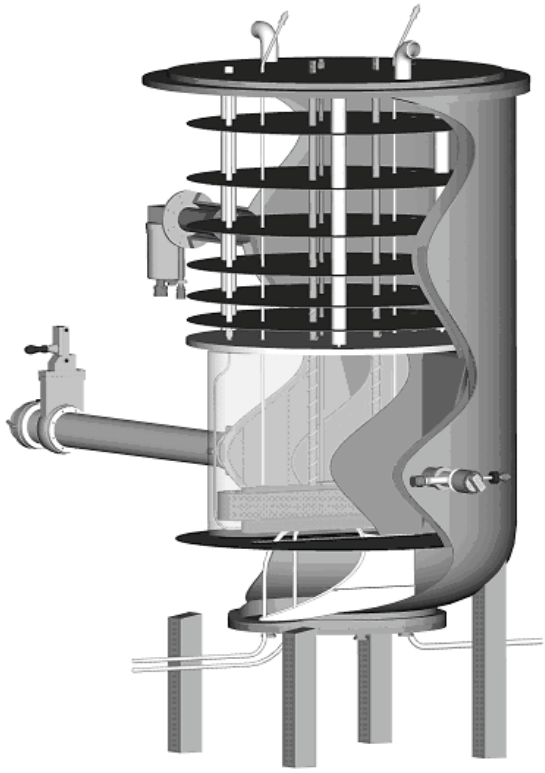

Fig. 6.2. Exploded view of the cryostat. A pipe (bottom right) conveys water into the cryostat and the bore of the magnet where separation occurs. At the end of the separation volume, the pipe divides into two. A vacuum is maintained between the inner and outer layers of the cryostat with a vacuum pump attached to the long pipe left of the center of the cryostat. The magnet is immersed in liquid helium, and several layers of superinsulation are used to dampen heat radiation. Liquid helium inlets are visible on the top plate.

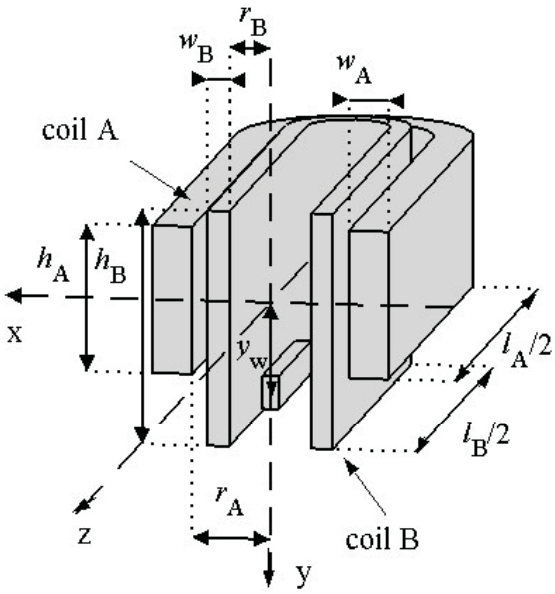

Fig. 6.3. Magnet geometry with two racetrack magnets.

TABLE 6.1
Magnet Specifications

PARAMETERS	NBTI MAGNET
l_A / l_B [mm / mm]	700 / 630
r_A / r_B [mm / mm]	48 / 25
w_A / w_B [mm / mm]	25 / 13
h_A / h_B [mm / mm]	90 / 129
y_w [mm]	43
D [mm]	24
Ic_A / Ic_B @ 4 T & 4.2 K [A / A]	400 / 647
A_A / A_B [mm^2 / mm^2]	0.567 / 0.950
Magnetic force density [T^2/m]	6e10^7
Magnetic force change in x / y direction [%]	3.7 / 5.9

to measure the flow velocity and temperature of the passing liquid. The pipe branched out at the end of the separation zone, and expansion tanks were installed on both lines to sample the liquids. Fig. 6.4 shows a photograph of the apparatus.

Fig. 6.4. The separator apparatus in operation. Pipes, canister, and the sampling assembly are in front and cryostat at the back. A Hall-sensor measured magnetic flux density with its display in the lower right corner.

6.2 Sample preparation

To separate dissolved metals, ions must be chemically attached to a larger magnetic particle, for which magnetite was used. Furthermore, an adsorbent was necessary between magnetite and ions because of their chemical linkage properties. The chosen adsorbent in all experiments was Molecular Sieve UOP Type 5 Å made by Fluka. The empirical formula of this molecular sieve is $Ca_nNa_{12}2n[(AlO_2)\ 12(SiO_2)] \cdot x\ H_2O$. Particles were crashed and sieved before they were used as adsorbent to a final particle size of < 50 μm. Magnetite, which particle size is < 5 μm, was used for magnetic seeding. Adsorbent and magnetite were coagulated by using $FeCl_3 \cdot 6H_2O$. Analytical grade reagents $Ni(NO_3)_2 \cdot 6H_2O$, $Cr(NO_3)_3 \cdot 9H_2O$, $FeCl_3 \cdot 6H_2O$, $(NH_4)Mo_7O_{24} \cdot 4H_2O$ were used to

prepare synthetic metalliferous solutions and analytical grade NaOH and HCl to adjust the pH of the solution. All samples were prepared with distilled water [82], [37].

Sorption tests were run at ambient 21°C. The amount of heavy metal ions removed from the solutions was determined by atomic absorption spectrophotometer (AAS), based on the differences in the metal ion concentration before and after the introduction of the molecular sieve. After sorption, magnetite particles and ferrugo, iron-hydroxide $Fe^{(III)}(OH)_3$, were added to the solutions at a pH of 7–8. Adsorption was studied as a function of adsorption time, silicate mass, and solution pH.

Adsorption proceeded rapidly, and the added silicate clearly enhanced it because of its greater adsorbing area. In addition, solution pH had an essential effect on ions removal, for adsorption intensified when pH was increased with protons competing for adsorption sites with metal ions. On the other hand, under basic conditions metal ions also precipitated as metal hydroxides. Thus adsorption is not the only mechanism to remove heavy metal ions from wastewaters. Microscopic studies showed that pH affected the coagulation of magnetite and silicate and that the most uniform silicate-magnetite network formed at pH 8, an observation supported by tests with a permanent magnet. Silicate was removed from magnetite by decreasing pH to 2 [49]. In experiments made as a function of adsorption time and pH, the initial concentration of each metal-ion was 50 mg/L and the mass of silicate was 1 g/L (results shown in Fig. 6.5).

Next, the adsorption time was fixed to 1 hour, and the effect of different silicate masses on adsorption was studied. Fig. 6.6 shows removal percentage as the silicate mass increased. Finally, adsorption tests were run by raising pH from acidic to alkaline with a fixed time of 1 hour and a silicate mass of 1 g/L. Fig. 6.7 shows that with slightly alkaline pH we could achieve 100% removal efficiency. As can be seen, sorption efficiency rises with increasing pH. There are two reasons for the rise. First, at low pH (acidic conditions), H^+ ions, which cause acidity, reduce the removal of metals by filling adsorption sites from silicate. Second, metal-hydroxides precipitate in alkaline conditions; that is, metals are removed from solutions not only by adsorption but also by precipitation [58].

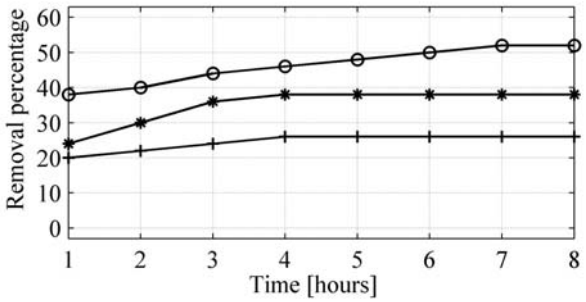

Fig. 6.5. Removal of metal ions in percentage over time. Symbols o, *, and + correspond to Ni^{2+}, Fe^{2+}, and Cr^{3+} ions, respectively.

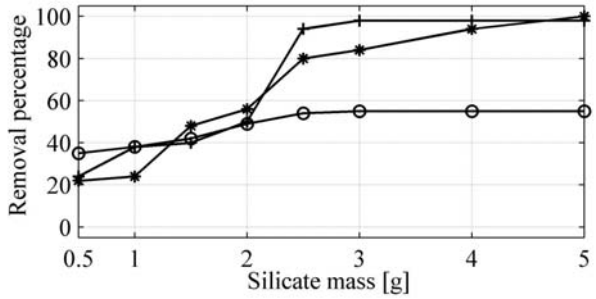

Fig. 6.6. Removal of metal ions in percentage by different silicate masses. Symbols o, *, and + correspond to Ni^{2+}, Fe^{2+}, and Cr^{3+} ions, respectively.

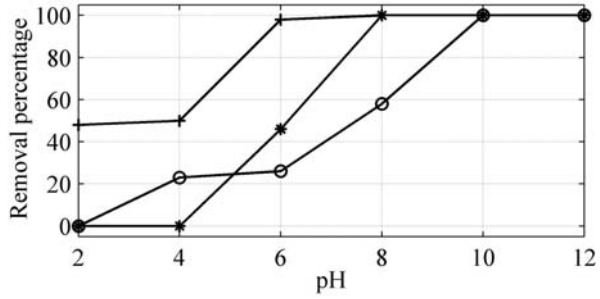

Fig. 6.7. Removal of metal ions in percentage over pH. Symbols o, *, and + correspond to Ni^{2+}, Fe^{2+}, and Cr^{3+} ions, respectively.

The next experiment was to find out how to get silicate and magnetite to link together. It was possible by using ferrugo and by adjusting the pH so that the coagulation occurs as efficiently as possible. After adding magnetite and ferrugo into the solution containing silicate, the concentration of free heavy metal-ions decreased. At the pH of 8, almost all free ions in the solution connected to silicate-ferrugo-magnetite-coagulants. After coagulation, a permanent magnet was placed near the graduated flask with the results that magnetic fraction started shifting towards the magnet. In about half a minute, the solution was clear. This know-how was used to prepare both synthetic and genuine steel mill wastewater.

6.3 Results and discussion

During the first test session, NbTi magnet and 50/50 pipe division was used. The synthetic wastewater contained 25 mg/L of dissolved Cr; the concentrations of genuine steel mill wastewater are shown in table 6.2. The latter contains Mo, which does not occur in cationic but oxy-anionic form in solutions. Therefore, it cannot attach itself to silicate, which is a cation exchanger. However, under suitable conditions, Mo-ions can be engaged with iron-hydroxides. At a pH of 8, Mo-ions linked directly to the ferrugo-induced magnetic network.

The main problem with these magnetic carriers is the instability of pH. At times, pH appeared stable and coagulation worked well, but after a couple of hours, pH decreased because metal-hydroxides precipitated. This could cause the magnetite-silicate network to break up and desorption of dissolved metals to occur. To an extent, this happened with the genuine steel mill wastewater, and the results thereof are not very reliable. The problem can be solved by adjusting pH over long time periods while simultaneously stirring the solution vigorously.

Results of genuine wastewater separation were not satisfactory because of the above pH stability problems. Only Mo-ions behaved as expected because, attached to ferrugo, they did not detach themselves from silicate when desorption occurred at a lower pH. Fig. 6.8 shows Mo-concentrations after separation together with Cr-concentrations of laboratory-made wastewater. The water flow velocity through the separation zone was 4.5 L/min for genuine and 7.0 L/min for laboratory-made wastewater. AAS spectrophotometer was used for analysis. At 3 T, the Cr concentration in synthetic wastewater dropped to 18% of the original whereas the Mo concentration showed an equally linear decrease after dropping quite rapidly to 6.2 mg/L at 1 T.

TABLE 6.2
HEAVY METAL CONCENTRATIONS IN ORIGINAL STEEL MILL WASTEWATER

Elements	Concentration before separation
Solid matter [mg / L]	8.8
Dissolved Cr [mg / L]	0.13
Dissolved Ni [mg / L]	<0.01
Dissolved Fe [mg / L]	0.05
Dissolved Mo [mg / L]	9.8
Total Cr [mg / L]	0.25
Total Ni [mg / L]	0.04
Total Fe [mg / L]	0.39
Total Mo [mg / L]	9.8

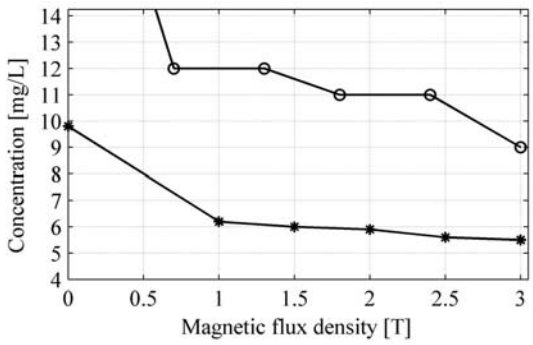

Fig. 6.8. A summary of results of the first separation tests. Symbols * and o correspond to Mo and Cr, respectively. Initial concentrations were Cr: 25 mg/L and Mo: 9.8 mg/L

In the second test session, an Nb_3Sn magnet was used and the pipe division changed to 25/75. Fig. 6.9 explains why the 25/75 division was tested here. Theoretically, 25/75 should yield better results than 50/50. Moreover, as the used Nb_3Sn superconducting wire had better current carrying characteristics than the NbTi one, higher magnetic flux density was expected of the Nb_3Sn-magnet. What happened was that the NbTi magnet performed better, and the 25/75 division gave rather unexpected results on separation efficiency.

NbTi-magnet reached 3.0 T, while the Nb_3Sn one performed well only up to 2.5 T, which was half of the expected value. Poor performance was related to the problems in coil manufacturing. The first reason was poor quality of the winding process. Also the used wax-based impregnation left the outermost layers of the coil too loose. At low temperatures even a slight movement of wire can release enough energy to raise the temperature over the critical temperature of the superconductor. Then the wire becomes normal conducting and transport current generated substantial amount of heat. Then the operating current, and thereby **B**, has to be lowered to zero to prevent damage to the coil [129]. This kind of sudden transition to normal conducting state was encountered above 2.5 T. Secondly, making of a magnet from Nb_3Sn requires a heat treatment that produces the superconducting phase in the wire. Heat treatment for the coil lasted about a month and temperature should be kept all the time within ±1 °C from the set point. Even a slight variation from the predetermined heat treatment program can result in imperfect formation of the superconducting Nb_3Sn phase.

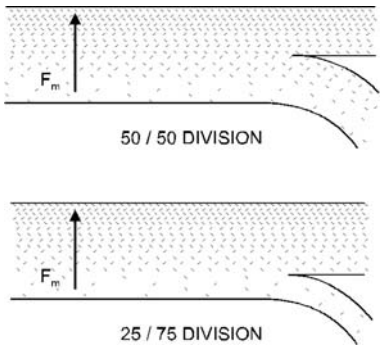

Fig. 6.9. Difference between pipe divisions 50/50 and 25/75. The catchment drops to half with 25/75 though cleaner samples are expected.

In the second session, only synthetic wastewater was tested because the steel-mill laboratory was not able to properly analyse the genuine waters. Already at the lowest magnetic flux density, 0.5 T, their concentrations dropped to about 60% of the initial value (see table 6.10). With increasing flux density, separation improved linearly, except in the case of Fe, whose concentration remained at 15 mg/L likely because the analytical grade chemicals used to build up the ion and magnetite network contained traces of Fe, which the AAS detected. Ni-ions separated in largest quantities: at the highest attained magnetic flux density, the Ni concentration dropped to 44% of the original. In the same magnetic field, the Cr-ion concentration dropped to 52%. In comparison, the first tests run with the NbTi magnet and 50/50 pipe division showed at 2.5 T a 2 mg/L better result for Cr. However, compared with Ni separation results, we can see that the result here was the same: after separation, concentrations were the same 11 mg/L for Ni-ions in the second session and for Cr-ions in the first session.

Interestingly, flow velocity variations had no observable effect on separation results, which were obtained at a flow velocity of 3 L/min. Increasing the velocity to 6 L/min affected only Fe

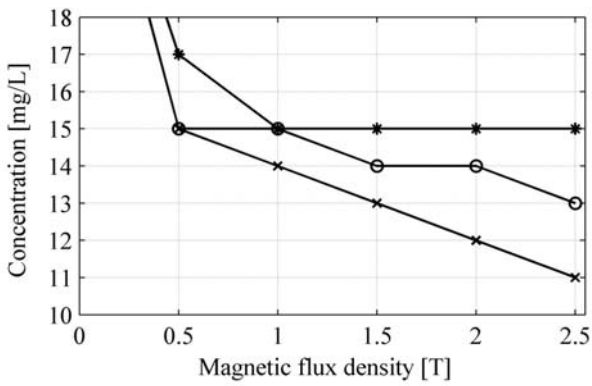

Fig. 6.10. Test results of the second separation tests. Symbols *, o, and x correspond to Fe, Cr, and Ni, respectively. The initial concentrations of all heavy metals were 25 mg/L.

concentrations by one mg/L. In addition, the 50/50 pipe division gave better results though the opposite was expected. Perhaps because inhomogeneously distributed in the volume, magnetite particles behaved unexpectedly in the turbulent conditions of the separation pipe.

6.4 Concluding remarks

In this chapter, magnetic separation of wastewaters containing heavy metals was studied with an open-gradient separator applying interchangeable pairs of NbTi and Nb_3Sn coils. The separator was designed and constructed during the project. In dissolved, that is, ionic form, heavy metals could be separated if they were first absorbed to a chemically-made magnetite-silicate network. The first test session with laboratory-made synthetic wastewater containing 25 mg/L of chromium showed 64% separation efficiency. The first tests with genuine steel mill wastewater did not work out as planned though molybdenum concentrations dropped to 56% of the original, and the concentration decreased linearly with magnetic field density. In the second test session, three wastewater batches containing 25mg/L of dissolved Ni, Cr, and Fe, respectively, were tested with a Nb_3Sn magnet with a **B** of up to 2.5 T. Results showed that already at 0.5 T heavy metal concentrations dropped to 60% of the original, and that at increased flux density, the concentrations decreased linearly. Therefore, superconducting magnetic separation is a promising alternative to conventional methods in large-scale wastewater processing. However, for the pursuit of internal water circulation, the OGMS-type separator is not the best alternative, since it only deflects the particles to the other side in the fluid stream. That way the particles are not removed, which would be necessary for continuous operation in an industrial plant. Therefore, other type of separator device is needed that could be, for example, a dry-type OGMS or high-gradient separator with cleanable filter, that is, a matrix-element.

Chapter 7

CONCLUSIONS

Recent successful medium-scale demonstrations have proved the technical feasibility of high temperature superconducting (HTS) devices in electrical power engineering. Now that these technologies are about to enter the market, it is not enough that the technology itself is studied in detail. The scientific community should pay special attention to the impacts of the new technology on society at large to lower the threshold from high quality prototype to commercial product and to avoid unpleasant surprises after its commercialization. For example, not until the 1970s were the CFC refrigerants seen as anything but miraculous substances, chemically inert, and inexpensive to produce. Similar notions persisted about SF_6 until the 1990s. Then CFCs suddenly appeared devastating to stratospheric ozone that protects us from solar radiation, and SF_6 turned out to have the highest global warming potential of all gases.

Though superconducting devices do not need any special chemicals, we would yet be well advised to find out the impacts these devices have on the environment. This thesis brought to light these impacts by following the framework of its four guiding, driving forces. First, it analyzed the production of superconductors with the aid of comparative LCA of conventional copper wire and

superconducting wire. Second, it evaluated the potential of HTS machinery to reduce emissions in European Union and particularly Finnish electrical networks. Then, LCA was applied to compare battery-based and superconducting energy storage solutions and cable systems in future distributed generation networks. Finally, the thesis demonstrated experimentally that superconducting magnetic separation harbors considerable potential for large-scale wastewater treatment.

The EuP directive calls for environmental assessment by manufacturers of electrical devices. The LCA made of superconductors in this thesis provides a good framework for device manufacturers to continue towards full environmental assessment of their particular devices. Note though that since this study focused only on the OK42 superconductor, its results are directly applicable only to MRI devices, which make use of this wire. In other devices, the proportions of NbTi and copper vary in the wire and should be observed in calculations. However, according to the data in this thesis, any combination of NbTi and copper in the finished wire is acceptable, and LCA can be conducted without difficulty.

The Kyoto protocol requires an enhancement in energy production efficiency. Because superconducting electrical machinery can operate at efficiencies higher than conventional devices, this thesis focused on the emission reduction potential of the former and found that up to 48% of the Kyoto target could be met with HTS-machinery. However, under free market conditions, HTS devices could not appreciably penetrate the market during the Protocol period. Yet this part of the study provides device manufacturers with important information about the break-even powers they could pursue. In addition, according to sensitivity analysis, it is more worthwhile to raise the efficiency of HTS devices than to aim at large production volumes.

DG networks have been proposed especially to satisfy the electricity needs of developing countries, which lack extensive power networks. In developed countries, DG would add to the versatility of energy sources and serve as platform for new technology. This study sought first to phase out irrelevant applications and then compare suitable superconductor applications with practicable solutions in the light of product life-cycles. The study concluded that of all superconducting power applications, only HTS SMES, flywheels with HTS bearings, and HTS cables were suitable for DG networks. However, among the non-superconducting applications only electrochemical batteries and power cables were suitable for comparative life-cycle assessment. While flywheels proved superior to conventional lead-acid batteries, they were equally competitive with the prospective vanadium-redox batteries, and SMESs were not competitive with any of the above in terms of their

environmental burden. However, since power quality issues are crucial in DG networks, SMES may emerge as a potential option because environmental issues are only one set of conditioning factors in developing future energy systems. On the other hand, cables appear as the most promising superconducting power application, and their potential role in DG networks is significant, because they boast low losses in areas where overhead lines are not practical and where distances are short. In terms of commercialization, a lot depends on the development of the 2G HTS wire.

For effective removal of concentrated materials from fluid streams, a superconducting magnetic separator was constructed and tested at our laboratory. With the aid of analytical grade chemicals, dissolved heavy metal ions in both steel mill and laboratory-made wastewater were attached to larger magnetic particles, which in turn were removed with the separator. Much work remains to be done to achieve ~100% separation efficiency, which is possible, though not with the OGMS-separator, which was constructed mainly to measure and obtain information about the separation of different materials.

In conclusion, the environmental impacts of superconducting power applications on society as a whole were of minor significance in this study. Conventional power applications are efficient, reliable, and relatively economical, because over the past century they have been extensively researched and developed. The drivers of superconductivity overriding in importance the environment are power quality issues, possible capital cost savings, and special applications, in which superconductivity becomes an enabling technology. In the power sector, the last mentioned include FCLs above 110 kV, fast-acting SMESs, and magnetic separators operating at above 2 T. In 1969, it was possible to send a man to the moon because enough political will-power was packed behind the Apollo space program. Similarly, if we applied all the available means to reduce environmental burdens from human activity, without interfering with economic growth, then in the spirit of ’69, superconducting power applications could be easily commercialized in the next decade. But only thorough techno-economical analysis would give us any certainty as to the practicality of the effort.

References

[1] ABB Ltd., Affolternstrasse 44, P.O. Box 8131, CH-8050 Zurich, Switzerland.
[2] ABB Motors & Drives, P. O. Box 603, 65101 Vaasa, Finland.
[3] R. Ackermann, *et al*., “Testing of a 1.8 MVA High Temperature Superconducting Generator”, *presented at the IEEE Power Engineering Soc. Annual Meeting, Emerging Technologies Panel Session*, Toronto, Canada. 2003.
[4] Adato Energia Oy, Mannerheimintie 76 A, 00101 Helsinki, Finland.
[5] M. Ahoranta, J. Lehtonen, R. Mikkonen, “Magnet Design for Superconducting Open Gradient Magnetic Separator,” *Physica C*, **386**, pp. 398-402, 2003.
[6] Alstom Power Corporation, 25 Avenue Kleber, 75795 Paris, France.
[7] American Electric Power, *2001–2002 Corporate Environmental Performance Report*, 2003. Available on-line at: http://www.aep.com/environmental/performance/envreport/Ceres.pdf.
[8] American Superconductor Corporation, Two Technology Drive, Westborough, MA, USA.
[9] R. U. Ayres, *Life Cycle Analysis: a Critique*. Working paper, INSEAD Centre for Management of Environmental Resources, Fontainebleau, France, 1994.
[10] J.-H. Bae, *et al*., "The Fabrication of Superconducting Magnet for MRI", *Physica C*, **372-376**, pp. 1342-1345, 2002.
[11] M. Bayergan, “A Vision of the Future Grid”, *IEEE Power Engineering Review*, **12**, pp. 10–12, 2001.
[12] J. Boehm, “Magnetic Separation – Superconductivity in Industry”, *IEEE Transactions on Applied Superconductivity*, **10**(1), pp. 710–715, 2000.
[13] C. M. Braams, P. E. Stott, *Nuclear Fusion – Half a Century of Magnetic Confinement Fusion Research*. IoP Publishing: Bristol, 2002.
[14] E. Brandt, “The Flux Line Lattice in Superconductors”, *Rep. Prog. Phys.* **58**, pp. 1465–1594, 1995.
[15] K. H. Bruch, D. Gohlke, *et al*. "Sachbilanz einer Ökobilanz der Kupfererzeugung und -verarbeitung", *Metall*, **49** pp. 252–257 & 318–324, 1995.
[16] E. Bryant, *Climate Process and Change*. Cambridge University Press: Cambridge, UK, 1997.
[17] P. Busquin in *Foreword from the Commissioner*, *New ERA for electricity in Europe – Distributed Generation: key issues, challenges and proposed solutions*. Luxembourg, 2003.
[18] Cambior Inc., *Environmental Performance Report of Niobium mining*. Longueuil, QC, Canada, 2000.
[19] P. C. Canfield, *et al*. “An overview of the basic physical properties of MgB_2”, *Physica C*, **385**, pp. 1–7, 2003.
[20] CBMM – Comphania Brasileira de Metallurgia e Mineracao, Araxa, Brazil.
[21] A. Chiba, *et al*., “Removal of Arsenic from Geothermal Water by High Gradient Magnetic Separation”, *IEEE Transactions on Applied Superconductivity*. **12**(1), pp. 952-954, 2002.
[22] Columbus Superconductors srl, Corso Perrone 24, 16152 Genova, Italy.
[23] T. A. Coombs in *Superconducting Magnetic Bearings*, *Handbook of Applied Superconductivity*. Vol. **2**, pp. 1441–1460. IoP Publishing: London, 1998.
[24] S. Crozier, D. M. Doddrell, "Compact MRI Magnet Design by Stochastic Optimization", *Journal of Magnetic Resonance*, **127**, pp. 233-237, 1997.
[25] Y. M. Dai, *et al*., ”Experimental Study on Chinese High-Sulphur Coal Cleaning by Superconducting High Gradient Magnetic Separation”, *Proceedings of the Low Temperature Engineering and Cryogenics conf.*, pp. p.03.3/1–5, 1990.
[26] Database of Environmental Load of 4000 Social Stocks, *Titanium*. Ecomaterials Center of Japanese National Institute for Materials Science, 1-2-1 Sengen, Tsukuba, Ibaraki 305–0047, Japan, 2003.
[27] R. M. Day, *Beyond Eco-Efficiency: Sustainability as a driver for innovation*. World Resources Institute (WRI): Washington, D.C., USA, 1998.
[28] R. Dhingra, J. G. Overly, G. A. Davis, *Life-cycle Environmental Evaluation of Aluminium and Composite Intensive Vehicles*. Report prepared for Oak Ridge National laboratory. Oakridge, TN, 1999.
[29] Directive of the European Parliament and of the Council, *On Establishing a Framework for the Setting of Eco-Design Requirements for Energy-Using Products and Amending Council Directives 92/42/EEC, 96/57/EC and 2000/55/EC*. Brussels, 2004.
[30] G. Donnier-Valentin, P. Tixador, “Considerations about HTS Superconducting Transformers”, *IEEE Transactions on Applied Superconductivity*, **11**(1), pp. 1498–1501, 2001.
[31] J.-L. Duchateau in *Superconducting Magnets for Thermonuclear Fusion*, *Handbook of Applied Superconductivity*. Vol. **2**, pp. 1261–1288. IoP Publishing: London, 1998.
[32] Edison S. p. A. Foro Buonaparte, 31, 20121 Milan, Italy.
[33] Endesa S. A. c/o Principe de Vergara, 187, 28002 Madrid, Spain.
[34] J. T. Eriksson, R. Mikkonen, J. Paasi, R. Perälä, L. Söderlund, ”A HTS synchronous motor at different operating temperatures”, *IEEE Transactions on Applied Superconductivity*, **7**, pp. 523–526, 1997.
[35] European Commission, *The Scope of Energy Saving in the EU Through the Use of Energy-efficient Electricity Distribution Transformers*. European Communities, 1999.

[36] European Commission, "EU average load factor of nuclear power generators", *Annual Energy Review,* 2001.
[37] D. Feng, C. Aldrich, H. Tan, "Removal of Heavy Metal Ions by Carrier Magnetic Separation of Adsorptive Particulates", *Hydrometallurgy*, **56**(3), 359–368, 2000.
[38] Y. Feng, *et al*., "High critical current density in MgB_2/Fe wires", *Physica C*, **406**, pp. 121–130, 2004.
[39] M. Frank, J, Frauenhofer, P. van Hasselt, W. Nick, H. W. Neümuller, G. Nerowski, "Long-term Operational Experience with first Siemens 400 kW HTS Machine in Diverse Configurations", *IEEE Transactions on Applied Superconductivity*, **13**, pp. 2120–2123, 2003.
[40] M. Franzreb, W. H. Höll, "Phosphate Removal by High-gradient Magnetic Filtration Using Permanent Magnets", *IEEE Transactions on Applied Superconductivity*, **10**(1), pp. 923–926, 2000.
[41] K. Funaki, *et al*., "Development of a 500-kVA-class Oxide-superconducting Power Transformer Operated at Liquid Nitrogen Temperature", *Cryogenics*, **38**, pp. 211–220, 1998.
[42] J. Gerhold in *Power Transmissions*, *Handbook of Applied Superconductivity*. Vol. **2**, pp. 1627–1690. IoP Publishing: London, 1998.
[43] J. Goerten, E. Clement, "Electricity prices for EU households on 1 July 2004", *Eurostat / Energy*, European Communities, 2004.
[44] G. Gillet, F. Diot, M. Lenoir, "Removal of Heavy Metal Ions by Superconducting Magnetic Separation", *Separation Science & Technology*, **34**(10), pp. 2023–2037, 1999.
[45] W. V. Hassenzahl, "Superconducting magnetic energy storage", *Proceedings of the IEEE*, **71**, pp. 1089–1098, 1983.
[46] W. V. Hassenzahl, D. W. Hazelton, B. K. Johnson, P. Komarek, M. Noe, C. Reis, "Electric Power Applications of Superconductivity", *Proceedings of the IEEE*, **92(10)**, pp. 1655–1674, 2004. References therein.
[47] J. T. Houghton, L. G. Meira Filho, J. Bruce, H. Lee, B. A. Callander, E. Haites, N. Harris, K. Maskel, *Climate Change 1994, Radiative Forcing of Climate Change and an Evaluation of the IPCC IS92 Emission Scenarios*, published for the Intergovernmental Panel on Climate Change, pp. 222. Cambridge University Press, UK, 1995.
[48] J. R. Hull in *Flywheels, The Encyclopedia of Energy* (ed. Cutler J. Cleveland) Vol. **2**, pp. 695–704. Elsevier Academic Press: San Diego, CA, USA, 2004.
[49] V. J. Inglezakis, A. A. Zorpas, M. D. Loizidou, H. P. Grigoropoulou, "Simultaneous Removal of Cu2+, Fe3+ and Cr3+ with Anions (SO4)2- and (HPO4)2- Using Clinoptilolite", *Mikroporous and Mesoporous Materials*, **61**, pp. 167–171, 2003.
[50] B. In-Su, K. Jin-O, K. Jae-Chul, C. Singh, "Optimal Operating Strategy for Distributed Generation Considering Hourly Reliability Worth", *IEEE Transactions on Power Systems*, **19**, pp. 287–292, 2004.
[51] International Council on Large Electric Systems (CIGRE), *Recommendations for SF_6 gas recycling*. References can be found from http://www.cigre-sc23.org/SF6/index.htm.
[52] International Energy Agency, *Implementing Agreement for a Cooperative Programme for Assessing the Impacts of High-Temperature Superconductivity on the Electric Power Sector*, 1990–2010.
[53] International Organization for Standardization, *ISO 14040 – Life Cycle Assessment*. Barrow, UK, 1996.
[54] Y. Iwasa, *Case Studies in Superconducting Magnets – Design and Operational Issues*. Definition of irreversibility field, pp. 405. Plenum Press, New York, USA, 1994.
[55] Y.-S. Jo, *et al*., "High Temperature Superconducting Synchronous Motor", *IEEE Transactions on Applied Superconductivity*, **12**(1), pp. 833–836, 2002.
[56] S. Kalsi, "Development Status of Superconducting Rotating Machines", in *IEEE Power Engineering Society Meeting 27–31 January*, pp. 401–403, New York, 2002.
[57] H. Kamerlingh-Onnes, "The Superconductivity of Mercury", *Comm. Phys. Lab. Univ. Leiden*, Nos. 122–124, 1911.
[58] N. Karapinar, "Magnetic Separation of Ferrihydrite from Wastewater by Magnetic Seeding and High-gradient Magnetic Separation", *International Journal of Mineral Processing*, **71**, pp. 45–54, 2003.
[59] Y. Kito, H. Okubo, N. Hayakawa, Y. Mita, M. Yamamoto, "Development of a 6600 V/210 V 100 kVA Hybrid-type Superconducting Transformer", *IEEE Transactions on Power Delivery*, **6**(2), pp. 816–823, 1991.
[60] H. Köfler in *Generators with Superconducting Field Windings*, *Handbook of Applied Superconductivity*. Vol. **2**, pp. 1497–1547. IoP Publishing: London, 1998.
[61] D. Larbalestier, A. Gurevich, D. Matthew Feldmann, A. Polyanskii, "High-T_c Superconducting Materials for Electric Power Applications", *Nature* **414**, pp. 368–377, 2001. References therein.
[62] Y. Laumond in *Transformers*, *Handbook of Applied Superconductivity*. Vol. **2**, pp. 1613–1626. IoP Publishing: London, 1998.
[63] J. Lehtonen, "AC Losses and Stability of High Temperature Superconducting Magnets", Tampere University of Technology Publications 306, 2000.
[64] J. Lehtonen, *et al*. "Design and Demonstration of Superconducting Power Link", *IEE Proceedings Generation, Transmission & Distribution*, **151**(6), pp.755–760, 2004.
[65] S. J. Lieberman, D. R. Kelland, "Magnetic Filtration of Aqueous Suspensions of Submicron Reactor Corrosion Products", *IEEE Transactions of Magnetics*, **MAG-20**(5), pp. 1195 – 1197, 1984.
[66] P. Magaud, G. Marbach, I. Cook in *Nuclear Fusion Reactors*, *The Encyclopedia of Energy* (ed. Cutler J. Cleveland) Vol. **4**, pp. 365–381. Elsevier Academic Press: San Diego, CA, USA, 2004.

[67] A. P. Malozemoff, *AMSC Second Generation HTS Wire – an Assessment*. American Superconductor Corporation, USA; 6/2004. Available on-line at: http://www.amsuper.com/documents/2GWhitePaper-July04_002.pdf.
[68] T. Masuda, *et al*. ”Experimental Results of a 30 m, 3-core HTSC Cable”, *Physica C*, **372–376**(3), pp. 1555–1559, 2002.
[69] B. McConnell, “Transformers – A Successful Application of High Temperature Superconductors”, *IEEE Transactions on Applied Superconductivity,* **10**(1) pp. 716–720, 2000.
[70] R. Mikkonen, “Highlights of SC Power Applications in Europe”, *IEEE Transactions on Applied Superconductivity*, **12**, pp. 782–787, 2002.
[71] R. Mikkonen, T. Kalliohaka, A. Korpela, J. Lehtonen, R. Perälä, ”A 0.2 MJ Cryogen Free Nb_3Sn SMES in UPS Application”, *Superconductor Science & Technology*, **16**, pp. 946–950, 2003.
[72] R. Mikkonen, L. Söderlund, "A 6 T Superconducting Wiggler for Synchrotron Radiation", *IEEE Transactions on Magnetics,* **32**, pp. 2617-2620, 1996.
[73] J. Mulholland, T. Sheahen, B. McConnell, *Analysis of Future Prices and Markets for High-Temperature Superconductors*. U.S. Department of Energy: Oakridge, TN, USA, 2003.
[74] K. Müller, J. Bednorz, “The Discovery of a Class of High Temperature Superconductors”, *Science* **237**, pp. 1133–1137, 1987.
[75] W. H.-G. Müller, D. Höpfel in *Magnetic Resonance Imaging and Spectroscopy (Medical Applications)*, *Handbook of Applied Superconductivity*, Vol. **2**, pp. 1213-1249. IoP Publishing: Bristol, UK, 1998.
[76] K. Mäkelä, J. Laurikko, H. Kanner, *Road Traffic Exhaust Gas Emissions in Finland. LIISA 2003 Calculation Software*, Technical Research Centre of Finland, Building and Transport, Research Report RTE 2814/04, 2004.
[77] W. Nick, K. Prescher, “Basic Design Considerations for a Medium-size Superconducting Magnetic Energy Storage System (SMES)”, *IEEE Transactions on Magnetics*, **32**, pp. 2268–2271, 1996.
[78] Nord Pool ASA Electricity Exchange, Oslo, Norway. *Spot price of a CO_2-ton allowance*, 11.10.2005.
[79] Outokumpu Poricopper Corp., Kuparitie, Pori, Finland.
[80] Outokumpu Poricopper Corp. *Environmental Report of Superconductor manufacturing plant*. Pori, Finland, 2002.
[81] J. Paasi, *et al*., ”Design and Performance of a 5 kJ HTS μ-SMES”, Advances in Cryogenic Engineering, Proceedings of the 1999 Cryogenic Engineering Conference, July 12-15, 1999, Montreal, Canada, **45**(A), pp. 779–786, 2000.
[82] O. Peralez-Perez, Y. Umetsu, H. Sasaki, “Precipitation and Densification of Magnetic Iron Compounds from Aqueous Solutions at Room Temperature”, *Hydrometallurgy*, **50**(3), pp. 223–242, 1998.
[83] Pirelli Cables and Systems Inc., PL 13, 02401 Kirkkonummi, Finland.
[84] J. Pitel, F. Chovanec, V. Hencl, “Application of Superconducting Magnet Systems to dry Magnetic Separation of Coal,” Magnetic and Electrical Separation, **4**(2), pp. 19–29, 1992.
[85] H. B. Püttgen, P. R. MacGregor, F. C. Lambert, “Distributed Generation: Semantic Hype of the Dawn of a New Era?”, *IEEE Power & Energy Magazine*, **1–2**/03, pp. 22–29, 2003.
[86] The Quantum Technology Corporation, *Brochure of Nitrogen Liquefier*, 1999.
[87] G. Ries, H. W. Neumüller, “Comparison of Energy Storage in Flywheels and SMES”, *Physica C*, **357–360**, pp. 1306–1310, 2001.
[88] P. H. Roberts, P. H. Diamond in *Magnetohydrodynamics, The Encyclopedia of Energy* (ed. Cutler J. Cleveland) Vol. **3**, pp. 705–732. Elsevier Academic Press: San Diego, CA, USA, 2004.
[89] H. Rogalla, J. Flokstra in *Josephson junctions*, *SQUID sensors*, *Handbook of Applied Superconductivity*. Vol. **2**, pp. 1757–1794. IoP Publishing: London, 1998.
[90] C.-J. Rydh, “Environmental Assessment of Vanadium Redox and Lead-acid Batteries for Stationary Energy Storage”, *Journal of Power Sources*, **80**, pp. 21–29, 1999.
[91] C. Sagan, *Cosmos*. Ballantine Books: New York, USA, 1980.
[92] N. Saho, H. Isogami, T. Takagi, M. Morita, “Continuous Superconducting-magnet Filtration System”, *IEEE Transactions on Applied Superconductivity,* **9**(2), pp. 398–401, 1999.
[93] S. Schoenung *Characteristics and Technologies for Long-vs. Short-Term Energy Storage — A Study by the DOE Energy Storage Systems Program*. SAND 2001-0765. Sandia National Laboratories, USA; 3/2001. Available on-line at http://infoserve.sandia.gov/sand_doc/2001/010765.pdf
[94] L. Schwartzkopf, J. Jiang, X. Cai, D. Apodaca, D. Larbalestier, “The use of the in-field critical current density J_C(0.1T), as a better descriptor of $(Bi,Pb)_2Sr_2Ca_2Cu_3O_x$/Ag tape performance”, *Appl. Phys. Lett.* **75**, 3168–3170, 1999.
[95] S. Schwenerly, et. al. “Performance of a 1-MVA HTS Demonstration Transformer”, *IEEE Transactions on Applied Superconductivity*, **9**(2), pp. 680–684, 1999.
[96] B. Seeber, *Handbook of Applied Superconductivity*. IoP Publishing: London, 1998.
[97] J. Seppälä, S. Koskela, M. Melanen, M. Palperi, "The Finnish Metals Industry and the Environment," *Resources, Conservation and Recycling*, **35**, pp. 61–76, 2002.
[98] R. Silberglitt, E. Ettedgui, A. Hove, “Strengthening the Grid: Effect of High-Temperature Superconducting Power Technologies on Reliability, Power Transfer Capacity and Energy Use”, *MR-1531-DOE*. RAND Science and Technology: USA, 2002. Available on-line at http://www.rand.org/publications/MR/MR1531/

[99] K. Sipilä, M. Vistbacka, A. Väätäinen, “Electricity Storing with Compressed Air Energy Storage”, Technical Research Centre of Finland (VTT), *VTT Research Notes* 1516, Espoo Press: Finland, 1993.
[100] E. Sissimatos, G. Harms, B. R. Oswald, ”Optimization of High-Temperature Superconducting Power Transformers”, *IEEE Transactions on Applied Superconductivity*, **11**(1), pp. 1574–1577, 2001.
[101] P. F. Smith, B. Colyer, "A Solution to the 'Training' Problem in Superconducting Magnets", *Cryogenics* **15**, pp. 201–207, 1975.
[102] V. Sokolovsky, V. Meerovich, I. Vajda, V. Beilin, “Superconducting FCL: Design and Application”, *IEEE Transactions on Applied Superconductivity*, **14**(3), pp. 1990–2000, 2004. References therein.
[103] J. V. Spandero, L. Langlois, B. Hamilton, “Assessing the Difference: Greenhouse-gas Emissions of Electricity Generation Chains”, IAEA Bulletin, **42**(2), pp. 19–24, 2000.
[104] Statistics Finland, *Energy Statistics 2000*. University Press, Helsinki, Finland, 2001.
[105] H. Stiller, *Material Intensity of Advanced Composite Materials*. Germany: Wuppertal Institute publication 90/1999.
[106] J. P. Stovall, *et al*. ”Operating Experience with the Southwire 30-meter High Temperature Superconducting Power Cable”, *Advances in Cryogenic Engineering*, **47**(A), pp. 591–598, 2002.
[107] M. Suenaga, A. Ghosh, Y. Hu, D. Welch, “Irreversibility Temperatures of Nb_3Sn and Nb-Ti”, *Physical Review Letters,* **66**, pp. 1777–1780, 1991.
[108] J. Svoboda, *Magnetic Methods for the Treatment of Minerals*. Elsevier, Amsterdam, The Netherlands, 1987.
[109] Teollisuuden Voima Oy Ltd., FIN-27160 Olkiluoto, Finland.
[110] D. R. Tilley, J. Tilley, *Superfluidity and Superconductivity*. 2nd ed., Adam Hilger Ltd., Bristol, UK, 1986.
[111] P. Tixador in *Fully Superconducting Generators*, *Handbook of Applied Superconductivity*. Vol. **2**, pp. 1553–1578. IoP Publishing: London, 1998.
[112] P. Tixador, H. Daffix, “Conceptual Design of an Electrical Machine with Both Low and High Tc Superconductors”, *IEEE Transactions on Applied Superconductivity*, **7**(4), pp. 3857–3865, 1997.
[113] W. Torres, *Reassessment of Superconducting Magnetic Energy Storage (SMES) Transmission System Benefits*, Electric Power Research Institute (EPRI) Technical Report no. 1 006 795, March 2002. References therein.
[114] O. Tsukamoto, “Ways for power applications of high temperature superconductors to go into the real world”, *Superconductor Science & Technology*, **17**, pp. S158–S190, 2004.
[115] J. Tuisku, *et al*., ”Cryogenic Design of an Isodynamic Magnetic Separator”, *IEEE Transactions on Applied Superconductivity*, **14**(2), pp. 1580–1584, 2004.
[116] K. Ueda, O. Tsukamoto, S. Nagaya, H. Kimura, S. Akita, “R&D of a 500 m Superconducting Cable in Japan”, *IEEE Transactions on Applied Superconductivity*, **13**(2), pp. 1946–1951, 2003. More references therein.
[117] The Union of Electricity Industry in Europe – Eurelectric, *Statistics and Prospects for the European Electricity Sector 1980 – 2020, EURPROG 2001*. 29th ed., 2001.
[118] United Nations Environment Programme (UNEP) Life Cycle Assessment: What it is and How to do it, UNEP Industry and Environment, 92 pages. Paris, France, 1996.
[119] United Nations Framework Convention on Climate Change (UNFCCC), *The Kyoto Protocol*. Kyoto, 1997.
[120] U.S. Environmental Protection Agency, *SF_6 Emission Reduction Partnership for Electric Power Systems*. On-line at: http://www.epa.gov/highgwp/electricpower-sf6/index.html.
[121] U.S. Congress, Office of Technology Assessment, *High-Temperature Superconductivity in Perspective, OTA-E-440*. U.S. Government Printing Office: Washington, D.C., USA, 1990.
[122] I. Vajda, *et al*., ”Operational Characteristics of Energy Storage High Temperature Superconducting Flywheels Considering Time Dependent Processes”, Physica C, **372–376**, pp. 1500–1505, 2002.
[123] I. Vajda, A. Györe, A. Szalay, V. Sokolovsky, W. Gawalek, ”Improved Design and System Approach of a Three Phase Inductive HTS Fault Current Limiter for a 12 kVA Synchronous Generator”, *IEEE Transactions on Applied Superconductivity*, **13(2)**, pp. 2000–2003, 2003.
[124] R. Van Berkel, "Life Cycle Assessment for Environmental Improvement of Minerals' Production," *Environment Workshop, Minerals Council of Australia*, October 2000.
[125] G. Vanderplaats, *Numerical Optimization Techniques for Engineering Design*. pp. 241-247, VR&D: Colorado Springs, CO, USA, 1999.
[126] J. Vlach, K. Singhal, *Computer Methods for Circuit Analysis and Design*. Van Nostrand-Reinhold Press: New York, USA, 1983.
[127] Wah Chang – Allegheny Technologies Inc., Albany, OR, USA.
[128] D. W. Willen, *et al*., ”Test Results of Full-scale HTS Cable Models and Plans for a 36 kV, 2 kA_{rms} Utility Demonstration”, *IEEE Transactions on Applied Superconductivity*, **11**, pp. 2473–2476, 2001.
[129] M. Wilson, *Superconducting Magnets*. Clarendon Press: Oxford, UK, 1997.
[130] A. M. Wolsky, *The likely Impacts on Environment, Safety, and Health from the Power Sector’s Future, Widespread Use of Superconducting Equipment*, a report for the IEA Group (see reference [52]), Argonne National Laboratory, USA, 1999.
[131] A. M. Wolsky, *The status of progress toward flywheel energy storage systems incorporating high-temperature superconductors*. A report for the IEA group (see reference [52]), Argonne National Laboratory, USA, 2000.

[132] A. M. Wolsky, *Today's Explorations Bearing Upon the Private Sector's Future Use of Magnets Incorporating High-Temperature Superconductors*, a report for the IEA group (see reference [52]), Argonne National Laboratory, USA, 2001.
[133] A. M. Wolsky, *HTS cable – Status, Challenge and Opportunity*, a report for the IEA Group (see reference [52]), Argonne National Laboratory, USA, 2004.
[134] K. Yamaguchi, *et al*., "70 MW Class Super-conducting Generator Test", *IEEE Transactions on Applied Superconductivity*, **9**, pp. 1209–1212, 1999.
[135] Y. Zhang, *et al*., "High critical current density $YBa_2Cu_3O_{7-x}$ thin films fabricated by ex-situ processing at low temperatures", *Superconductor Science&Technology*, **17**, pp. 1154-1159, 2004.

Publication **I**

T. Hartikainen, J. Lehtonen and R. Mikkonen

"Role of HTS Devices in Greenhouse Gas Emissions Reduction"

Superconductor Science & Technology, **16**, pp. 963-969, 2003.

INSTITUTE OF PHYSICS PUBLISHING SUPERCONDUCTOR SCIENCE AND TECHNOLOGY

Supercond. Sci. Technol. **16** (2003) 963–969 PII: S0953-2048(03)62740-5

Role of HTS devices in greenhouse gas emission reduction

Teemu Hartikainen, Jorma Lehtonen and Risto Mikkonen

Institute of Electromagnetics, Tampere University of Technology, 33101 Tampere, Finland

Received 28 April 2003
Published 23 July 2003
Online at stacks.iop.org/SUST/16/963

Abstract
By applying high temperature superconductors (HTS) in generators, transformers and synchronous motors it is possible to improve their efficiency. Higher efficiency saves electrical energy and thus reduces greenhouse gas (GHG) emissions as well. The reduction of GHG emissions is becoming a topical issue due to the Kyoto Protocol which requires the European Union (EU) to reduce its emissions by 8% from the 1990 levels between 2008 and 2012. This environmental viewpoint can accelerate the commercialization of HTS applications if certain efficiency and sufficiently large power range are reached. In this paper, a detailed study about the replacement of existing devices by HTS ones is made in order to find the efficiency level and the power range where HTS becomes competitive. Finland is taken, as an example of an EU country, to present accurate figures of saved electricity. The structure of energy production and consumption was investigated and the emission data from different types of power plants were screened. The potential savings were allocated to the reduced usage of coal. Finally, an expanded view towards the possible emissions reduction gained by superconducting technology in the whole EU is presented. A market penetration model was introduced to investigate the time-scale in which conventional devices can be replaced with HTS devices.

1. Introduction

Recent successful demonstration projects of medium scale have shown the technical feasibility of high temperature superconducting (HTS) devices in electric power engineering [1, 2]. Now that these kinds of technologies are emerging into the market, it is not sufficient that the technology itself has been studied in detail. The scientific community should pay special attention to the impact of this new technology on the surrounding society in order to lower the step from a high quality prototype to the commercial product and to avoid any unpleasant surprises after the commercialization. So far, there have been only a few such studies of superconductor technology and they have received only a limited audience [3, 4]. In this paper, a method to analyse the role of HTS devices in greenhouse gas (GHG) emission reduction is presented.

Today it is unquestionable that the burning of fossil fuels increases the GHG content of the atmosphere. The major greenhouse gases from human activity in order of importance are: carbon dioxide (CO_2), methane (CH_4), nitrous oxide (NO_2) and halocarbons (CFCs) [5]. In 1997 the industrialized countries signed a contract called the Kyoto Protocol, which requires them to lower their GHG emissions by at least 5% below the level of 1990 between 2008 and 2012. The European Union (EU) agreed to 8% reductions and Finland, in particular, should freeze its GHG emissions to the level of 1990. The Kyoto Protocol states that an enhancement in energy efficiency should be exploited [6].

HTS provides one way to improve the energy efficiency. Energy will be saved by utilization of HTS-based generators, transformers and synchronous motors in power stations and heavy industry facilities. The commercialization of HTS transformers and rotating machines requires that they are superior to the conventional systems. Environmental viewpoints can help the breakthrough of HTS-based applications if certain efficiency and a sufficiently large power range are reached. Here a detailed study about the replacement of existing devices by HTS ones is made in order to find the efficiency level and the power range where HTS becomes competitive.

As an example of an EU country, the accurate figures of GHG emission reduction potential are set forth from Finland because the detailed statistical data of large electrical

Table 1. Efficiencies for conventional transformers and generators.

Transformers		Generators	
Power P_n (kVA)	Efficiency η_c	Power P_n (kVA)	Efficiency η_c
1	0.9100	500	0.960
5	0.9295	1000	0.966
10	0.9512	3000	0.970
50	0.9731	5000	0.973
100	0.9802	10 000	0.977
200	0.9818	15 000	0.980
500	0.9867	20 000	0.982
800	0.9877	40 000	0.984
1000	0.9900	60 000	0.985
10 000	0.9920	80 000	0.987
30 000	0.9933	100 000	0.988
50 000	0.9945	130 000	0.988
130 000	0.9949	250 000	0.988
250 000	0.9952	370 000	0.988
370 000	0.9956	500 000	0.988
500 000	0.9960	750 000	0.988
1 000 000	0.9977	1 000 000	0.988

machinery as well as the emission data were freely available. Finally, an expanded view towards the possible emission reduction achieved by HTS technology in the whole EU is presented. A comprehensive set of background information is presented to enable other analysts to repeat the calculations for their own countries.

2. Analysis

So far, the efficiency figures for future commercial HTS machinery cannot be precisely expressed because the efficiency depends on many different issues, such as material properties, tape geometry and cooling systems. Also in many cases it is not suitable to optimize the machine only for the lowest possible losses [7, 8]. Therefore, one aim of this study is to examine what efficiency these HTS machines should reach so that they could considerably save energy and GHG emissions. On the other hand, the efficiencies for conventional machinery, η_c , can be accurately given as a function of the rated nominal power. The efficiencies for transformers and generators as a function of their power are presented in table 1 [3][1,2]. Efficiency for synchronous motors, η_{sm}, can be given as

$$\eta_{sm}(P) = 1.667 \times 10^{-9} P + 0.955,$$

where P is nominal power in Watts[3]. For the study of achievable reduction in GHG emissions, the ratio of the losses in a HTS device to the losses in a corresponding conventional one, a, is used as a variable to express the efficiency of HTS devices, η_{sc}.

$$\eta_{sc} = 1 - a(1 - \eta_c). \tag{1}$$

HTS-based machinery is most competitive in systems with high nominal power. The break-even power, P_{be}, is defined so that it is reasonable to replace a conventional device i having nominal power $P_n^i \geqslant P_{be}$ with a superconducting one. However, P_{be} is not uniquely defined but it depends strongly on the optimization criteria. In general, P_{be} is different for transformers, generators and synchronous motors and it also depends on the application. For example, in transportation systems P_{be} is much lower than in stationary applications, because weight of the device plays a crucial role in moving systems [7]. In addition to the efficiency, P_{be} contributes strongly to the achievable reduction of GHG emissions. When the number of HTS devices replacing conventional devices in the power grid increases the total savings in electrical energy rise as well.

[1] Alstom Power Corporation, 25 Avenue Kleber, 75795 Paris, France.
[2] Muuntosähkö Oy–Trafox, Niittylänpolku 4, 00620 Helsinki, Finland.
[3] ABB Motors & Drives, PO Box 603, 65101Vaasa, Finland.

Table 2. GHG emissions from electricity production.

Energy vector	$e_k w_h$ (Direct)	$e_k w_h$ (In-direct)
Hard coal	790–1017	176–289
Natural gas	362–575	77–113
Hydro	0	4–236
Solar (photovoltaic)	0	100–280
Wind	0	10–48
Nuclear	0	9–21

The range of GHG emissions from electricity production in grams of CO_2 equivalent per kWh. The first values are direct emissions from burning and the second values indicate indirect emissions during life cycle. The exact value depends on the state of technology [8].

Next, the saved electricity is transformed to reductions in GHG emissions. The generation of electricity from fossil fuels is a significant source of GHG emissions. For example, the generation of electricity created 16.6 Mt of CO_2-eq. (megatonnes of CO_2-equivalent) or 22% of Finland's total 76 Mt of CO_2-eq. GHG emissions in the year 1999 [9]. When the use of electricity is more efficient, less energy needs to be produced. The maximum reduction in GHG emissions is achieved when the most polluting power plants are eliminated. Hard coal burning produces highest life-cycle emissions per generated kWh as can be seen from table 2. Coal-fired power stations worldwide consume over 2500 million tons of coal each year to produce 38% of the total generated electricity [10]. In Finland, the share of hard coal was 8.4 TWh or 10.6% [9, 11]. Therefore, it is clear that the proportion of hard coal in electricity generation shall be reduced. In this analysis, the saved energy is allocated for reduced use of hard coal and then converted to grams of CO_2-equivalent per kWh, which is a common way of reporting the GHG emissions. For hard coal, an average value of emissions per kWh, e_{kWh}, is 1 kg of CO_2-eq./kWh [10].

The total GHG emissions saved, e_{tot}, when all conventional devices having $P_n^i \geqslant P_{be}$, where P_n^i is the nominal power of device i, are replaced with superconducting ones are obtained from

$$e_{tot} = e_{kWh} T \sum_{i=1}^{N} P_{ave}^i \left(\eta_{sc}^i(a) - \eta_c^i\right), \tag{2}$$

where η_{sc}^i and η_c^i are the efficiencies of the superconducting and the conventional device i, respectively, P_{ave}^i is the average power delivered to the device i during the period of study T and N is the number of devices having $P_n^i \geqslant P_{be}$. Here generators, transformers and motors are arranged in decreasing order (i.e. $P_n^i \geqslant P_n^{i+1}$) and T is one year. Components of the electric

power grid are not loaded with the nominal power all the time. The average power delivered to the device i in a scale of one year, P^i_{ave}, is usually given as

$$P^i_{\mathrm{ave}} = k^i P^i_{\mathrm{n}}, \tag{3}$$

where k^i is the load factor of the device i. Together equations (2) and (3) yield

$$e_{\mathrm{tot}}(P_{\mathrm{be}}, a) = e_{\mathrm{kWh}} T \sum_{i=1}^{N} k^i P^i_{\mathrm{n}} \left(\eta^i_{\mathrm{sc}}(a) - \eta^i_{\mathrm{c}}\right). \tag{4}$$

An estimate about k^i for transformers is 0.4–0.6 and for synchronous motors is 0.75. Generators of nuclear power, hydroelectric and thermal power have an average $k^i = 0.94$, 0.59 and 0.36, respectively [9]. Here, the dependence of the average efficiency on the load factor is neglected.

To study what influence the variation of a and P_{be} have on the total GHG emissions saved, the concept of sensitivity needs to be introduced. The sensitivity of e_{tot} with respect to a variable x is defined as [12]

$$S^{e_{\mathrm{tot}}}_x = \frac{\mathrm{d}e_{\mathrm{tot}}/e_{\mathrm{tot}}}{\mathrm{d}x/x}$$

In this case x is either a or P_{be}. $S^{e_{\mathrm{tot}}}_{P_{\mathrm{be}}}$ is computed with finite differencing while $S^{e_{\mathrm{tot}}}_a$ can be calculated analytically from equation (4).

When equation (4) is applied the nominal power distribution of transformers and electrical machines must be known in detail before an accurate analysis about the influence of P_{be} and a on the reduction in GHG emissions can be made. In Finland, the electricity is generated by 875 power generators that have the rated nominal capacity totalling 17.2 GW. The ratings of transformers in electric power plants follow quite closely the ratings of the generators. The peak power of a certain transformer is just fixed slightly over the corresponding generator. Due to the need for many voltage levels in transmission grid, the total capacity of transformers is over five times higher than the capacity of generators. This also implies that there are significantly more devices on the lower end of the power scale. In total, there are 132282 transformers in Finland's power grid, the largest being 1000 MVA. Their total capacity is 94428 MVA.[4] Figure 1 presents the distribution of nominal power of generators and transformers in operation in Finnish power stations.

Industry consumes 53% of the total electricity supply and from this study's point of view, possible savings can be attributed to synchronous industrial motors. In the class over 1 MW, there are about 450 synchronous motors in operation in the Finnish industry with the combined power totalling 2.85 GW. The large number of powerful synchronous motors is due to the dominant position of paper industry in Finland. Large-scale wood processing requires lots of power with steady pace (see footnote 3).

Finally, the time-scale in which the conventional devices can be replaced with HTS ones is studied. Here only the replacement of existing devices is studied without examining the future market growth of electrical devices. The replacement rate of devices can be computed as a function of

[4] Adato Energia Oy, Mannerheimintie 76 A, 00101 Helsinki, Finland.

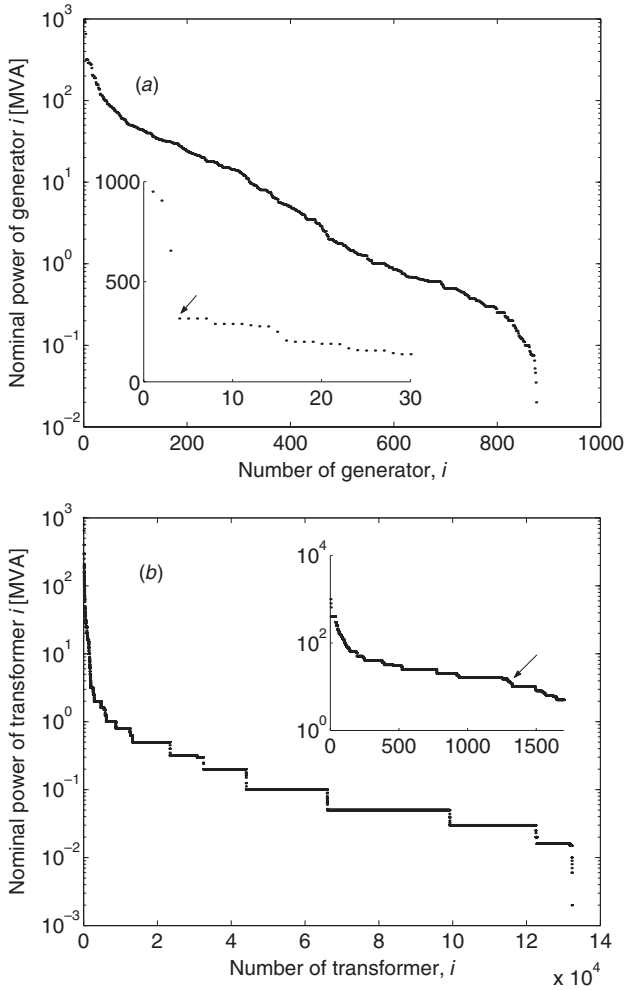

Figure 1. The nominal power of each (a) generator and (b) transformer operating in Finnish power grid. The inset is a zoom from the first values of the curve. The arrow points to the most sensitive power level.

time. The number of devices, N_{b}, which will be written off during year j (here j equals zero at the moment) is given as

$$N_{\mathrm{b}}(j) \approx \sum_{l=1}^{\infty} n_l \int_{l+j-1}^{l+j} f(T_{\mathrm{ave}}, \sigma_t)\,\mathrm{d}t, \tag{5}$$

where n_l is the number of devices installed l years ago, $\int_t^{t+\Delta t} f\,\mathrm{d}t$ is the probability that a device will be written off in the time interval $[t, t + \Delta t]$, T_{ave} and σ_t are the average value and the standard deviation of the lifetime. $N_{\mathrm{b}}(j)$ can be calculated after an equation for n_l is found. The total number of devices operating in the network at the moment, N, can be given as

$$N = \sum_{l=1}^{\infty} n_l F_l(T_{\mathrm{ave}}, \sigma_t), \tag{6}$$

where F_l is the probability that these devices are still operating. When the market increases $p(l)$% during year l

$$n_l = \frac{n_1}{\prod_{l'=1}^{l} (1 + p(l')/100)}, \tag{7}$$

where $\prod_{l'=1}^{l}(1+p(l')/100)$ reduces to $(1+p(l')/100)^l$ if $p(l)$ is constant over time. Now equation (6) becomes

$$N = \sum_{l=1}^{\infty} n_1 \frac{1-\int_{-\infty}^{l} f(T_{\mathrm{ave}},\sigma_t)\,\mathrm{d}t}{\prod_{l'=1}^{l}(1+p(l')/100)}. \tag{8}$$

The terms in the summation decrease rapidly as l increases. Therefore, only first $T_{\mathrm{ave}} + 2\sigma_t$ terms are taken into account and

$$N \approx n_1 \sum_{l=1}^{T_{\mathrm{ave}}+2\sigma_t} \frac{1-\int_{-\infty}^{l} f(T_{\mathrm{ave}},\sigma_t)\,\mathrm{d}t}{\prod_{l'=1}^{l}(1+p(l')/100)}, \tag{9}$$

gives a good enough approximation for the original infinite sum in equation (8). Now, the number of devices installed l years ago can be solved from equations (7) and (9).

$$n_l \approx \frac{N}{\prod_{l'=1}^{l}(1+p(l')/100)} \left\{ \sum_{l=1}^{T_{\mathrm{ave}}+2\sigma_t} \frac{1-\int_{-\infty}^{l} f(T_{\mathrm{ave}},\sigma_t)\,\mathrm{d}t}{\prod_{l'=1}^{l}(1+p(l')/100)} \right\}^{-1}. \tag{10}$$

When equation (10) is substituted to equation (5)

$$N_{\mathrm{b}}(j) \approx N \left\{ \sum_{l=1}^{T_{\mathrm{ave}}+2\sigma_t} \frac{1-\int_{-\infty}^{l} f(T_{\mathrm{ave}},\sigma_t)\,\mathrm{d}t}{\prod_{l'=1}^{l}(1+p(l')/100)} \right\}^{-1} \times \left\{ \sum_{l=1}^{T_{\mathrm{ave}}+2\sigma_t} \frac{\int_{l+j-1}^{l+j} f(T_{\mathrm{ave}},\sigma_t)\,\mathrm{d}t}{\prod_{l'=1}^{l}(1+p(l')/100)} \right\},$$

is obtained. It should be noted here that all written off devices are not replaced by HTS ones, new conventional devices are still installed. The market penetration model is used in order to take into account that HTS devices like any application of new technology will gradually take over markets from the old competitors. For example, in electric power sector 20 years is a typical time-scale for market penetration of new equipment. The empirical equation describing the market share of a new product as a function of time yields

$$N_{\mathrm{r}}(j) = \frac{\beta N_{\mathrm{b}}(j)}{1+\mathrm{e}^{2(\gamma-j)/\alpha}},$$

where N_{r} is the number of installed HTS devices during year j and α, β and γ are the fitting parameters [3]. Thus, the total number of HTS devices operating in year j is

$$N_{\mathrm{r,tot}}(j) = \sum_{j'=1}^{j} N_{\mathrm{r}}(j').$$

It is worth noting that $N_{\mathrm{r,tot}}$ is only the statistical expectation value. The expectation value, $e_{\mathrm{r}}(j)$ for the achieved GHG emission reductions is achieved with the change of variable

$$e_{\mathrm{rpl}}(j) \approx \frac{e_{\mathrm{tot}}}{N} N_{\mathrm{r,tot}}(j).$$

Correspondingly, the total emission reduction potential due to the device replacements is

$$e_{\mathrm{b}}(j) \approx \frac{e_{\mathrm{tot}}}{N} \sum_{j'=1}^{j} N_{\mathrm{b}}(j').$$

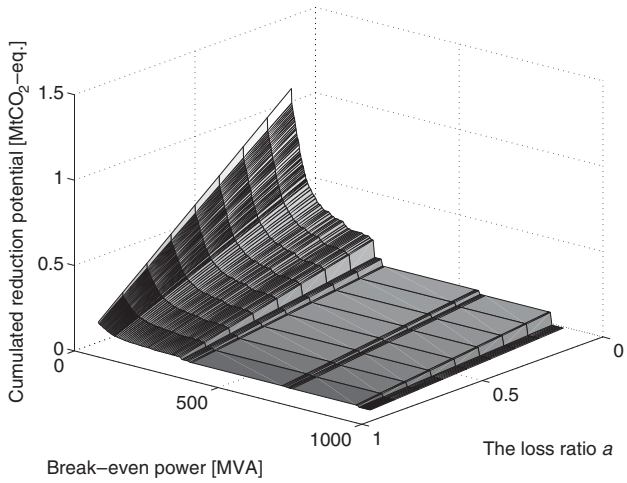

Figure 2. Saved GHG emissions as a function of break-even power and efficiency (in terms of loss ratio a) for HTS generators.

3. Results and discussion

Figure 2 shows the possible reduction in GHG emissions for generators as a function of P_{be} and a according to equation (4). The achievable emission reduction is a linear function of a. On the other hand, it is estimated that the utilization of HTS windings in power devices can reduce losses to approximately half compared to the conventional devices [3, 4]. Therefore, the most interesting information is obtained when the emission reduction is examined as a function of P_{be} in the vicinity of $a = 50\%$. Figure 3 presents three curves corresponding to the different efficiencies of HTS devices, computed with $a = 40\%$, 50% and 60%. Naturally, when $e_{\mathrm{tot}}(P_{\mathrm{be}}; a = 0.5)$ is known the reduction potential in GHG emissions for the given efficiency of superconducting devices can be computed as

$$e(P_{\mathrm{be}}; a) = \frac{(1-a)}{0.5} \cdot e(P_{\mathrm{be}}; 0.5).$$

Different institutes have used slightly different criteria to determine the technological and economical limitations for choosing the P_{be}s. The American Superconductor corporation has used $P_{\mathrm{be}} = 750$ kW for synchronous motors and $P_{\mathrm{be}} = 100$ MVA for transformers and generators to calculate possible energy savings potential[5]. Applying these P_{be}s 0.21–0.32 Mt of CO_2-eq. savings with HTS synchronous motors (all units to be replaced, also hereafter), 0.21–0.31 Mt with HTS generators (40 units to be replaced) and 0.15–0.34 Mt with HTS transformers (100 units to be replaced) can be obtained. In total, this means 0.57–0.97 Mt of CO_2-eq. reduction annually, as allocated for hard coal. The range is due to varying values of a and the load factor of transformers, k_{TR}.

However, a 30 MVA HTS transformer with $\eta = 99.97\%$ was designed by a French group [13] so it is reasonable to settle the P_{be} for transformers below that. The US Department of Energy (DOE) suggested $P_{\mathrm{be}} = 20$ MVA, 100 MVA and 375 kW for transformers, generators and synchronous motors, respectively. These values would give 0.21–0.32 Mt with HTS synchronous motors, 0.21–0.31 Mt with HTS generators

[5] American Superconductor Corporation, Two Technology Drive, Westborough, MA, USA.

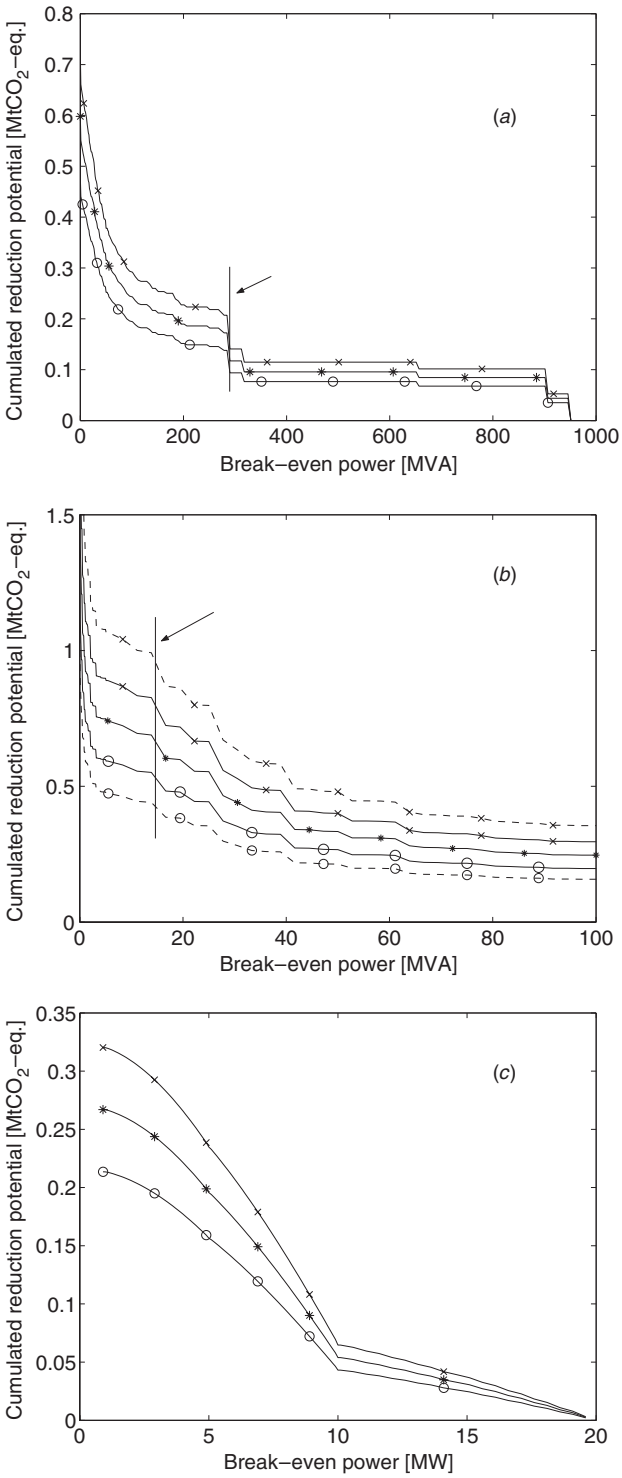

Figure 3. Saved GHG emissions as a function of break-even power for (*a*) generators, (*b*) transformers and (*c*) synchronous motors. The symbols ×, ∗ and ○ correspond to $a = 40\%$, 50% and 60%, respectively. The variable a is the loss ratio of HTS devices to corresponding conventional ones. The solid lines in (*b*) indicate saved emissions when the load factor $k = 0.5$ and the dash lines show the range when $0.4 \leqslant k \leqslant 0.6$.

(40 units to be replaced) and 0.36–0.80 Mt with HTS transformers (774 units to be replaced). As combined, 0.78–1.43 Mt reductions can be obtained.

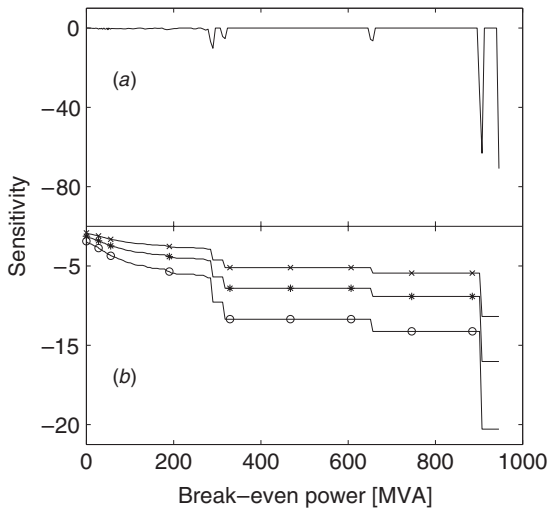

Figure 4. Sensitivity of saved GHG emissions to the variables (*a*) P_{be} and (*b*) a. The symbols ×, ∗ and ○ correspond to $a = 40\%$, 50% and 60%, respectively.

From the emissions point of view, it can be seen from figure 3 that above certain power level the savings cumulate much stronger than below that level. These steps are for transformers at 12.5 MVA, for generators at 300 MVA and for synchronous motors at 1 MW. They arise simply from the power distribution of the devices, as can be seen from the insets of figure 1. These P_{be}s would mean 0.21–0.32 Mt with HTS synchronous motors, 0.15–0.22 Mt with HTS generators (7 units to be replaced) and 0.44–0.99 Mt with HTS transformers (1303 units to be replaced). In total, this is 0.8–1.53 Mt of CO_2-eq. or 5–9% of total GHG emissions from electricity production. A close estimate would be 1.14 Mt of CO_2-eq., that is when superconductivity cuts the losses to half, i.e. $a = 50\%$ and $k_{TR} = 0.5$.

With the P_{be}s that the American Superconductor has used, $4.6 \pm 1.2\%$ of GHG emissions from electricity generation could be avoided. The DOE's P_{be}s give $6.7 \pm 2.0\%$ reduction. When the P_{be}s are optimized with respect to GHG emissions in Finnish power grid they agree well with estimates by DOE. For generators below 300 MVA the achievable reduction in GHG emissions increases smoothly with decreasing P_{be}. However, it is not economically viable to lower the P_{be} below the step because more devices need to be built without notable decrease in emissions. Consequently, 300 MVA for generators and 12.5 MVA for transformers are suggested as P_{be}s to be pursued.

The sensitivities $S_{P_{be}}^{e_{tot}}$ and $S_{a}^{e_{tot}}$ for generators are presented in figure 4. The importance of sensitivity can be illustrated as follows. If $a = 40\%$ is used with $P_{be} = 300$ MVA 0.22 Mt of CO_2-eq. reduction can be obtained with seven generators to be replaced. In order to achieve the same reduction potential with $a = 50\%$, P_{be} has to be lowered to 170 MVA and 14 generators are to be replaced. That is, e_{tot} is more sensitive to changes in a than in P_{be}. The average $S_{P_{be}}^{e_{tot}}$ between 170 MVA and 300 MVA is −0.38 while $S_{a}^{e_{tot}}$ between $a = 40\%$ and $a = 50\%$ is −4.38, i.e. over tenfold. In general, above 300 MVA e_{tot} is more sensitive to ascending of a than to the descending of P_{be}, except at 900 MVA where little variation in P_{be} results in major change in saved GHG emissions. Thus, the reductions

in emissions are achieved rather by boosting up the efficiency of the devices than by increasing the manufacturing volume. Figure 4(*a*) shows only one curve, because the sensitivity with respect to P_{be} is independent of the value of a. Sensitivities for transformers and synchronous motors are not shown because the curve for transformers is similar to that of generators, except hundredfold in magnitude. For synchronous motors it is not relevant because all conventional motors are above 1 MW and therefore replaced by HTS ones when any of the presented P_{be} criteria is used.

There are some changes to this scenario when all of the EU countries are considered. The biggest difference is the rife usage of combined heat and power in Finland. Also the load factors of nuclear and hydroelectric power are lower than those in Finland, but k^i is higher for thermal power instead. These together mean that the relative emissions per generated kWh are higher in EU than in Finland. The share of synchronous motors in other EU countries is roughly half of Finland's. In 1998, the total generation of electricity in the EU was 2490 TWh, and it created 933 Mt of CO_2 emissions [9]. The target for the Kyoto Protocol is 852 Mt [6]. In the year of comparison, the total generation in Finland was 70 TWh with 19 Mt of CO_2 emissions [9]. According to the analysis about the Finnish power grid, 1.1–2.2% of the total electricity generation could be saved with HTS devices. When that energy is allocated for reduced use of hard coal, 27–53 Mt of CO_2 emission reduction in the whole EU can be obtained. If the saved electricity is allocated evenly for all forms of electricity generation, the percentual savings in EU is higher than that in Finland due to EU's higher relative e_{kWh}. Thus, in view of the Kyoto Protocol, the utilization of HTS machinery alone would result in 33–65% of the required reduction in emissions.

It has been assigned that the lifetimes of electrical machines are normally distributed and the average lifetimes are 31, 35 and 40 years for motors, generators and transformers, respectively. The market of electrical power devices has been increasing about 4.7% per year during 1960s and 1970s, 2.7% per year during 1980s and 1.7% per year after 1990 [3]. According to this data the market penetration of HTS machinery is estimated and the achieved GHG emission reductions are presented in figure 5. Because the standard deviation of the lifetime σ_t is unknown, the range in the number of replaced devices is obtained by assuming $5\text{y} \leqslant \sigma_t \leqslant 20\text{y}$. The theoretical maximum in GHG emission reduction is achieved with an assumption that all new units are HTS ones. In the near future only few of the devices are to be replaced but the write-off rate reaches a maximum after 25–30 years. Thus, it will take at least 20 years to realize 50% of the total reduction potential in GHG emissions. However, in reality an even longer period of time is needed because market penetration of HTS devices is not ideal. Mulholland *et al* estimated the coefficients of the market penetration model for HTS devices [3]. They appear in table 3. When their estimates are used only 13% of generators, 17% of transformers and 30% of synchronous motors are replaced with HTS ones after 25 years. It should be noted that the estimates are pessimistic because the coefficients include the fact that small devices are not replaced. This was already taken into account here with the concept of P_{be}. Also, the new

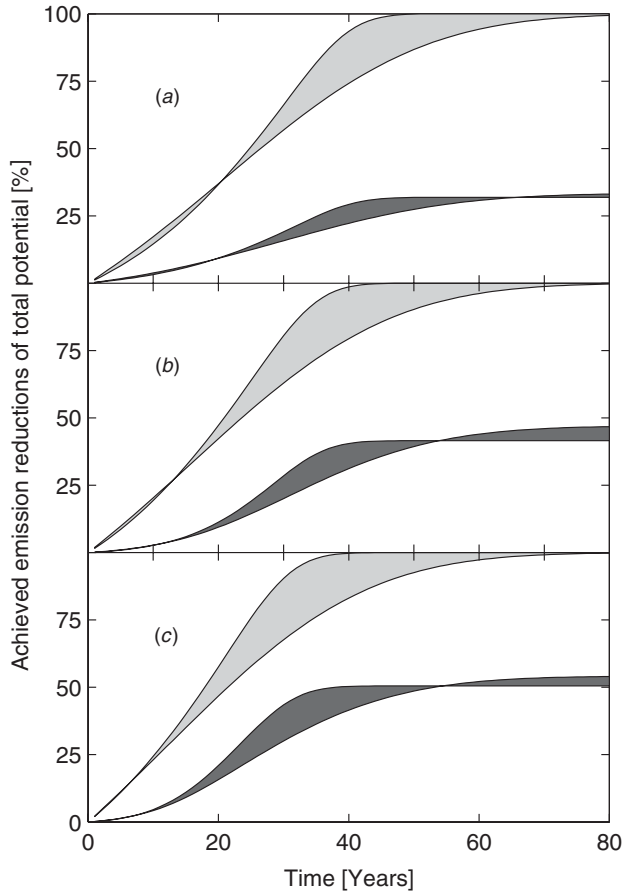

Figure 5. The total GHG emissions as a function of time according to the market penetration model: (*a*) generators, (*b*) transformers and (*c*) synchronous motors. Light grey correspond to e_b/e_{tot} and dark grey to e_{rpl}/e_{tot}. The range is due to variation $5\text{y} \leqslant \sigma_t \leqslant 20\text{y}$.

Table 3. The coefficients of the market penetration model.

Machine	α (years)	β	γ (years)
Generators	44.39	0.50	11
Transformers	17.76	0.80	10
Synchronous motors	10.68	0.75	12

advantages of HTS machinery, e.g., the positive impact on environmental issues, were not resolved when determining the coefficients. Instead, they were determined from contemporary technological viewpoints, such as the insensitivity to load variations and higher stability in HTS generators and the absence of fire hazards, overload capability and lower noise levels in HTS transformers.

4. Conclusion

Detailed study about the replacement of existing conventional transformers, generators and synchronous motors by HTS ones was made in order to find the levels of efficiency and nominal power that make HTS devices competitive from the environmental point of view. The study concentrated on the potential to reduce greenhouse gas (GHG) emissions in the Finnish electric power grid when the production and

consumption of electricity together with the causes for GHG emissions were taken into account. The limits for the break-even power of superconductivity, P_{be}, were constructed according to previous economical and technological estimates combined with presented GHG emission analysis. The suggested $P_{be} = 1$ MW, 300 MVA and 12.5 MVA for motors, generators and transformers, respectively, can lead to 0.8–1.53 Mt of CO_2-eq. emission reduction annually in Finland. The range is due to uncertainty in the efficiencies of future commercial devices. In the EU, the corresponding reduction potential is 27–53 Mt of CO_2 or 33–65% of the required reduction in emissions according to the Kyoto Protocol. Thus, in environmental considerations HTS devices are ahead of their conventional counterparts. However, according to the market penetration model based on the write-off rate of present electrical machinery the minimum time to achieve 50% of the reduction potential is 20 years. Finally, according to a sensitivity analysis it is more desirable to improve the efficiency of HTS devices than to aim for the manufacturing of large quantities.

Acknowledgments

The authors would like to express their gratitude to Terho Savolainen from Statistics Finland for supplying the detailed data of nominal power distribution of utility generators and transformers and to Juhani Mantere from ABB Motors for information on synchronous motors. This work was partly supported by National Technology Agency of Finland, Prizztech Ltd, Outokumpu Advanced Superconductors Ltd, TVO, Fortum Foundation, SVK-Pool and the Academy of Finland.

References

[1] Malozemoff A P, Maguire J, Gamble B and Kalsi S 2002 *IEEE Trans. Appl. Supercond.* **12** 778
[2] Mikkonen R 2002 *IEEE Trans. Appl. Supercond.* **12** 782
[3] Mulholland J, Sheahen T and McConnell B 2001 *Analysis of Future Prices and Markets for High Temperature Superconductors* (Oakridge, TN: US Department of Energy)
[4] Wolsky A M 1999 *The Likely Impacts on Environment, Safety and Health from the Power Sector's Future Widespread Use of Superconducting Equipment* (Argonne, Illinois: Argonne National Laboratory, USA)
[5] Bryant E 1997 *Climate Process & Change* (Cambridge: Cambridge University Press)
[6] United Nations Framework Convention on Climate Change (UNFCCC) 1997 *The Kyoto Protocol* (Kyoto: UNFCCC Press)
[7] Tixador P and Daffix H 1997 *IEEE Trans. Appl. Supercond.* **7** 3857
[8] Sissimatos E, Harms G and Oswald B R 2001 *IEEE Trans. Appl. Supercond.* **11** 1574
[9] Statistics Finland 2001 *Energy Statistics 2000* (Helsinki: Helsinki University Press)
[10] Spandero J V, Langois L and Hamilton B 2000 *IAEA Bull.* **42** 19
[11] Vuori S, Lautkaski R, Lehtilä A and Suolanen V 2002 *VTT Research Notes* 2127 (Espoo)
[12] Vlach J and Singhal K 1983 *Computer Methods for Circuit Analysis and Design* (New York: Van Nostrand-Reinhold)
[13] Donnier-Valentin G and Tixador P 2001 *IEEE Trans. Appl. Supercond.* **11** 1498

Publication **II**

T. Hartikainen, J. Lehtonen and R. Mikkonen

"Reduction of Greenhouse-gas Emissions by Utilization of Superconductivity in Electric-power Generation"

Applied Energy, **78**, pp. 151-158, 2004.

Available online at www.sciencedirect.com
SCIENCE DIRECT®
Applied Energy 78 (2004) 151–158
APPLIED ENERGY
www.elsevier.com/locate/apenergy

Reduction of greenhouse-gas emissions by utilization of superconductivity in electric-power generation

Teemu Hartikainen*, Jorma Lehtonen, Risto Mikkonen

Institute of Electromagnetics, Tampere University of Technology, 33101 Tampere, Finland

Received 18 June 2003; received in revised form 9 July 2003; accepted 12 July 2003

Abstract

The reduction of greenhouse-gas (GHG) emissions is becoming a topical issue due to the Kyoto Protocol which requires the European Union (EU) to reduce its emissions by 8% from the 1990 levels by between 2008 and 2012. The main source for GHG-emissions is energy production. Superconducting electrical machinery is starting to emerge into the market of power devices. High-temperature superconducting (HTS) windings in generators and transformers can approximately halve the losses compared to conventional devices. Higher efficiency saves electrical energy and also reduces GHG-emissions as well. In this paper, the reduction potential of GHG-emissions in the EU by HTS-machinery is calculated. The replacement of existing devices by HTS ones is considered from the environmental point-of-view. The structure of energy production for the EU was investigated and the emission data from different type of power plants were screened. The potential energy savings were converted to saved GHG-emission tonnes.

Keywords: Emissions reduction; Energy efficiency; Kyoto Protocol; Superconductivity

1. Introduction

The first calculations of the increasing greenhouse effect (GHe) were made in late 1800s. Without GHe, the mean temperature of our planet would be 33 K lower and

* Corresponding author. Fax: +358-3-3115-2160.
E-mail address: teemu.hartikainen@tut.fi (T. Hartikainen).

0306-2619/$ - see front matter
doi:10.1016/S0306-2619(03)00158-2

the present-type of life forms wouldn't exist. Water vapour is the main greenhouse gas, accounting for 75% of the natural GHe.

Today it is unquestionable that the burning of fossil fuels increases the greenhouse gas (GHG) content of the atmosphere. The major greenhouse gases from human activity, in order of importance, are: carbon dioxide (CO_2), methane (CH_4), nitrous oxide (NO_2) and halocarbons (CFCs). Over 20 Gt of CO_2 annually are emitted into the atmosphere by human activity, but this is still only about 3% of the natural flow through the air–ground interface [1].

In 1997, the industrialized countries signed the Kyoto Protocol, which requires them to lower their GHG-emissions by at least 5% below the level of 1990 between 2008 and 2012. The European Union (EU) as a whole agreed to an 8% reduction. The Kyoto Protocol states that the efficiency of energy production shoud be enhanced [2]. In this study, high-temperature superconductivity (HTS) is examined as a way of improving the energy-production efficiency. The phenomenon of superconductivity means zero electrical resistivity below critical values of temperature, current density and external magnetic-flux density. T_C is a few Kelvins in classical metallic superconductors. The new era in superconductivity research began in 1986 when a Swiss group reported HTS in Ba-doped $LaCuO_3$, a ceramic oxide material [3]. In just a few years, many HTS-materials were found with T_C over 100 K and soon liquid nitrogen (LN_2) cooled HTS-magnets were proposed for electric appliances. Recent successful demonstration projects on a medium scale have shown the technical feasibility of HTS-devices in electric power engineering [4,5]. Energy will be saved by utilization of HTS-based generators and transformers in power plants and substations.

Figures for potential GHG-emissions reduction are calculated from European statistical data. It should be noted that this analysis doesn't consider the economic aspects of the case. Calculations are made purely by observing the technological limitations. Earlier, a similar study was made for Finland's electric-power grid for which exact statistics for every installed machine were available [6]. Such statistics are not obtainable for the whole EU.

2. Background for analysis

The efficiencies of superconducting machinery are not clear-cut, but depend on many different issues, such as, among other things, the properties of the chosen HTS-material, the geometry of the superconducting tapes and the cooling system which can be based on either LN_2 or mechanical cryocoolers. All of these influence the losses of the devices and thus it is not possible to precisely express the efficiency figures of superconducting devices. A superconducting 30 MVA transformer, with an efficiency of 99.97%, was designed by a French group [7], but in reality it is not suitable to optimize the machines only for the lowest possible losses. In moving systems, for example, the weight of the device plays a crucial role and optimization should take that into account [7,8]. According to current knowledge, by utilizing HTS windings in power devices it is possible to reduce losses to approximately half

compared to that of the conventional devices [9,10]. The ratio, a, of the losses in the HTS-device to the losses in the corresponding conventional one can be used to express the efficiencies of HTS-devices, η_{sc}.

$$\eta_{sc} = 1 - a(1 - \eta_c) \tag{1}$$

where η_c is the efficiency of the corresponding conventional device and in this paper, $a = 0.5$ was used as stated previously. Table 1 presents the efficiencies for conventional transformers and generators as a function of their power [9,11,12].

The saved energy could be allocated, for example, for reduced use of hard coal or peat in electricity production and then converted to grams of CO_2-equivalent per kWh, which is a common way of reporting the GHG-emissions.

Generation of electricity is the largest individual contributor to greenhouse gas emissions in the EU. In 1999, CO_2-emissions from electricity generation were 913.6 Mt, while total CO_2-emissions from fuel combustion were 3085 Mt. This is approximately 80% of the total greenhouse-gas emissions from the EU [13]. Table 2 shows the GHG-emissions from different electricity-generation chains. For example, a typical coal/peat-fired power plant in the EU has an average value of emissions per kilowatt-hour $e_{kWh} = 1140$ g of CO_2-eq./kWh [14]. When the total electricity production from all sources is considered, an average European value is estimated to be 475 g of CO_2-eq./kWh.

Table 1
Efficiencies for conventional transformers and generators [9,11,12]

Transformers Power P_n(kVA)	Efficiency η_c	Generators Power P_n(kVA)	Efficiency η_c
1	0.9100	500	0.960
5	0.9295	1000	0.966
10	0.9512	3000	0.970
50	0.9731	5000	0.973
100	0.9802	10,000	0.977
200	0.9818	15,000	0.980
500	0.9867	20,000	0.982
800	0.9877	40,000	0.984
1000	0.9900	60,000	0.985
10,000	0.9920	80,000	0.987
30,000	0.9933	100,000	0.988
50,000	0.9945	130,000	0.988
130,000	0.9949	250,000	0.988
250,000	0.9952	370,000	0.988
370,000	0.9956	500,000	0.988
500,000	0.9960	750,000	0.988
1,000,000	0.9977	1,000,000	0.988

Table 2
GHG-emissions from electricity production [14][a]

Energy vector	e_{kWh} (Direct)	e_{kWh} (In-direct)
Hard coal or peat	790–1017	176–289
Natural gas	362–575	77–113
Hydro	0	4–236
Solar (photovoltaic)	0	100–280
Wind	0	10–48
Nuclear	0	9–21

[a] The range of GHG-emissions from electricity production in grams of CO_2 equivalent per kilowatt-hour. The first values are direct emissions from burning and the second values indicate indirect emissions during life-cycle. The exact value depends on the state of technology [14].

3. Analysis and discussion

The generation of electricity in the EU in 1999 was 2531 TWh and the maximum net generating capacity was 575 GW [13]. The current annual growth rate in production is 1.7%. Typically electricity is generated at 10–20 kV and stepped up by transformers to 275–400 kV for transmission by overhead lines. Three more transformation points are required for a fully functioning electrical-network, a pattern that is standardized throughout the EU. Transformers are responsible for approximately one third of the total network losses which are, on average, 6% of the generated electricity. The rest, 4%, is consumed mainly in overhead transmission lines [15]. The power distribution of transformers in the EU can be seen from Fig. 1. This was constructed from Finnish statistics—there are 30-times more transformers in the EU than in Finland, the networks are identical and the electricity consumption is 30-times larger in the EU [15]. The transformers were arranged so that $P_n^i >= P_n^{i+1}$, where P_n^i is the nominal power of transformer i. In utility use the transformers are not loaded with the nominal power all the time. The average power delivered to the device i in a scale of one year, P_{ave}, is calculated from

$$P_{ave}^i = kP_n^i, \tag{3}$$

where k is is the load factor of the transformers. An estimate for k is 0.4–0.6. Now the energy savings potential for transformers, E_S^{tr}, can be calculated from

$$E_S^{tr} = T\sum_{i=1}^{N} P_{ave}^i\left(\eta_{sc}^i - \eta_c^i\right), \tag{4}$$

where N is the total number of transformers and T is the period of study: here 1 year is used.

To obtain an improvement in the efficiency of transformers, it is reasonable to apply superconductivity only above a certain power level which is denoted as the break-even power, P_{be}. Devices whose nominal power is above P_{be} are replaced by

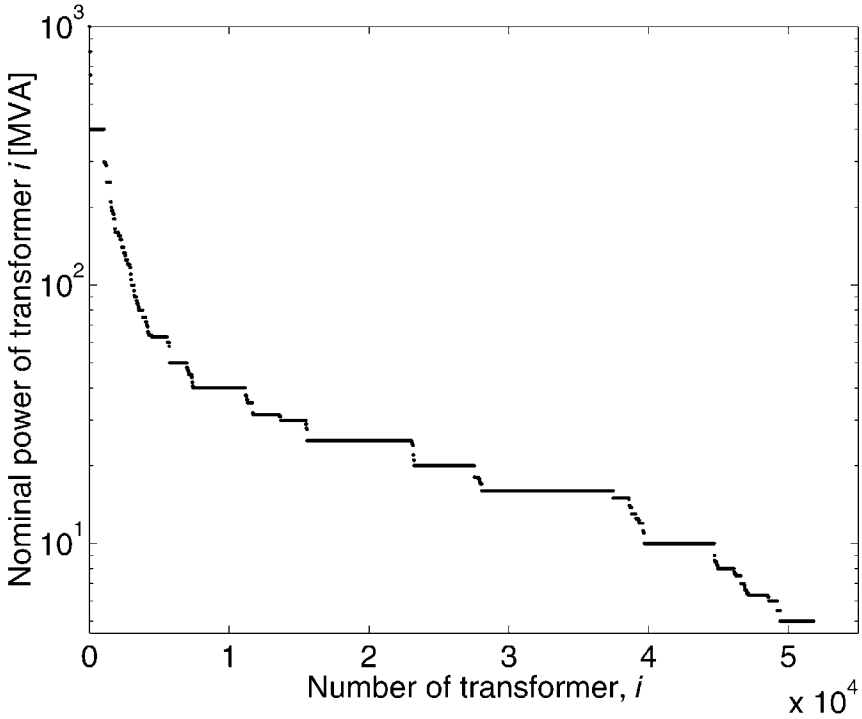

Fig. 1. The power distribution of transformers in the EU. Only transformers with a nominal power of 5 MVA or above are included [13,15].

superconducting ones. For transformers, $P_{be} = 12.5$ MVA was chosen for this study because it is technologically attainable and there are many devices at this power level, so the savings potential rapidly increases [6]. Eq. (4) gives $E_S^{tr} = 20.67$ TWh with $k = 0.5$. Fig. 2 presents the dependence of savings potential on P_{be}.

However, a similar analysis cannot be used for generators in the EU, because the contribution of sources to electricity production differs between Finland and the EU average. Contribution of the sources to electricity production in the EU in 1999 was as follows: conventional thermal power 52% (55% of which by coal/peat-fired power plants), nuclear power 34%, hydro power 13% and wind power 1%.

It is reasonable to use superconductivity in generators only above 100 MVA [5,6]. Therefore, generators of nuclear power and coal/peat-fired thermal power plants as well as combined cycle gas turbine (CCGT) power plants are involved. This is a rather pessimistic simplification, because there could be a few other thermal power plants with over 100 MVA generators but exact statistics do not exist. The possible savings in generators were thus calculated from electricity-production statistics with

$$E_S^j = \frac{E_G^j}{\eta_c^j}\eta_{sc}^j - E_G^j, \tag{2}$$

where j refers to the source (i.e nuclear, coal/peat-fired thermal, CCGT), E_G is generated electricity (TWh) and E_S is the savings potential (TWh): η_{sc} is calculated from Eq. (1). Results for all 15 EU countries are presented in Table 3 [16]. In spite of the simplification, the results calculated for Finland with Eq. (2) agree relatively well

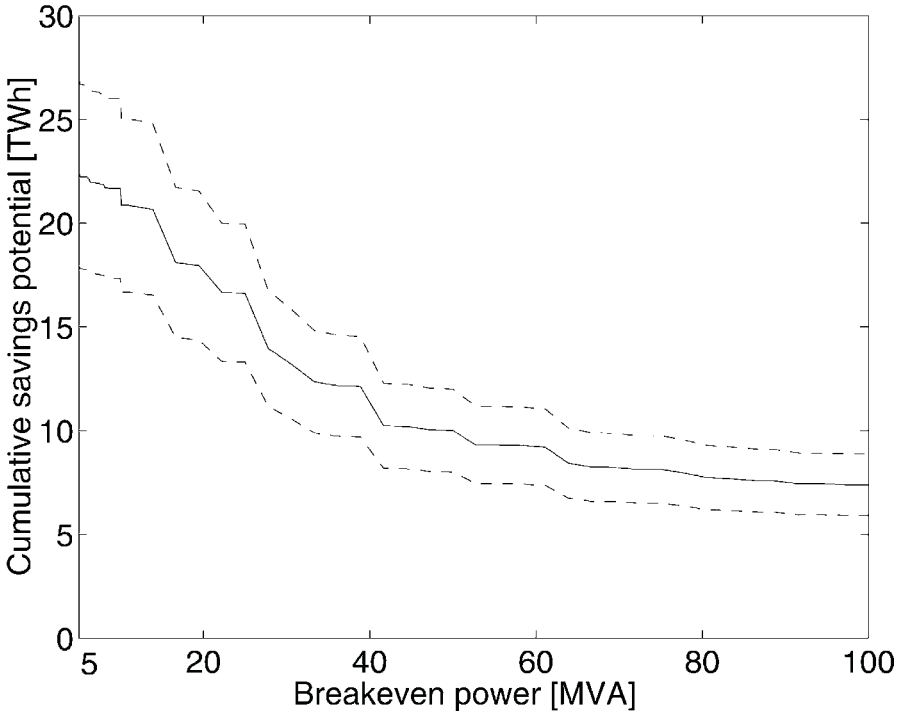

Fig. 2. Annual energy savings potential with respect to P_{be} for transformers. The solid line indicates the savings potential when $a = 0.5$, and $k = 0.5$, while the dashed lines show the range when $0.4 < k < 0.6$.

Table 3
Annual savings potential in generators in different EU countries [16]

Country	Savings potential in TWh
Austria	0.02429
Belgium	0.42024
Germany	2.52389
Denmark	0.09838
Spain	0.87929
Finland	0.21255
France	2.44008
United Kingdom	1.86923
Greece	0.17733
Ireland	0.05466
Italy	0.81595
Luxembourgh	0
Netherlands	0.22227
Portugal	0.18170
Sweden	0.43785
EU-15[a]	10.3577

[a] EU-15 means the total savings potential of all 15 EU countries.

with the results in [6]. The difference is only −5% compared to the calculation from generator statistics for conventional steam-turbines over 100 MVA. The difference is due to the fact that there are some gas turbines in Finland that utilizise generators above 100 MVA. In Spain and Italy, oil is widely used for large-scale electricity generation. According to their electricity companies, in Spain approximately 90% and in Italy approximately 80% of the electricity generated by oil is produced with generators over 100 MVA [17,18].

When discussing the combined annual savings potential in generators and transformers, E_S, which depend linearly on a, the savings with different a-values can be calculated easily from

$$E_S(a) = \frac{(1-a)}{0.5} E_S(0.5).$$

The savings in energy can be converted to savings in GHG-emissions by multiplying E_S with e_{kWh}. If the total savings potential is allocated for reduced usage of hard coal/peat in electricity generation this multiplication gives $E_S = 35.25$ Mt of $CO_{2\text{-eq}}$. This is 48% of the needed reduction in CO_2-emissions from electricity generation according to the Kyoto Protocol. More relevant would be to use the average European value introduced earlier. Thus the savings potential becomes $E_S = 14.74$ Mt of $CO_{2\text{-eq}}$ or 20% of the Kyoto Protocol requirement. In [6], the GHG-emissions reduction was examined by the write-off rate of conventional devices according to their normal life-span. Here the maximum achievable reduction is presented. There are several other issues which affect the write-off rate than just the usual life-time of devices: for example, political decisions for committing to the Kyoto Protocol.

4. Conclusion

Due to the need to reduce greenhouse-gas (GHG) emissions, the reduction potential by utilizing high temperature superconducting (HTS) devices in electric-power generation in the European Union (EU) was examined. The flow of electricity in the EU and the GHG-emissions from power generation were presented and savings with HTS generators and transformers were calculated. By widespread utilization of HTS in the EU, 31 TWh of electrical energy could be saved annually. This is 1.2% of the total generation. In GHG-emissions, this means 14.7 Mt of $CO_{2\text{-eq.}}$ with average European value for emissions per kWh. This is approximately 20% of the needed reduction in CO_2-emissions from electricity generation required by the Kyoto Protocol.

References

[1] Bryant E. Climate process & change. Cambridge University Press. Cambridge; 1997.

[2] United Nations Framework Convention on Climate Change.The Kyoto Protocol. Kyoto; 1997.
[3] Müller KA, Bednorz JG. The discovery of a class of high-temperature superconductors. Science 1987;237:1133–7.
[4] Mikkonen R. Highlights of SC power applications in Europe. IEEE Trans Appl Supercond 2002; 12(1):782–7.
[5] Malozemoff AP, Maguire J, Gamble B, Kalsi S. Power applications of high-temperature superconductors: status and perspectives. IEEE Trans Appl Supercond 2002;12(1):778–81.
[6] Hartikainen T, Lehtonen J, Mikkonen R. Role of HTS-devices in greenhouse-gas emissions reduction. Superconductor Science & Technology 2003;16:963–9.
[7] Tixador P, Daffix H. Conceptual design of an electrical machine with both low and high tc superconductors. IEEE Trans Appl Supercond 1997;7(4):3857–65.
[8] Sissimatos E, Harms G, Oswald BR. Optimization of high-temperature superconducting power transformers. IEEE Trans Appl Supercond 2001;11(1):1574–7.
[9] Mulholland J, Sheahen T, McConnell B. Analysis of future prices and markets for high temperature superconductors. U.S. Department of Energy; 9/2001.
[10] Wolsky AM. The likely impacts on environment, safety and health from the power sector's future widespread use of superconducting equipment. Argonne National Laboratory, USA; 11/1999.
[11] Alstom Power Corporation, 25 Avenue Kleber, 75795 Paris, France.
[12] Muuntosähkö Oy - Trafox, Niittylänpolku 4, 00620 Helsinki, Finland.
[13] Statistics Finland. Energy statistics 2001. Finland: Helsinki University Press; 2002 (References therein).
[14] Spandero JV, Langois L, Hamilton B. Assessing the difference: greenhouse-gas emissions of electricity generation chains. IAEA Bulletin 2000;42(2):19–24.
[15] European Commission. The scope for energy saving in the EU through the use of energy-efficient electricity distribution transformers. European Communities; 1999.
[16] The Union of Electricity Industry in Europe—Eurelectric. Statistics and prospects for the European electricity sector (1980–1999) (2000–2020) (EURPROG 2001). 29th ed.; 2001.
[17] Endesa S.A. C/ Principe de Vergara, 187, 28002 Madrid, Spain.
[18] Edison S.p.A. Foro Buonaparte, 31, 20121 Milan, Italy.

Publication **III**

T. Hartikainen, A. Korpela, J. Lehtonen and R. Mikkonen

"A Comparative Life-Cycle Assessment Between NbTi and Copper Magnets"

IEEE Transactions on Applied Superconductivity, **14**, pp. 1882-1885, 2004.

A Comparative Life-Cycle Assessment Between NbTi and Copper Magnets

Teemu Hartikainen, Aki Korpela, Jorma Lehtonen, and Risto Mikkonen

***Abstract*—Magnetic Resonance Imaging (MRI) devices can utilize either a conventional copper magnet or a superconducting NbTi magnet. In this study, copper and NbTi large bore magnets were designed by numerical optimization procedure for optimum wire length. The optimized magnets represent roughly the main coils of an MRI system. Then, Life Cycle Assessment (LCA) was used to compare the environmental impact of these two types of magnets. LCA is an established tool to investigate the interaction between a product and the environment. In the inventory phase of LCA all material inputs, energy consumption, wastes and emissions to air and water are assessed, beginning from the extraction of raw materials and ending to the delivery of products from the factories. The optimization results showed that the construction of the copper magnet requires much more wire than the NbTi one. However, the manufacturing of NbTi/Cu wire requires more raw materials and is more energy-intensive than the manufacturing of copper wire per unit ton. Thus, more wastes and emissions to air and water are generated during the production of NbTi/Cu wire, but when the magnets were compared the results became reversed.**

***Index Terms*—Copper, life cycle assessment, magnet design, NbTi.**

I. Introduction

SUPERCONDUCTING wires are competing with traditional copper conductors in magnet applications such as magnetic resonance imaging (MRI). Superconductors are used in systems which are unrealizable without them, or in which they save considerable extents of energy. So far the comparisons between superconducting and traditional copper magnets have been made from economical or purely technical point of view. Nowadays environmental issues are also considered in policymaking. Therefore, scientific studies are required also from this point of view.

The concepts of sustainable development and eco-efficiency were introduced to the general public in 1992 Earth Summit in Rio de Janeiro. The definitions of them are "development that meets the needs of the current generation without undermining future generations' ability to meet their own needs." and "strategy to improve the environmental performance of a company or a nation by the use of performance indicators.", respectively [1]. The life cycle assessment (LCA) is one such indicator to deal with the complex interaction between a product and the environment. It is '*from-cradle-to-grave*' approach where all environmental impacts starting from the extraction of raw materials and energy to final disposal of the product are assessed [2].

A formal LCA study is divided into four main categories: goal and scope definition (GSD), life cycle inventory analysis (LCI), impact assessment (LCIA) and interpretation [3].

In this paper, comparative LCA study is made for magnets wound of copper and NbTi/Cu wires. Outokumpu Poricopper produces both wires. The share of subcontractors and transports were also taken into account. The copper and NbTi magnets to be compared must have similar performance. Therefore, a numerical optimization study, based on Sequential Quadratic Programming (SQP) and Finite Element Method (FEM), is exploited for the design of both magnets. The magnet volume is minimized when the maximum achievable magnetic flux density and the bore diameter are taken as constraints. The properties of optimized copper and NbTi magnets correspond roughly to the ones encountered in MRI systems [8]. Then the minimum lengths of copper and NbTi/Cu wires are computed as a function of the required field in the magnet bore. Once the optimal magnet geometries are known results from the LCA are applied.

II. Magnet Design

The coil design can be formulated as a constrained optimization problem:

$$\begin{aligned}&\text{minimize } F(\mathbf{X})\\&\text{subject to } \mathbf{g}(\mathbf{X}) \leq 0\end{aligned}$$

where $F(\mathbf{X})$ is the object function, $\mathbf{X}$ the vector containing the optimization parameters and $\mathbf{g}(\mathbf{X})$ the vector of the constraint functions. SQP is an iterative optimization algorithm that divides the problem into two sub problems, which are solved at each iteration. The minimum of $F(\mathbf{X})$ is achieved when $\mathbf{X}$ is updated as $\mathbf{X}_{k+1} = \mathbf{X}_k + \delta_k \mathbf{d}_k$, where δ_k is the step length, $\mathbf{d}_k$ the search direction and k the iteration index. δ_k and $\mathbf{d}_k$ are determined separately. The search direction is found by solving a quadratic problem with linear constraints:

$$\begin{aligned}&\text{minimize } \frac{1}{2}\mathbf{d}_k^{\mathrm{T}} H_k \mathbf{d}_k + \nabla F(\mathbf{X}_k)^{\mathrm{T}} \mathbf{d}_k\\&\text{subject to } \nabla g_j^{\mathrm{T}} \mathbf{d}_k + g_j(\mathbf{X}_k) \leq 0, \quad j = 1, \ldots, n\end{aligned}$$

where H_k is a positive definite approximation of the Hessian matrix and n is the number of constraint functions. H_k is updated at each iteration with the Broyden-Fletcher-Goldfarb-Shanno (BFGS) method [7]. The step length is then

Manuscript received October 20, 2003. This work was supported by the National Technology Agency of Finland, Prizztech Ltd., TVO, Outokumpu Advanced Superconductors, Fortum Foundation, SVK-pool and the Academy of Finland.

The authors are with the Institute of Electromagnetics, Tampere University of Technology, Tampere, Finland (e-mails: teemu.hartikainen@tut.fi; aki.korpela@tut.fi; jorma.r.lehtonen@tut.fi; risto.mikkonen@tut.fi).

Digital Object Identifier 10.1109/TASC.2004.830891

obtained from a one-dimensional unconstrained problem by minimizing the merit function

$$\Psi(\delta_k) = F(\mathbf{X}_k + \delta_k \mathbf{d}_k) + \sum_{j=1}^{n} p_j \max\{0, g_j(\mathbf{X}_k + \delta_k \mathbf{d}_k)\} \tag{1}$$

where p_j is a penalty parameter. In this study, the SQP was carried out with Matlab.

The object function of the optimization is the volume of the solenoidal coil, which can be expressed as

$$V(\mathbf{X}) = \pi(b^2 - a^2)d,$$

where a, b and d are the inner radius, the outer radius and the axial length of the coil, respectively.

The optimized geometry of the coil must fulfill the following constraints:

- The magnetic flux density in the center of the coil, B_0, has to be at least equal to the pre-defined value, B_{lim}. In NbTi magnet the operation current, I_{op}, equals the coil critical current, I_c^k. In copper magnet I_{op} is determined by the maximum allowable current density, $J_{\text{cu}} = 10\ \text{A/mm}^2$. The values of B_{lim} used here are 1.5 T for NbTi magnet and 0.2 T for copper magnet [8], [20].
- The thickness of the coil, $b-a$, and the axial length of the coil must be at least equal to the diameter of the wire, $\varnothing$.

Thus, $\mathbf{X} = [a, b, d]$ and $g(\mathbf{X}) = [B_{\text{lim}} - B_0(a, b, d, I_{\text{op}}), \varnothing - (b-a), \varnothing - d]$.

The critical current of the NbTi coil was obtained from the measured short sample data, I_c^w. For NbTi (model name OK42, $\varnothing = 0.85$ mm) [9]

$$I_c^w(B, 4.2\ \text{K}) = -93B\ \frac{\text{A}}{\text{T}} + 747\ \text{A}. \tag{2}$$

The critical current density of the coil is reduced from the short sample value due to mechanical stresses. This reduction was assumed to be 20% [10]. Furthermore, a filling factor of 55% was assumed for these coils wound of round wire [11]. Thus, the current density of a coil can be expressed as

$$J_c^k = 0.55 \cdot 0.80 \cdot \frac{I_c^w}{S_{\text{sc}}}, \tag{3}$$

where S_{sc} is the cross-section of the superconducting wire. Then, Finite Element Method is used to solve the magnetic flux density $\mathbf{B} = \nabla \times \mathbf{A}$, where $\mathbf{A}$ is the vector potential, from

$$\nabla \times \frac{1}{\mu_0} \nabla \times \mathbf{A} = \mathbf{J}, \tag{4}$$

where μ_0 is the vacuum permeability. All the field computations are carried out with Femlab.

In the beginning of the first iteration the optimization algorithm needs an initial guess for the geometry parameters of the coil. The inner radius of the initial guess, 500 mm, was chosen according to a typical geometry of an MRI device [21]. Then, I_{op} was calculated for both coils. In NbTi one I_{op} depends on the coil geometry and has to be calculated at each iteration. In copper coil, which has the wire diameter of 1 mm, I_{op} was constant and given by $I_{\text{op}} = J_{\text{cu}} S_{\text{cu}} \approx 7.85$ A. After I_{op} and thus $\mathbf{J}$ were known, B_0 was calculated from (4). The solution is in the feasible region, if all the requirements defined by the constraints are fulfilled. In this situation the penalty parameter in the (1) is zero and SQP starts to minimize the coil volume. If the solution is not a feasible one, the coil geometry is changed to the direction given by the search direction $\mathbf{d}_k$.

TABLE I
DESIGN PARAMETERS OF THE OPTIMIZED COILS

	Copper	NbTi
Inner radius (mm)	500.1	502.1
Outer radius (mm)	644.1	520.2
Axial length (mm)	366.6	412.3
Operation current (A)	7.85	263.8
Magnetic flux density (T)	0.20	1.50
Coil volume (dm^3)	150.8	8.25
Wire diameter (mm)	1.0	0.85
Total wire length (m)	105600	7993
Coil mass (kg)	738	38

The initial geometries were $\mathbf{X}_0 = [500, 550, 50]$ mm and [500, 700, 200] mm for NbTi and copper coils, respectively. The optimization of NbTi coil converged to a feasible solution of $\mathbf{X} = [502.1, 520.2, 412.3]$ mm after 24 iterations. This solution had $I_{\text{op}} = 263.8$ A and $B_0 = 1.50$ T. Thus, the minimum coil volume existed in the limit of B_0. The optimized NbTi coil geometry resulted in the volume of 8.25 dm^3 and had the total wire length of approximately 7993 m. The density of copper wire is 8.9 kg/dm^3 while the density of OK42 is 8.36 kg/dm^3 [9], [19]. Thus the total mass of NbTi magnet is 38 kg.

The optimization of copper coil converged to a feasible solution of $\mathbf{X} = [500.1, 644.1, 366.6]$ mm after 30 iterations. As $I_{\text{op}} = 7.85$ A and $B_0 = 0.20$ T, the minimum coil volume existed again in the limit of B_0. The volume and the total wire length of the optimized copper coil were 150.8 dm^3 and 105 600 m, respectively. The total mass of the copper coil was 738 kg.

This suggestive study indicates the reason for the interest toward superconductivity in MRI applications. As a copper coil is replaced with an NbTi one, multifold magnetic flux densities are achieved with remarkable size and mass reduction. The design parameters of the optimized copper and NbTi coils are presented in Table I.

III. LIFE CYCLE ASSESSMENT

A. Goal and Scope Definition (GSD)

In GSD the intended application and the reason for carrying out the study are determined. The goal setting in turn defines the needed scope of the study.

During the last decade, companies adopted environmental management as one of their basic functions. LCA for Outokumpu's copper products was made in 2000 as part of a larger study of the Finnish metals industry [4]. Outokumpu's wire is widely used for MRI magnets. Since they are wound both from copper and NbTi/Cu wire, MRI is a suitable application to carry out a comparative LCA study. This study is also part of a research project where the environmental impact of widespread usage of superconducting technology is studied. The scope of this LCA is coupled with the system boundaries in LCI chapter.

B. Life Cycle Inventory-Analysis (LCI)

The work in LCI part is divided in four substeps. First, all processes involved in the life cycle of the product have to be identified. Ultimately, every process start with the extraction of

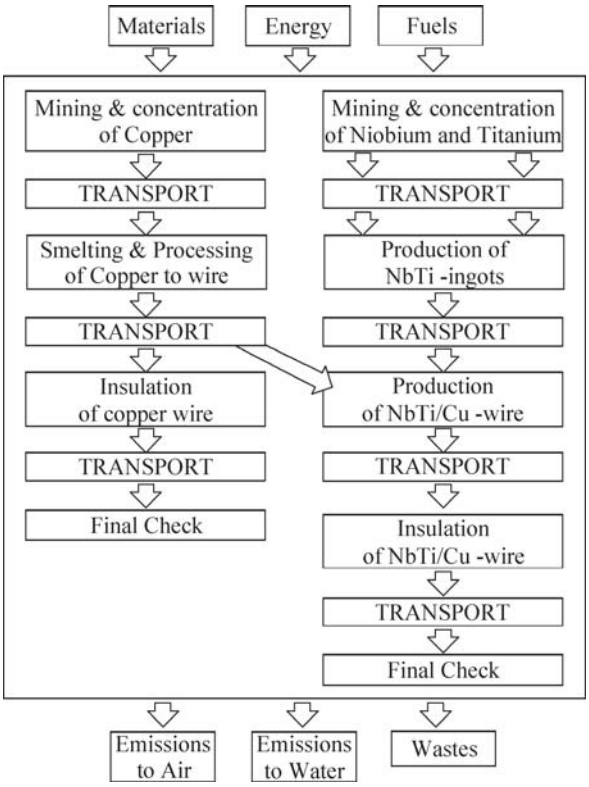

Fig. 1. Process flow chart and LCA system boundaries of copper and NbTi.

raw materials and energy from the ground and finally the inputs re-enter the environment in the form of emissions to air, water and land. A process flow chart is constructed to clarify the path of materials. Secondly, the quantitative data are collected. The third step is to define the system boundaries to get a manageable size for the LCA study. Finally, the inputs and outputs from all processes are adjusted to relate to the functional unit [2]. One ton of NbTi/Cu wire at the factory gate was chosen as the functional unit of this study. Same quantity was used in [4].

The application of LCA to process technology normally excludes product use, recycling and waste disposal from system boundaries. Such method is often referred to as '*cradle-to-gate*' assessment and it is applied also in this study [5]. The system boundaries are presented with a process flow chart in Fig. 1. Since this study is a comparative analysis, only the differences between the production of copper and NbTi/Cu wire need to be addressed.

The product systems comprise the extraction of elements Nb, Ti and Cu and their processing stages to wire, as well as fuels and energy production and the numerous transports. Processing of NbTi requires quite a few stages more than copper and wire production from NbTi is far more complex and therefore energy intensive. Table II shows the LCI for mining, concentration and processing stages of cathode copper and NbTi-ingots [12]–[15]. These materials are used in copper and NbTi/Cu wire production.

The LCI data shown in Table II is not thorough. The usage of chemicals in Nb and Ti processing are unknown. The niobium processing companies consider also their energy usage as proprietary information [17], [18].

TABLE II
LCI FOR MINING, CONCENTRATION AND PROCESSING OF COPPER AND NbTi

	Copper	NbTi
Vector	1 ton of cathode-copper	1 ton of NbTi-ingots
Net energy use	48.5 GJ	376 GJ
Mine tailings	28.8 tons	905 tons
Water usage	4 000 litres	1 303 800 litres (*)
SO_2	23 kg	not available
CO	4.45 kg	42.4 kg
NO_x	11.43 kg	20.6 kg
CO_2	3.69 tons	20.4 tons

(*) Water usage of titanium processing is not available.

TABLE III
LCI FOR PRODUCTION AND INSULATION OF COPPER AND NbTi/Cu-WIRE

	Copper wire	NbTi/Cu wire
Vector	1 ton of product	1 ton of product
Net energy use	55.4 GJ	151.4 GJ
Water usage	1 000 litres	527 053 litres
SO_2	7.5 kg	11.3 kg
CO	2.85 kg	3.90 kg
NO_x	8.32 kg	25.25 kg
CO_2	3.31 tons	9.06 tons
HNO_3	-	280 kg
HF	-	5 kg
C_3H_7OH (propanol)	-	30 kg

Therefore, LCI data of titanium is used for niobium also while considering that 2 tons of niobium raw material, FeNb, are needed in concentration of 1 ton of pure niobium [12]. The composition of superconductor grade NbTi ingot is 53% Nb and 47% Ti [17].

The next step is the production of wire and insulation of the finished product. Table III presents the LCI for these stages [12], [16]. The net energy use, 10.2 GJ, and emissions of all the transports shown in Fig. 1 are included in the data of Table III [9], [12]. The ratio of copper and NbTi materials in the finished wire, OK42, is 4:1. The total materials intake is included in the calculations but is not released [9].

C. Life Cycle Impact Assessment (LCIA)

The inventory table constructed in LCI is used as input to life cycle impact assessment where formalized evaluation is made for classification. However, the impact categories to be included in this classification are not completely agreed upon and even tougher problem arises with valuation and weighing of the impact. Is, for example, the increasing greenhouse effect more serious problem than acidification and if so how serious it is? For these reasons the impacts of LCI presented here were not assessed; results from LCI were used as is [2], [6].

IV. RESULTS, DISCUSSION AND LIFE CYCLE INTERPRETATION

When copper wire is compared to superconducting NbTi/Cu wire, the addenda copper data from Tables II and III are compared to combined NbTi and copper data from Tables II and III while taking into account the material shares in NbTi/Cu wire. Table IV presents the results from this calculation.

Results show that while the net energy use of NbTi/Cu production is almost three times the copper wire production, the

TABLE IV
COMPLETE LCI FOR COPPER AND NbTi/Cu-WIRE

	Copper wire	NbTi/Cu wire
Vector	1 ton of end-product	1 ton of end-product
Net energy use	103.9 GJ	284.6 GJ
Mine tailings	28.8 tons	905 tons
Water usage	5 000 litres	856 235 litres
SO_2	30.5 kg	29.88 kg (*)
CO	7.3 kg	18.10 kg
NO_x	19.75 kg	39.64 kg
CO_2	7.0 tons	17.14 tons
HNO_3	-	280 kg
HF	-	5 kg
C_3H_7OH (propanol)	-	30 kg

(*) The share of NbTi mining, concentration and processing is not available.

TABLE V
LCI FOR COPPER AND NbTi MAGNETS

	Copper magnet	NbTi magnet
Net energy use	76.8 GJ	10.81 GJ
Mine tailings	21.3 tons	34.4 tons
Water usage	3 690 litres	32 537 litres
CO_2	5.17 tons	0.65 tons

difference in water usage is 170-fold. Differences in air emissions are about 2–3-fold. However, fair comparison between conventional and superconducting technology, as far as environmental issues are considered, can be made only by comparing the applications where the technologies are used. Therefore, by taking into account the differences in weights of the magnets studied here, completely different results as obtained as seen from Table V for the most interesting vectors.

Still, the water consumption for NbTi magnet manufacturing is 9-fold the copper magnet but the energy use and emissions are only fractions. It should be noted that this comparison applies only to the magnets designed here. Coils of e.g., electrical machines need to be studied individually while the results from Table IV are generally applicable.

V. CONCLUSION

In order to obtain information about the environmental impacts of superconducting technology, a comparative life cycle assessment between copper and NbTi/Cu wire was carried out. First, a resistive and a superconducting magnet for MRI operation were designed with numerical optimization procedure. The results showed that the copper coil weights 738 kg while the NbTi one weights 38 kg. Then, life cycle assessment (LCA) was conducted for NbTi/Cu wire and the results were compared with previous LCA data for copper wire. Finally, the LCA data was adjusted so that the comparison between copper and NbTi magnet was possible. Results showed that from environmental point of view the NbTi magnet is more preferable because the energy consumption and CO_2-emissions of manufacturing are 14% and 13% of copper magnet, respectively. However, NbTi magnet construction needs 8.8 times more water and produces 1.6 times more mine tailings than copper magnet construction.

ACKNOWLEDGMENT

The authors would like to thank K. Korpela and J. Teuho from Outokumpu Poricopper for helpful information concerning NbTi/Cu wire production.

REFERENCES

[1] R. Day. (1998, March) Beyond Eco-Efficiency: Sustainability as a Driver for Innovation. Sustainable Enterprise Perspectives. . [Online]http://www.wri.org/wri/meb/sei/beyond.html
[2] United Nations Environment Programme (UNEP), *Life Cycle Assessment: What It Is and How to Do It*. Paris, France: UNEP Industry and Environment, 1996.
[3] International Organization for Standardization, ISO 14 040—Life Cycle Assessment, Barrow, UK, 1996.
[4] J. Seppälä, S. Koskela, M. Melanen, and M. Palperi, "The Finnish metals industry and the environment," *Resources, Conservation and Recycling*, vol. 35, pp. 61–76, 2002.
[5] R. Van Berkel, "Life cycle assessment for environmental improvement of minerals' production," in *Environment Workshop*, October 2000.
[6] R. U. Ayres, *Life Cycle Analysis: A Critique*. Fontainebleau, France: Working paper, INSEAD Centre for Management of Env. Resource, 1994.
[7] G. Vanderplaats, *Numerical Optimization Techniques for Engineering Design*. Colorado Springs, CO: VR&D, 1999, pp. 241–247.
[8] *Handbook of Applied Superconductivity*, 1st ed., IOP Publishing Ltd., Bristol, UK, 1998, pp. 1213–1249.
[9] Outokumpu Poricopper Corp., , Kuparitie, Pori, Finland.
[10] P. F. Smith and B. Colyer, "A solution to the 'training' problem in superconducting magnets," *Cryogenics*, vol. 15, pp. 201–207, 1975.
[11] R. Mikkonen and L. Söderlund, "A 6 T superconducting wiggler for synchrotron radiation," *IEEE Trans. Magn.*, vol. 32, pp. 2617–2620, 1996.
[12] K. H. Bruch and D. Gohlke *et al.*, "Sachbilanz einer Ökobilanz der Kupfererzeugung und-verarbeitung," *Metall*, vol. 49, pp. 252–257, 1995.
[13] "Environmental Performance Report of Niobium Mining," Cambior Inc., Longueuil, QC, Canada, 2000.
[14] *Database of Environmental Load of 4000 Social Stocks, Titanium*. Tsukuba, Japan: Ecomaterials Center of Japanese National Institute for Materials Science, 2003.
[15] R. Dhingra, J. G. Overly, and G. A. Davis, *Life-Cycle Environmental Evaluation of Aluminum and Composite Intensive Vehicles*. Oakridge, TN: Oak Ridge National laboratory, 1999.
[16] "Environmental Report of Superconductor Manufacturing Plant," Outokumpu Poricopper Corp., Pori, Finland, 2002.
[17] W. Chang, , Allegheny Technologies Inc., Albany, OR, USA.
[18] CBMM, Comphania Brasileira de Metallurgia e Mineracao, Araxa, Brazil.
[19] M. Wilson, *Superconducting Magnets*. Oxford: Clarendon Press, 1983.
[20] J.-H. Bae *et al.*, "The fabrication of superconducting magnet for MRI," *Physica C*, vol. 372–376, pp. 1342–1345, 2002.
[21] S. Crozier and D. M. Doddrell, "Compact MRI magnet design by stochastic optimization," *J. Magn. Res.*, vol. 127, pp. 233–237, 1997.

Publication **IV**

T. Hartikainen, J. Lehtonen and R. Mikkonen

”Environmental Advantages of Superconducting Devices in a Distributed Generation Network”

submitted to *Applied Energy*

Environmental Advantages of Superconducting Devices in a Distributed Generation Network

Teemu Hartikainen[1], Risto Mikkonen[1] and Jorma Lehtonen[2]

[1]Institute of Electromagnetics, Tampere University of Technology, 33101 Tampere, Finland

e-mail: teemu.hartikainen@tut.fi tel: +358 3 3115 2014 fax: +358 3 3115 2160

[2]Applied Energy Research Inc., Yliopistonkatu 45 A 5, 33500 Tampere, Finland

Abstract

Distribute generation (DG) is emerging as an alternative to centralized electricity generation system. The goals of DG include the minimization of the environmental impacts of energy production and introduction of new renewable energy sources to the distribution network. Superconducting devices are also proposed for DG because of their high efficiency as well as smaller size and more stable operation during peak loads. This study concentrates on the environmental benefits of superconducting machinery by comparing suitable devices with their competitors in DG-network. Exploitable superconducting devices in DG include superconducting magnetic energy storages (SMES), flywheels and cable systems. Life-cycle assessment (LCA) is used as a tool in comparisons of energy storage devices suitable for DG: SMESs, flywheels and batteries. In LCA, all material inputs, energy consumption, wastes, and emissions are assessed over the life-cycle of the product. Finally, commercialization schedule for HTS-cables is presented and an unconventional concept for DG-network is suggested for further examination.

Keywords: distributed generation (DG), environment, life cycle assessment (LCA), superconductivity

1. Introduction

Environmental issues have become increasingly important in decisions about energy policy. However, these issues are often phrased in ambiguous terms such as "environmentally friendly technology," "green products," and "sustainable development." Superconducting technology is eagerly praised as environmentally friendly, but fair comparisons are missing which would show whether certain technologies are environmentally superior. Here, this issue is addressed by comparing superconducting devices with their rivals in distributed generation networks.

Distributed generation (DG) can be defined as electricity generation connected to a distribution network or a customer site with less than 10 MW of power delivered [1] [2]. DG should not be confused with renewable energy generation. Renewables can be exploited in DG and are very much encouraged by certain lobbying groups, though non-renewable technologies are also considered in DG-systems [3]. Traditionally, electricity is generated in large power stations, located near resources or at logistical optimums, and delivered through a high voltage transmission grid and locally through medium voltage distribution grids. DG aims to add versatility of energy sources and reliability of supply and reduce emissions and dependence on fossil fuels. In addition, DG can contribute to the reduction of transmission losses and help introduce new developments such as fuel cells and superconducting devices [1]. Fig. 1 illustrates the differences between a central plant and a DG model.

Superconductivity means zero electrical resistivity below the critical values of current density, external magnetic flux density, and temperature. In classical metallic superconductors, T_C is lower than -250 °C. These low-temperature superconductors

(LTS) can be drawn into wire and wound as regular copper conductors. During operation, LTSs are typically cooled by liquid helium at 4.2 K (-269 °C) and therefore need a special insulation vessel called a *cryostat*.

Classical superconductors have been commercialized in magnetic resonance imaging (MRI) devices and in industrial magnetic separation. Unfortunately, as electrical machinery is considered, LTSs become economically viable only at powers exceeding 1000 MVA. The so-called high temperature superconductors (HTS) were discovered in 1986, and they renewed interest in network appliances. The possibility to operate in liquid nitrogen (LN_2) at 77 Kelvins considerably simplifies cryostat design and lowers cooling losses, thereby lowering the break-even power. Recently, successful medium-scale demonstrations have shown that HTS-devices are technically feasible in electric power engineering [4], [5]. However, the operating temperature in the demonstrations has so far been in 20–30 Kelvin range. Development work of HTS-materials is nowadays concentrated around the so-called 'Second Generation' (2G) materials, which are yttrium-based copper oxides (YBCO) applying thin film technology. The goal is to develop these conductors comparable in price and performance to LTS ones, while operating in the temperature of LN_2.

In a previous study, we showed that when used in a full-scale network, HTS-devices could reduce greenhouse gas (GHG) emissions from electricity generation by 3–6 % [6]. HTS-based generators, motors, and transformers were found to have break-even powers (P_{be}) of 100 MVA, 1 MVA, and 20 MVA, respectively, and they reduced losses by 50% compared with their conventional counterparts. However, with DG, HTS-machinery is not applicable because of the 10 MW limit. Large MW-class

motors are used only in heavy industry, which cannot be located under a DG-network. Here we examine the feasibility of the other superconducting power applications: cables, fault current limiters (FCL), and magnetic energy storages (SMES) [7].

2. Comparative analysis of energy storage solutions

Energy storage is becoming increasingly important in electrical networks because the energy sources considered in DG are typically less reliable steady-power suppliers than traditional power stations. Therefore, we need storage unless we are ready to accept intermittent electricity supply and operation at lower, that is, non-optimal efficiency. Suitable storage technologies are based on either electrical (batteries, SMES) or mechanical (flywheels, compressed air, pumped water storage) devices [9]. For example, with flywheels the Meissner-effect of superconductivity can be exploited in bearings. By blocking the magnetic field from its interior, a piece of yttrium-based YBCO-material in superconducting state possesses complete diamagnetic properties and thus provides frictionless levitating bearing [7].

The recent blackouts in Europe and the USA have raised questions about the reliability of electricity transmission network. Also, power quality issues (PQI) are on stage, especially because of the varying nature of these new maturing energy technologies and their increased need of power converters. Harmonic distortion in current and voltage challenges equipment manufacturers. Superconducting FCLs and SMESs offer certain benefits here, but PQIs are beyond the scope of this article. Instead, FCLs are to be compared with traditional circuit breakers, and SMESs and flywheels with HTS-bearings with other proposed energy storage solutions only in

environmental terms. An established tool, called life-cycle assessment, (LCA) is used in the environmental analysis of energy storage devices, while a more common approach is taken with cables. In LCA, all material inputs, energy consumption, wastes, and emissions are assessed, beginning from the extraction of raw materials and ending with the delivery of products from the factories [12].

Storage methods that use air-compression can be divided in two types: compressed air energy storage (CAES), and compressed air storage (CAS). The main component of both concepts is natural gas driven turbine generator. A compressor is used during off-peak hours to compress air into underground caves (CAES) or vessels (CAS), which is then released to combustion chamber during usage hours. As a result, the efficiency of the turbine generator will be higher [9]. CAES-plants have been built since the 1970s but their minimum feasible power is tens or even hundreds of MWs, thus being too large for DG-systems [10]. The development of the CAS concept is at the design stage, so it is not possible to conduct a LCA yet. However, since the fuel of the turbine generator is natural gas, rough estimates of GHG-emissions of this "storage method" can be calculated from the data of table 1, while keeping in mind that the efficiency of the plant is twice of conventional gas-turbine plant. Thus, emissions are halved and fall into a range of 220–344 g($CO_{2\text{-eq}}$)/kWh.

Table 1 shows, for comparison, the range of GHG-emissions from electricity production in grams of CO_2-equivalent per kWh [g($CO_{2\text{-eq}}$)/kWh]. The first values are direct emissions from combustion, while the second values indicate indirect emissions during life cycle. The exact number depends on the state of technology [6].

The case of pumped water storage can be reduced to simple hydropower plant, in which environmental insult is mainly due to construction of the dam and auxiliary structures. It can be estimated that the higher emission number of hydropower in table 1, 236 g($CO_{2\text{-eq}}$)/kWh, is suitable for pumped water storages, which have low utilization rate and are typically constructed in artificial rather than in natural formations. This is approximately the same amount of emissions that photovoltaic solar cells have per kWh, but five times more than wind power and eleven times more than nuclear power. Comparison to the CAS concept reveals that from the emissions point of view these storage methods are equal, if state-of-the-art turbine generators are used.

The energy storage methods that remain under comparison here are SMES, flywheel, and batteries. A good environmental assessment between conventional lead-acid batteries and their prospective replacements vanadium-redox batteries was conducted in [11], and those results are exploited in this analysis. The lead-acid batteries are commercial, while the vanadium-redox batteries are demonstrational ones under development, as is the flywheel system. The studied SMES system is of theoretical design. The functional unit (FU) of [11], *an electricity storage system with a power rating of 50 kW, a storage capacity for 450 kWh and an average delivery of 150 kWh electrical energy per day for 20 years*, is applied also in this study. This FU yields two possible systems with maximum capacity of 450 kWh. The first possibility is a system for diurnal usage with 150 kWh of energy in storage daily. This is suitable, for example, for peak-hour load leveling in a DG-network. The second is an autonomous system for three days power back-up with 450 kWh energy stored, exemplifying the electricity requirements for several remote houses for 10–70 persons. Selection

between these systems affects the depth-of-discharge (DOD) in lead-acid batteries and the amount of flywheels in operation. That in turn leads to varying endurance of the stack membranes in batteries and changes in refrigeration requirements in flywheels. Therefore, two different cases are studied, and a range between the results is given in table 2. With vanadium-redox batteries, it is possible to use deep DODs without interfering the lifetime of stack membranes. The SMES system is one complete unit and thus refrigeration is independent of energy stored.

The SMES was designed to be a LTS, NbTi-based system with liquid helium cooling and *in situ* liquefier, because HTSs are not yet developed enough to hold competitive current densities with LTSs in SMES magnets. According to design principles presented in [14] and [15], a 450 kWh SMES system would need 856 kg of NbTi wire, 5933 kg of stabilizing copper, and 52.3 t reinforcing material (stainless steel) per FU. Earlier, a LCA has been made for NbTi-wire, and the results can be employed for this concept [13]. The production statistics for SMES in table 2 include wire production data from that study. A SMES under normal operating conditions doesn't lose any amount of the stored energy, thus yielding to electrical efficiency of 100 %. However, heat leaks through the cryostat create losses that must be eliminated by appropriate cooling. The needed power conditioning systems naturally dissipate energy, but the amount is considered equal in all applications, and thus neglected. From [15] it was possible to estimate the cooling requirements and rate the liquefier capacity at 45 l/h. A Linde TCF50 liquefier with a weight of 8.5 tons and energy consumption of 132 kW was chosen.

The designed flywheel system consists of 45 units of 10 kWh Boeing flywheels with superconducting YBCO bearings [16], [17]. The flywheels itself are made of carbon fiber, which production is very intensive considering materials and energy, but LCAs for it have been conducted only partly [18]. Need of YBCO material in bearings is a mere 9.6 kg per FU and is thus neglected from this LCA. Cooling of the YBCO bearings can be handled either by liquid nitrogen or by mechanical cryocooler. Depending on usage (diurnal or three days back-up) either 15 of total 45 or all flywheel units are running, and this reflects to the differences in refrigeration power and thus to losses.

The stack membranes of the battery systems have to be changed four to six times during the functional unit of 20 years, because average lifetime of a membrane is 3–5 years, depending on DOD. The first values in lead-acid battery column are for 5-year stack membranes while the second ones are for 3-year membranes. The more often the membranes need replacement, the more materials are needed and emissions accumulate. However, both vanadium and lead are recyclable materials. The impact of recycling and re-assembling of the batteries is scrutinized, and results are included in the numbers of table 2. In contrast to membrane lifetimes, the flywheel system has a designed lifetime of 25 years and the SMES system of 30 years, and this is taken into account in the production parameters [11], [17].

The very first impression from table 2 is that the designed SMES system is an absurd energy storage application because it stores about one GWh but needs over 23 GWh for refrigeration during the 20 years of operation. However, this analysis only verifies the fact that LTS SMES is not economically viable. In a HTS SMES with similar

performance and liquid nitrogen cooling, the dissipation would be only 6 kW and thus losses, in 20 year period, 1051 MWh [19]. Therefore, fully developed HTS wires would considerable increase interest in SMES devices too. Another peculiarity of the SMES is that while electrical efficiency is 100%, losses from refrigeration account for total efficiency of 5% over 20 years. A similarly sized HTS SMES would yield to 50% total efficiency. That kind of system falls slightly behind the flywheels and batteries by economical or environmental standards, but on the other hand, SMES is the only storage method without any degradation in the quality of electricity, and is therefore a prominent choice if PQIs are considered.

The flywheel seems favorable from environmental point of view; energy usage of production is moderate and losses are low. Unfortunately, emission data is incomplete at the moment because LCAs for production of carbon fiber and YBCO are not available yet. One disadvantage is the volume of flywheel system; it requires 37 times more space than an average battery installation for the same energy storage capacity. On the other hand, the absence of sulphuric acid and toxic lead — which lead-acid battery system needs 30–44 tons — in flywheels are important advantages over battery systems. The average electricity losses of flywheels, including the cooling requirements, are equal to those of prospective vanadium batteries, while their losses are approximately 75% of the losses in lead-acid batteries.

The only common factor with all of the presented energy storage devices: CAS, pumped water storage, SMES, flywheel, and batteries, is greenhouse gas emissions in $g(CO_{2\text{-eq}})$/kWh. This number gives the emissions generated to discharge 1 kWh of electricity from the storages, without considering the emissions from charging them.

Depending on source of electricity, the amount of emissions from generation needs to be added to given in-direct emissions shown in table 2 and the in the chapter discussing CAS and pumped water storage. Simply by comparing the numbers one can see that vanadium-redox batteries show the best performance, and flywheels come second.

3. Comparison of superconducting and conventional cable systems

The cable system connects the production and the consumption sites of the network, and it consists of wires and switchgear and controlgear assemblies. In DG-networks, cables are favoured over overhead lines because the transmission distances are short and thus losses are low. From environmental point of view, the biggest problem lies within circuit breakers that utilize sulphur hexafluoride (SF_6) gas as insulator to prevent electric arcs. SF_6 is the most potent greenhouse gas ever evaluated with global warming potential up to 36500 times that of CO_2 [20]. However, in DG-networks, the usage of SF_6 in circuit breakers is minimum because they are most suited for high voltages, and thus the environmental benefit of replacing them by lower switchgear ratings made possible by superconducting FCLs, is negligible.

Nowadays, typical conventional cable for DG-networks is a 10–20 kV 3-phase ground cable that utilizes aluminum conductors and polyethylene PEX plastic as electric insulator. Losses for such cables in a range of 1.5–8.5 MW at nominal current ratings are in the range of 50–65 W/m [21]. In superconducting HTS-cables, there are two different competing designs called the room temperature dielectric (RTD) and the cryogenic dielectric (CD). Fig. 2 illustrates the differences between these designs. The

advantages of RTD-design are usability of common insulating materials and smaller total cable diameter. The CD-design offers higher overall current density along with lower losses. Development work of HTS-cables is concentrating nowadays on CD-design [22]. By computations based on [23], the losses of future HTS-cables incorporating YBCO material would lie to the range of 15–25 W/m including LN_2-cooling requirements. True comparison of these cables would need designing a complete DG-network with certain power sources and PCS-systems, but there would be so many different choices of power ratings, devices, and geographical issues considering the cables that indistinguishable results would yield.

It is suggested that a dc-transmission system incorporating underground cables would be the best alternative to interconnect different DG-networks together [8]. Here superconducting cables would suit excellently, not least with their ability to automatically limit over-currents. But the possibility to distribute electricity with dc within the DG-network should also be studied by power engineers. A common dc voltage in the whole system would make the system simpler and thus more durable; the only need for power converters being at generation and consumption sites.

Commercialization schedule along with market penetration model for HTS-cables is also presented here. It is estimated that the 2G-wires would become commercial in 2007 and the first profitable year for HTS-cables in the market would be 2010 [24], [25]. Fig. 3 shows the estimated market penetration curves for HTS-cables in DG-networks. In the entire electricity network, the asymptotic market share that HTS-cables could reach is 45%, and the market penetration is estimated to be quite fast [24]. The formula generating these curves is:

$$F(u) = b\frac{e^{(u-c)/a}}{e^{-(u-c)/a} + e^{(u-c)/a}} = \frac{b}{1+e^{-2(u-c)/a}}, \quad (1)$$

where F gives the market share in year u. Parameter b is the asymptotic maximum value, c is the halfway point in time, that is, when $u = c$, half of the market is captured and $F = b/2$. Parameter a determines the speed with which market share is captured.

Since the DG-networks are an emerging market and are aimed for platforms of modern technology, one can expect that the share of superconducting cables in DG exceeds the 45% value of entire network. As an example, superconducting transformers and synchronous motors with powers above their P_{be}s, could reach 80% and 75% share in the entire network, respectively [24]. The future DG-networks can be designed to fully utilize the advantages brought about by superconducting cables. In that case, superconducting cables could reach market shares at least comparable or even exceeding that of transformers in entire network. Thus, the upper limit of market share for superconducting cables was estimated to be 85%. The market penetration is estimated to be rather steep, because HTS-cables are not going to replace the conventional ones but instead the DG-networks would start out already superconducting.

With the lowest market share, 45%, average losses at nominal current in cables of a DG-network would fall into a range of 39–53.5 W/m, which means approximately 20% reduction in losses of electricity and thus in GHG-emissions from transmissions losses. The higher market share, 85%, yields average losses of 20–31 W/m, which is gives 56% reduction, both in losses and in GHG-emissions.

4. Conclusion

Environmental impacts of utilizing superconductivity in distributed generation (DG) networks were studied. Three suitable superconducting applications for DG were found, magnetic energy storages (SMES), flywheels incorporating superconducting bearings, and cable systems. Life-cycle assessment (LCA) used as a tool for comparisons between conventional batteries and superconducting alternatives in energy storage devices. It was found out that in environmental terms flywheels outweigh conventional lead-acid batteries and are equally competitive with prospective vanadium-redox batteries. The designed SMES don't show such competence, but a SMES incorporating high temperature superconductors (HTS) offers far better performance. Superconducting cables were found to have 60–70 % lower losses than conventional ones, while simultaneously having the ability to prevent over-currents. Finally, commercialization schedule for HTS-cables in DG-networks was examined.

References

[1] New ERA for electricity in Europe — Distributed Generation: key issues, challenges and proposed solutions, Luxembourg: Office for Official Publications of the European Communities, 2003.

[2] B. In-Su, K. Jin-O, K. Jae-Chul, C. Singh IEEE Trans. Power Syst. 19 (2004) 287–292.

[3] H. Puttgen, P. MacGregor, F. Lambert Distributed Generation: Semantic Hype of the Dawn of a New Era?, IEEE Power & Energy Magazine, January/February 2003.

[4] R. Mikkonen, IEEE Trans. Appl. Supercond. 12(1) (2002) 782–787.

[5] A. Malozemoff, J. Maguire, B. Gamble S. Kalsi, IEEE Trans. Appl. Supercond. 12(1) (2002) 782–787.

[6] T. Hartikainen, J. Lehtonen R. Mikkonen, Supercond. Sci. Technol. 16 (2003) 963-969. References therein.

[7] B. Seeber, Handbook of Applied Superconductivity, 1912 pages, IoP Publishing Ltd. London 1998.

[8] M. Bayergan, IEEE Power Engineering Review, (Dec 2001) 10–12.

[9] S. Schoenung, Characteristics and Technologies for Long-vs. Short-Term Energy Storage — A Study by the DOE Energy Storage Systems Program, Sandia National Laboratories, SAND 2001-0765, March 2001. Available on-line at http://infoserve.sandia.gov/sand_doc/2001/010765.pdf

[10] K. Sipilä, M. Vistbacka and A. Väätäinen, Electricity storing with compressed air energy storage, Technical Research Centre of Finland, VTT Research Notes 1516, Espoo 1993.

[11] C. Rydh, J. Power Sources 80 (1999) 21–29.

[12] International Organization for Standardization, "ISO 14040 – Life Cycle Assessment," Barrow, UK, 1996.

[13] T. Hartikainen, A. Korpela, J. Lehtonen, R. Mikkonen, IEEE Trans. Appl. Supercond. 14(2) (2004) 1882–1885.

[14] W. Nick, K. Prescher, IEEE Trans. Magn. 32 (1996) 2268–2271.

[15] G. Ries, H. -W. Neumueller, Physica C 357–360 (2001) 1306–1310.

[16] A. M. Wolsky, The Status of Progress Toward Flywheel Energy Storage Systems Incorporating High-Temperature Superconductors, Argonne National Laboratory Report, 17 Oct 2000.

[17] R. Silberglitt, E. Ettedgui and A. Hove, Strengthening the Grid: Effect of High-Temperature Superconducting Power Technologies on Reliability, Power Transfer Capacity and Energy Use, RAND Science and Technology, MR-1531-DOE, 136 pages, 2002. Available on-line at http://www.rand.org/publications/MR/MR1531/

[18] H. Stiller, Material Intensity of Advanced Composite Materials, Wuppertal Institute publication Nr. 90, 1999.

[19] The Quantum Technology Corporation, Brochure of Nitrogen Liquefier, 1999.

[20] A. M. Wolsky, The likely impacts on environment, safety, and health from the power sector's future, widespread use of superconducting equipment, Argonne National Laboratory Report, 21 Dec 2000. References therein.

[21] Pirelli Cables and Systems Oy, PL 13, 02401 Kirkkonummi, Finland.

[22] A. M. Wolsky, HTS cable — Status, Challenge and Opportunity, Argonne National Laboratory Report, 28 Sep 2004.

[23] T. Masuda, *et. al.*, Physica C, 372–376(3) (2002) 1555–1559.

[24] J. Mulholland, T. Sheahen and B. McConnell, Analysis of Future Prices and Markets for High Temperature Superconductors, U.S. Department of Energy Report, Draft, June 2003.

[25] Alexis P. Malozemoff, AMSC Second Generation HTS Wire – and Assessment, American Superconductor Corporation Report, 25 pages, June 2004. Available on-line at: http://www.amsuper.com/documents/2GWhitePaper-July04_002.pdf

TABLE 1

GHG-EMISSIONS FROM ELECTRICITY PRODUCTION IN GRAMS OF CO_2-EQUIVALENT PER KWH [6]

Energy vector	Direct emissions / kWh	In-direct emissions / kWh
Hard coal or peat	790–1017	176–289
Natural gas	362–575	77–113
Hydropower	0	4–236
Solar (photovoltaic)	0	100–280
Wind	0	10–48
Nuclear	0	9–21

TABLE 2

LCA BETWEEN SMES, FLYWHEEL AND BATTERIES OVER 20 YEARS OF USAGE

		SMES	Flywheel	Lead-Acid Battery	Vanadium Battery
Dimensions	Mass [kg]	98 000	27 035	47 974	23 601
	Volume [m3]	800	260	4.3	9.6
Production	Water [m3]	4 718	7 200	6.4–9.6	11.3
	Energy [GJ]	2 669	1 225	1 062–1593	281
	Lead [kg]	0	0	29 400–44 100	0
	Vanadium [kg]	0	0	0	2 309
	Superconductor [kg]	856	9.6	0	0
	Copper [kg]	5 933	0	130–195	184
	Carbon fiber [kg]	0	2 988	0	0
	Steel [kg]	52 333	18 640	0	2 516
	Sulphuric Acid [kg]	356	N/A	4 600–6900	6 103
	Nitric Acid [kg]	1900	N/A	0	0
Electricity	Net delivery [MWh]	1095	1095	1095	1095
	Electrical efficiency	100 %	88–92 %	75 %	72–88 %
	Refrigeration [W]	132 000	450–1350	~0	~0
	Losses [MWh]	23 126	200–358	365	150–425
	Total efficiency	5 %	75–85 %	75 %	72–88 %
Emissions	Nox [kg]	563	36	242–363	45
	SO2 [kg]	404	57	215–323	28
	CO [kg]	133	N/A	57–86	5
	CO2 [tons]	433	173	148–222	46
	[g(CO2-eq) / kWh]	416	159	145–217	44

Denotation N/A means data not available. Emissions from electricity production to charge the storages are not included. Emissions for flywheel are only from production of the required steel and energy.

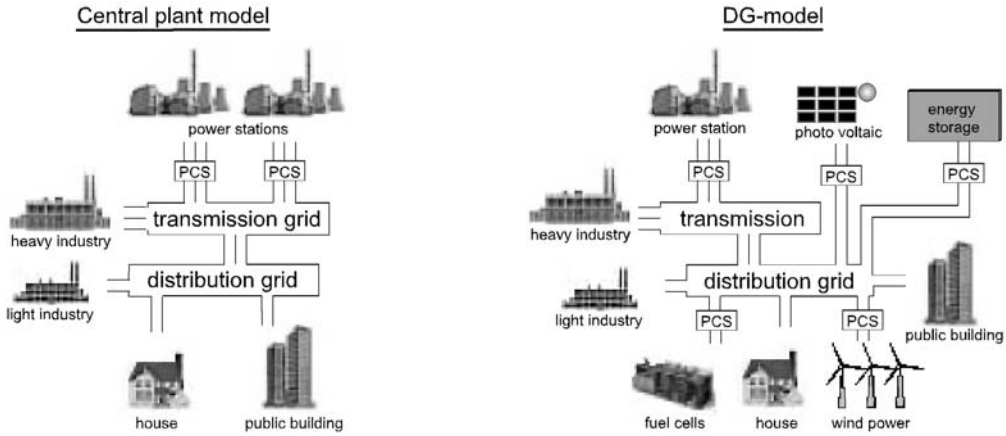

Fig. 1. Schematic diagram of traditional central plant model and one referred to as DG-model. PCS stands for power-conditioning system.

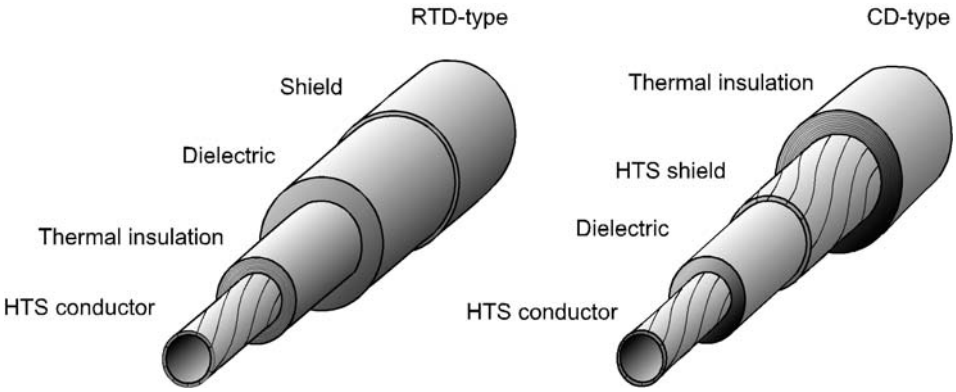

Fig. 2. Schematic presentation of the two designs for superconducting cable: room temperature dielectric (RTD) and cryogenic dielectric (CD) design.

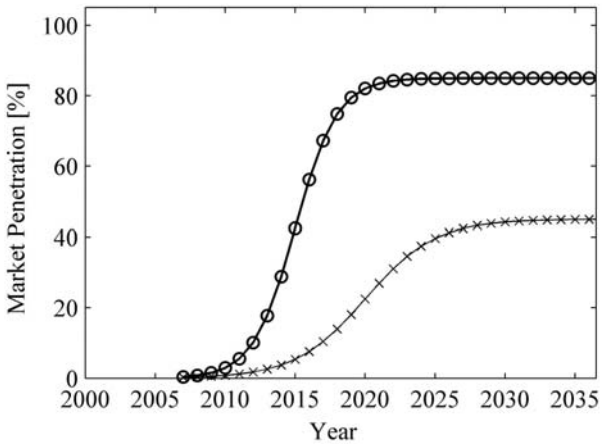

Fig. 3. Estimated market penetration of HTS-cables over the next 30 years. Symbols o and x denote to upper and lower limits for market share in DG-networks, respectively.

Publication **V**

T. Hartikainen, J.-P. Nikkanen and R. Mikkonen

”Magnetic Separation of Industrial Waste Waters as an Environmental Application of Superconductivity”

IEEE Transactions on Applied Superconductivity, **15**, pp. 2336-2339, 2005.

Magnetic Separation of Industrial Waste Waters as an Environmental Application of Superconductivity

Teemu Hartikainen, Juha-Pekka Nikkanen, and Risto Mikkonen

***Abstract*—Open gradient magnetic separation enables continuous operation of the separator without the need of matrix-elements. Such a separator consisting of liquid helium cryostat and an interchangeable pair of NbTi and Nb3Sn coils were designed and constructed for testing the separation of various substances. As an environmental application, synthetic and genuine steel mill waste waters were purified with the separator. Synthetic waste water contained dissolved Cr while genuine steel mill waste water contained Cr, Fe, Ni and Mo both in particle and in ionic form. Chemical treatment was needed to make the dissolved metals susceptible for magnetic field; this was achieved with the help of an adsorbent and ferromagnetic magnetite. Separated sludge was collected by attached pipeline. Cleaned waste water was first pH-treated and then analyzed by AAS-spectroscopy. Results showed that open gradient separator is a promising alternative for matrix-type separators.**

***Index Terms*—Environment, magnetic separation, superconductivity, waste water.**

I. Introduction

MAGNETIC separation has been used by mining industry since the 1840's in concentration of magnetic ore and removal of magnetizable particles from slurries [1]. The advent of high field superconducting magnets in the 1960's gave rise to superconducting separators that were first used in refining kaolin clay. Lately, environmental applications have attained interest, and several superconducting separators have been built to various water purification processes and also to sulfur removal from combustible coal [2]–[6].

Successful separation depends on experimentally optimized parameters, such as size and magnetic susceptibility of particles to be separated, applied magnetic force density, and flow velocity through separation zone. The force needed for separation is proportional to the product of magnetic flux density, $\mathbf{B}$, and its gradient. In open gradient magnetic separators, the gradient can be created by magnet design and is limited to 0.05 T/mm [7]. This work is part of a research project where a superconducting isodynamic open gradient magnetic separator is designed, constructed and tested with different slurries to determine the optimum separation conditions.

Manuscript received October 4, 2004. This work was supported in part by the National Technology Agency of Finland, by Prizztech Ltd., by Outokumpu Advanced Superconductors Ltd., by Teollisuuden Voima Ltd., by SVK-pool, and by Fortum Foundation.

T. Hartikainen and R. Mikkonen are with the Institute of Electromagnetics, Tampere University of Technology, Tampere 33101, Finland (e-mail: teemu.hartikainen@tut.fi).

J.-P. Nikkanen is with the Institute of Materials Science, Tampere University of Technology, Tampere 33101, Finland.

Digital Object Identifier 10.1109/TASC.2005.849660

In this paper, first test results of the separation with synthetic and genuine steel mill waste waters are presented. Tests were conducted with NbTi racetrack coils with magnetic flux density in separation zone up to 3 T. First, design and construction of magnet system and the cryostat are reviewed. Second, the chemical preparation and separation results of synthetic waste water are presented. Third, test results and issues concerning the steel mill waste water are discussed, and finally, development ideas for the separator are considered.

II. Design and Testing of Cryostat and Magnet

The design of the cryostat was aimed to minimize evaporation of liquid helium that is used to cool the NbTi coils and current leads. The cryostat is a cylindrical vessel constructed from AISI 316 L stainless steel. The total height and diameter of the outer vessel are 2.2 mm and 1.62 m, respectively. The outer vessel wall thickness is 6 mm, while the thickness of top- and bottom plates is 20 mm. The top plate of the cryostat supports the coils and their bracket structure along with current leads and instrumentation. Between inner and outer vessel there are 40 layers of MLI-superinsulation in vacuum. Evaporated helium gas cools the radiation shield that reaches the vacuum space. Two ion-pumps are attached in between vessels in order to keep an appropriate vacuum regardless of possible leak.

The current leads that feed the coils consist of two parts. The upper part is made of brass tube with inner and outer diameters of 20 mm and 32 mm, respectively. The hollow structure with large diameter was used in order to exploit the cooling with vaporized helium efficiently. The thickness of the tube was optimized with respect to the total heat load [8].

In isodynamic open gradient magnetic separation, high and nearly constant magnetic force density is needed. Solenoid, racetrack and saddle-shape coils were studied to find a suitable magnetic field distribution. The two last mentioned turned out to give the best results, and racetrack geometry was chosen due to manufacturing issues. The coils and separation zone are illustrated in coordinate system in Fig. 1 with model dimensions r_{A}, r_{B}, w_{A}, w_{B}, h_{A}, h_{B}, l_{A}, l_{B}. S is y-directional distance between the center points of the coils [9].

The magnetic force density distribution is sensitive to changes in the ratio of coil operating currents. These fluctuations are avoided when the coils are connected in series and current fed by single power source. The critical currents Ic_{A} and Ic_{B} are short-sample values of the NbTi wires with cross sectional areas A_{A} and A_{B}. The dimensions, wire specifications, magnetic force density and its uniformity are presented in Table I for the NbTi magnets [9].

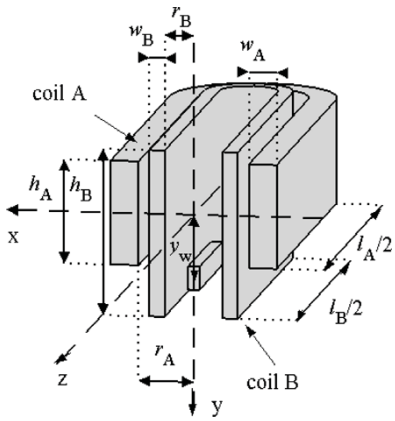

Fig. 1. Magnet geometry with two racetrack magnets [9].

TABLE I
MAGNET SPECIFICATIONS [8]

Parameters	NbTi Magnet
l_A / l_B [mm / mm]	700 / 630
r_A / r_B [mm / mm]	48 / 25
w_A / w_B [mm / mm]	25 / 13
h_A / h_B [mm / mm]	90 / 129
y_w [mm]	43
S [mm]	24
Ic_A / Ic_B @ 4 T & 4.2 K [A / A]	400 / 647
A_A / A_B [mm^2 / mm^2]	0.567 / 0.950
Magnetic force density [T^2/m]	6e10^7
Magnetic force change in x / y direction [%]	3.7 / 5.9

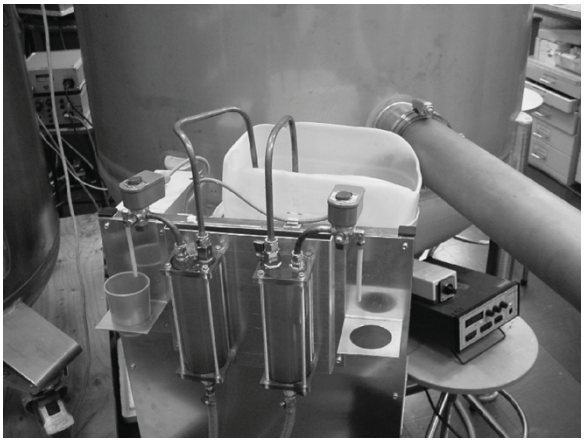

Fig. 2. Picture of the separator apparatus in operation. Pipes, canister and the sampling assembly are in front and cryostat is in background. A Hall-sensor measures magnetic flux density and its display is in lower right corner.

The waste waters are pumped to the separation zone through a pipe from a canister. A water flow meter by IFM Electronic is attached to the pipe to examine the flow velocity and temperature of the passing liquid. The pipe branches out in the end of the separation zone and expansion tanks are installed to both lines in order to take samples of the liquids. A photograph of the apparatus is seen in Fig. 2.

Fig. 3 shows the training effect measured from quench currents of the coils. The last quench occurred at 144 A, which is lower than expected. The reason for this is not clear but may arise from manufacturing of the coils; the interior of the coils may not be completely filled with impregnating compound. Thus, a little movement by certain wire can trigger the quenches.

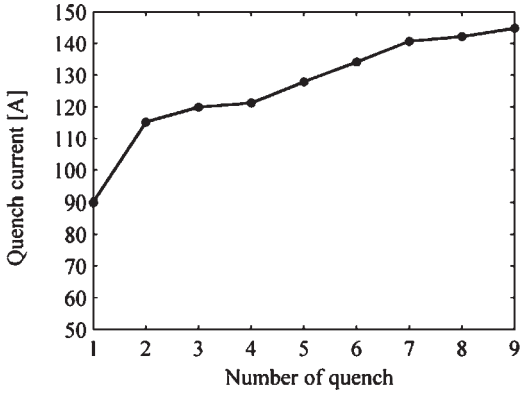

Fig. 3. Measured quench current as a function of consecutive quenches.

III. TESTS WITH SYNTHETIC WASTE WATER

In order to separate dissolved metals, the ions need to be chemically attached to a larger magnetic particle. In this case magnetite was used. An adsorbent is needed between magnetite and ions because of chemical linkage properties. The chosen adsorbent in all experiments was Molecular Sieve UOP Type 5 Å made by Fluka. Empirical formula of this molecular sieve is $Ca_nNa_{12}2n[(AlO_2)\ 12(SiO_2) \cdot \times H_2O$. Particles were crashed and sieved before using as adsorbent so that final particle size was $< 50\ \mu m$. Magnetite, which particle size is $< 5\ \mu m$, was used for magnetic seeding. Adsorbent and magnetite were coagulated by using $FeCl_3 \cdot 6H_2O$. The analytical grade reagents $Ni(NO_3)_2 \cdot 6H_2O$, $Cr(NO_3)_3 \cdot 9H_2O$, $FeCl_3 \cdot 6H_2O$, $(NH_4)Mo_7O_{24} \cdot 4H_2O$ were used for the make-up of synthetic metalliferous solutions. Analytical grade NaOH and HCl were used to make adjustments in the pH levels of the solution. All samples were made in distilled water [10], [11].

Sorption tests were performed at an ambient temperature of 21°C. The amount of heavy metal ions that were removed from solutions were determined by use of atomic absorption spectroscopy (AAS), based on the differences in the metal ion concentration before and after introducing the molecular sieve. After sorption, magnetite particles and ferrugo, which is an iron-hydroxide $Fe^{(III)}(OH)_3$, were added to the solutions at pH level 7–8. Adsorption was studied as a function of adsorption time, silicate mass and solution pH [12].

The adsorption was found to be a rapid process. Addition of silicate had a clear influence on the adsorption because of greater adsorbent area. Solution pH has also an essential effect on the removal of ions. Adsorption was enhanced when pH was increased because protons are competing of the adsorption sites with metal ions. On the other hand, in basic conditions metal ions also precipitate as metal hydroxides. Thus, adsorption is not the only mechanism for removal of heavy metal ions from waste waters. The microscopic studies indicated that pH has influence on the coagulation of magnetite and silicate. The most uniform silicate-magnetite network was found at pH 8. The tests with

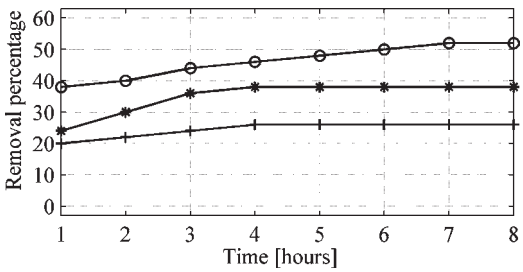

Fig. 4. Removal percentage of metal ions over several hours. Symbols o, $*$ and $+$ correspond to Ni^{2+}, Fe^{2+} and Cr^{3+} ions, respectively.

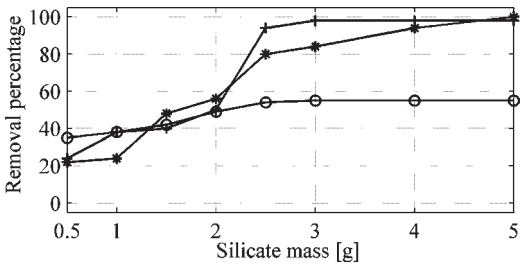

Fig. 5. Removal percentage of metals ions by different silicate masses. Symbols o, $*$ and $+$ correspond to Ni^{2+}, Fe^{2+} and Cr^{3+} ions, respectively.

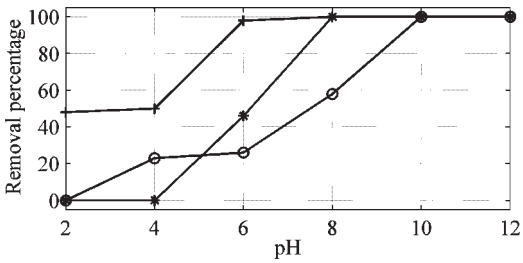

Fig. 6. Removal percentage of metals ions over pH. Symbols o, $*$ and $+$ correspond to Ni^{2+}, Fe^{2+} and Cr^{3+} ions, respectively.

a permanent magnet support this observation. The silicate was removed from magnetite by decreasing pH to 2 [13].

In experiments made as a function of adsorption time and pH, initial concentration of each metal-ion was 50 mg/L and the mass of silicate was 1 g/L. The results are shown in Fig. 4.

Next, the adsorption time was fixed to 1 hour and the influence of different silicate mass on adsorption was studied. Fig. 5 shows the removal percentage with increasing mass of silicate. Finally, adsorption tests by raising pH from acidic to alkaline were conducted with fixed time, 1 hour and silicate mass, 1 g/L. It appears from Fig. 6. that with slightly alkaline pH it is possible to obtain 100% removal efficiency. As can be seen, the sorption efficiency rises with increasing pH. There are two reasons for the rise. First, when the pH is low (acidic conditions), H^+ ions, which cause the acidity, reduce the removal of metals by filling the places of adsorption from silicate. The second reason of better removal in alkaline conditions is the precipitation of metal-hydroxides. This means that the reason of metal removal from solutions is not only adsorption but also precipitation [14].

The next experiment was to find out how to get silicate and magnetite to link together. It was possible by using ferrugo, and by adjusting the pH so that the coagulation is as efficient as possible. After adding magnetite and ferrugo into the solution

TABLE II
Cr CONCENTRATION IN SYNTHETIC WASTE WATER WITH MAGNETIC FIELD

Magnetic flux density	Cr concentration after separation
Initial value 25 mg / L	
0.7 T	6 mg / L
1.3 T	6 mg / L
1.8 T	5.5 mg / L
2.4 T	5.5 mg / L
3.0 T	5.5 mg / L

TABLE III
HEAVY METAL CONCENTRATIONS IN ORIGINAL STEEL MILL WASTE WATER

Elements	Concentration before separation
Solid matter [mg / L]	8.8
Dissolved Cr [mg / L]	0.13
Dissolved Ni [mg / L]	<0.01
Dissolved Fe [mg / L]	0.05
Dissolved Mo [mg / L]	9.8
Total Cr [mg / L]	0.25
Total Ni [mg / L]	0.04
Total Fe [mg / L]	0.39
Total Mo [mg / L]	9.8

containing silicate, the concentration of free heavy metal-ions decreased. With pH 8, almost all free ions of the solution were connected to silicate-ferrugo-magnetite-coagulants. After coagulation, a permanent magnet was placed near to the graduated flask. The result was that magnetic fraction started to move toward the magnet and after about half a minute, the solution was clear. This know-how was used in preparation of both synthetic and genuine steel mill waste water.

The laboratory made synthetic waste water contained initially dissolved Cr concentration of 25 mg/L. Table II presents the magnetic flux densities where samples of separated synthetic waste water were taken, along with results of analysis performed for the samples. Flow velocity of waste water through the separation zone was 7 L/min. AAS-spectroscopy was used to determine the Cr concentrations in the purified samples. Three concurrent analyses for each sample were run, and Table II shows mean value of the results. With the NbTi coils, 3 T was the highest magnetic flux density achieved. At that flux density, only 18% of the original concentration was present. As can be seen from the results, concentration lowers in steps with increasing magnetic flux density. Thus, it can be assumed that with higher fields, separation efficiency enhances further.

IV. TESTS WITH STEEL MILL WASTE WATER

The separation tests were performed also for genuine waste water from local steel mill with concentrations shown in Table III. The genuine waste water contains Mo, which does not occur in cationic form in solutions, but is in oxy-anionic form. Therefore, it is impossible to attach into silicate, which is a cation exchanger. However, Mo-ions are possible to engage with iron-hydroxides in suitable conditions. With pH 8, the Mo-ions linked directly to the magnetic network brought about by ferrugo.

The main problem with these magnetic carriers is the instability of pH. Sometimes the pH might seem stable and coagulation good enough, but after a couple of hours pH has

TABLE IV
Mo CONCENTRATIONS IN GENUINE WASTE WATER WITH MAGNETIC FIELD

Magnetic flux density	Mo concentration after separation
1.0 T	6.2 mg / L
1.5 T	6.0 mg / L
2.0 T	5.9 mg / L
2.5 T	5.6 mg / L
3.0 T	5.5 mg / L

decreased because of precipitation of metal-hydroxides. Thus, magnetite-silicate network breaks up, and desorption of dissolved metals can occur. In some extent, this happened with the genuine steel mill waste water and therefore the obtained results are not very reliable. The problem can be solved by adjusting pH over long periods of time while simultaneously stirring the solution efficiently.

The results from genuine waste water separation were not satisfactory because of problems with pH stabilization. Only the Mo-ions behaved correctly because they were attached to the ferrugo and thus not released from silicate when desorption occurred with lowered pH. Table IV shows the results of Mo-concentrations after the separation. The flow velocity of waste water through separation zone was 4.5 L/min.

V. CONCLUSION

Magnetic separation of two types of industrial waste waters were studied with an isodynamic open gradient separator applying a pair NbTi-coils. The separator was designed and constructed during the project, and this paper summarizes those phases, along with first test results and chemical treatment done on the waste waters to make them susceptible to magnetic field. It was found that heavy metals in dissolved i.e. ionic form could be separated, if they were first absorbed to chemically made magnetite-silicate network. Tests with laboratory-made synthetic waste water containing 25 mg/L of chromium showed separation efficiency of 82%. The first tests with genuine steel mill waste water didn't yet work out as planned, but it was found out that molybdenum concentrations dropped to 55% of the original, and concentration decreased linearly with magnetic flux density.

REFERENCES

[1] J. Svoboda, *Magnetic Methods for the Treatment of Minerals*. Amsterdam: Elsevier, 1987.

[2] A. Chiba *et al.*, "Removal of arsenic from geothermal water by high gradient magnetic separation," *IEEE Trans. Appl. Supercond.*, vol. 12, no. 1, pp. 952–954, Mar. 2002.

[3] G. Gillet, F. Diot, and M. Lenoir, "Removal of heavy metal ions by superconducting magnetic separation," *Separation Sci. Technol.*, vol. 34, no. 10, pp. 2023–2037, 1999.

[4] N. Saho, H. Isogami, T. Takagi, and M. Morita, "Continuous superconducting-magnet filtration system," *IEEE Trans. Appl. Supercond.*, vol. 9, no. 2, pp. 398–401, 1999.

[5] Y. M. Dai *et al.*, "Experimental study on Chinese high-sulphur coal cleaning by superconducting high gradient magnetic separation," in *Proc. Low Temp. Eng. and Cryogenics Conf.*, 1990, p. 03.3/1-5.

[6] J. Pitel, F. Chovanec, and V. Hencl, "Application of superconducting magnet systems to dry magnetic separation of coal," *Magn. Elect. Separation*, vol. 4, no. 2, pp. 19–29, 1992.

[7] J. Kopp, "Superconducting magnetic separation," *IEEE Trans. Magn.*, vol. 24, pp. 745–748, 1988.

[8] J. Tuisku, M. Ahoranta, A. Korpela, J. Lehtonen, R. Mikkonen, and R. Perälä, "Cryogenic design of an isodynamic magnetic separator," *IEEE Trans. Appl. Supercond.*, vol. 14, no. 2, pp. 1580–1584, Jun. 2004.

[9] M. Ahoranta, J. Lehtonen, and R. Mikkonen, "Magnet design for superconducting open gradient magnetic separator," *Physica C*, vol. 386, pp. 398–402, 2003.

[10] O. Peralez-Perez, Y. Umetsu, and H. Sasaki, "Precipitation and densification of magnetic iron compounds from aqueous solutions at room temperature," *Hydrometallurgy*, vol. 50, no. 3, pp. 223–242, 1998.

[11] D. Feng, C. Aldrich, and H. Tan, "Removal of heavy metal ions by carrier magnetic separation of adsorptive particulates," *Hydrometallurgy*, vol. 56, no. 3, pp. 359–368, 2000.

[12] B. E. Morgan, O. Lahav, R. R. Hearne, and R. E. Loewenthal, "A seeded ambient temperature ferrite process for treatment of AMD waters: magnetite formation in the presence and absence of calcium ions under steady state operation," *Water South Africa*, vol. 29, no. 2, 2003.

[13] V. J. Inglezakis, A. A. Zorpas, M. D. Loizidou, and H. P. Grigoropoulou, "Simultaneous removal of Cu^{2+}, Fe^{3+} and Cr^{3+} with anions $(SO_4)^{2-}$ and $(HPO_4)^{2-}$ using clinoptilolite," *Mikroporous and Mesoporous Mater.*, vol. 61, pp. 167–171, 2003.

[14] N. Karapinar, "Magnetic separation of ferrihydrite from wastewater by magnetic seeding and high-gradient magnetic separation," *Int. J. Mineral Processing*, vol. 71, pp. 45–54, 2003.

Publication **VI**

T. Hartikainen and R. Mikkonen

”Open-gradient Magnetic Separator with Racetrack Coils Suitable for Cleaning Aqueous Solutions”

IEEE Transactions on Applied Superconductivity, **16**, 2006. *In press.*

Open-gradient Magnetic Separator with Racetrack Coils Suitable for Cleaning Aqueous Solutions

Teemu Hartikainen and Risto Mikkonen

Abstract— **Superconductivity enables magnetic fields in a magnitude of 5–10 times greater than conventional electromagnets. Applied to magnetic separation, use of superconducting magnets opens the possibility to separate sub-micron sized paramagnetic particles. Open-gradient magnetic separation (OGMS) enables continuous operation without the need of matrix-elements. Such a separator consisting of liquid helium cryostat and an Nb_3Sn coils were designed and constructed for testing the separation of various slurries. The separation parameters, such as size and magnetic susceptibility of particles to be separated, applied magnetic force density, and flow velocity have to be experimentally optimized. In isodynamic separation, high gradient and nearly constant and homogenous magnetic force density distribution in separation zone are created by magnet design. Here the superconducting OGMS was used in purification of synthetically made solutions emulating industrial wastewaters. Performance of the used Nb_3Sn magnet is discussed and proposals for developing the performance of racetrack magnets are given. Finally, a simple permanent magnet separator was constructed and tested with wastewater.**

Index Terms—**Superconducting magnets, magnetic separation, waste materials, industrial applications.**

I. Introduction

MAGNETIC separation can be described as a method of separating particles in relation to their magnetic properties. This long-standing engineering practice is mainly used by the mining industry for concentration of minerals and for purification of different slurries. Efficient usage of magnetic separation in minerals processing has encouraged its use also in wastewater treatment. During the 1970's, development of high-field superconducting magnets along with high-gradient separation process made it possible to separate fine, weakly magnetic particles [1], [2]. Later for example viruses, algae, phosphate, and even dissolved pollutants have been removed by magnetic seeding technique, which enhances the magnetic properties of materials to be removed [3]–[6]. Magnetic purification accelerates considerably the separation of sludge from liquid, and thus leads to increased processing rates compared to conventional decantation and mechanical filtration.

This paper presents the results from steel mill wastewater purification with a superconducting isodynamic open-gradient magnetic separator (OGMS). Three solutions emulating real wastewaters were tested. The solutions were synthetically made and each contained 25 mg/liter of dissolved Cr, Fe and Ni, respectively. Real factory wastewaters were also tested during the first test session [9], but since there were problems associated with proper analyses of cleaned samples, only synthetic wastewaters were run through the separator this time to obtain more accurate analyses. The magnet system had interchangeable pairs of NbTi and Nb_3Sn coils with applied **B** in working volume up to 3 T in magnitude. The water pump unit had stepless control of flow velocity and velocities up to 7 liters per min (L/min) were achieved. Later simple separator based on permanent magnets, generating one tenth of the **B** in NbTi device, was constructed with flow velocities up to 12 L/min. Here, the operation of the separators is explained and impacts of the results are discussed.

II. Procedure of Separation

A. Basic Theory

The force, $\mathbf{F}_m$, needed to separate materials in a magnetic separator is proportional to magnetic flux density, **B**, its gradient $\nabla\mathbf{B}$, magnetic susceptibility of the particle to be separated, χ, and volume, V, of the particle by the following formula [1]:

$$\mathbf{F}_m = \frac{\chi}{2\mu_0} V \nabla(\mathbf{B}\cdot\mathbf{B}), \qquad (1)$$

where μ_0 is the permeability of vacuum. There are two ways of creating the needed field gradient, namely by the help of a ferromagnetic matrix or by so-called open-gradient magnetic separation. By installing a ferromagnetic material, typically iron, in the volume where **B** is present, gradient of **B** is created, and thus particles possessing positive χ move towards the ferromagnetic matrix. In OGMS, $\nabla\mathbf{B}$ is created by magnet design, and particles are deflected in the separation volume.

Manuscript received September 19, 2005. This work was supported by National Technology Agency of Finland, Prizztech Ltd., Outokumpu Advanced Superconductors Ltd., and SVK-pool.

Teemu Hartikainen and Risto Mikkonen are with Institute of Electromagnetics, Tampere University of Technology, P.O.Box 692, Tampere, 33101 Finland, (phone: +358-3-31152014; fax: +358-3-31152160; e-mail: teemu.hartikainen@tut.fi).

The magnetic susceptibility of each particle determines the direction and angle of this deflection. The OGMS-device was also made isodynamic, which means that $\mathbf{F}_m$ is nearly constant throughout the working volume of the separator. This way the influence of variable parameters on the results of separation can be studied [7]. Also, cleaning of the matrix is difficult due to pertaining magnetic forces, so therefore OGMS was chosen to the present application [8].

B. Properties of the Separator

The dissolved pollutants in the wastewater needed first chemical treatment to become susceptible for magnetic field. The ions were attached to magnetite, Fe_3O_4, by the help of analytical grade chemicals. This adsorption process is explained in detail in reference [9]. Then, wastewater containing ferromagnetic magnetite particles (which included all of the dissolved materials) was pumped to the separation volume through a pipe from a canister. The pipe was divided in two at the end of the homogenous force density distribution area, i.e. at the end of separation volume. Then, the cleaned wastewater should flow from the lower pipe. Two pipe constructions were used, one divided the pipe diameter by 50/50 while the other one by 25/75, that is, cleaned wastewater flowed through the smaller pipe. Fig. 1. presents schematically the experimental set-up.

The cryostat was a cylindrical vessel measuring 2.2 m in height and 1.62 m in diameter, and it is shown as exploded view in Fig. 2. Detailed design is explained more thoroughly in reference [10]. The magnet consists of two racetrack-shaped coils measuring ~70 cm in length. As mentioned earlier, two pair of magnets were designed and manufactured, more closely explained in [7]. The first tests were conducted with coils wound of NbTi and with the 50/50 pipe construction. Results from those tests are presented in [9]. They are shortly summarized in Fig. 3 to give the reader some basis for comparison between test sessions. Here, the test results with Nb_3Sn-coils and separation pipe modified to 25/75 division are presented. Theoretically, the 25/75 division should yield better separation results than the 50/50 one as shown schematically in Fig. 4.

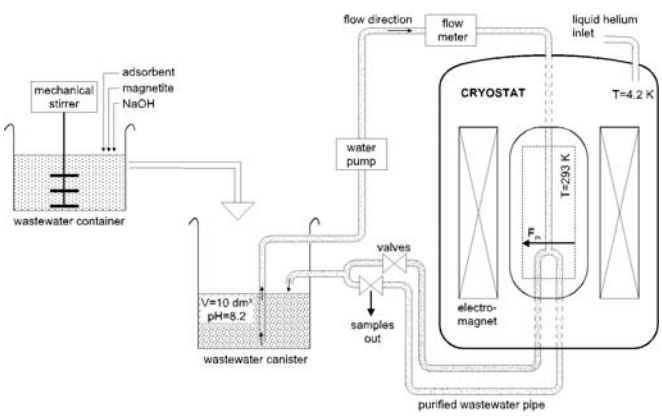

Fig. 1. Schematic presentation of experimental set-up. The direction of magnetic force, $\mathbf{F}_m$, is shown inside the separation volume.

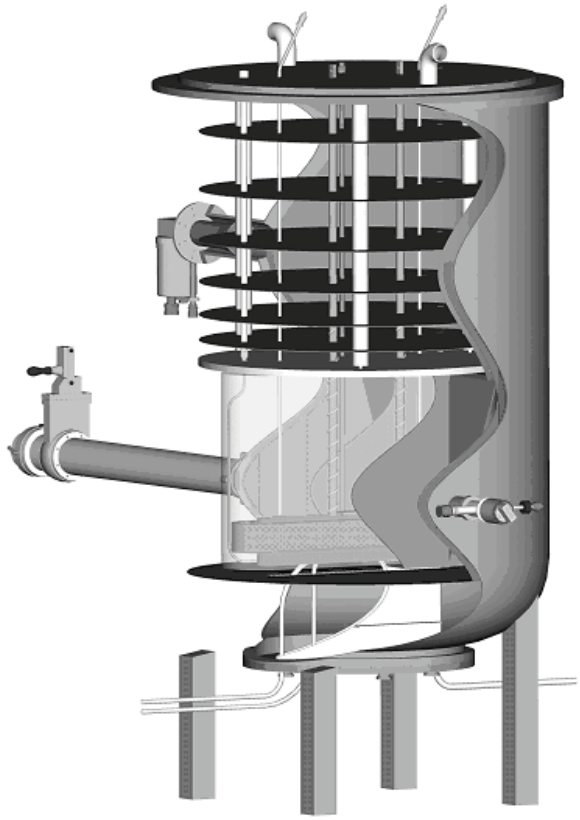

Fig. 2. Exploded view of the cryostat. The pipe conveys water flow from the lower right, into the cryostat, and to the bore of the magnet where separation occurs. At the end of the separation volume, pipe is divided in two.

With constant $\mathbf{F}_m$, information about the efficiency of magnetic separation under wide range of operating conditions can be obtained. Based on the results of the superconducting separator, a simple device applying permanent magnets was constructed. The pipe assembly was removed from the system, and three stacks of Nd-Fe-B permanent magnets were installed along the pipe close to the pipe junction. Each stack had five magnets sized 11cm*5cm*0.8cm [length*width*height] and they generated an approximate magnetic flux density of 0.3 T. Now, $\nabla\mathbf{B}$ varies inside the pipe and therefore the magnetic force cannot be determined uniquely. Thus, the results are not comparable to the superconducting device having the same $\mathbf{B}$.

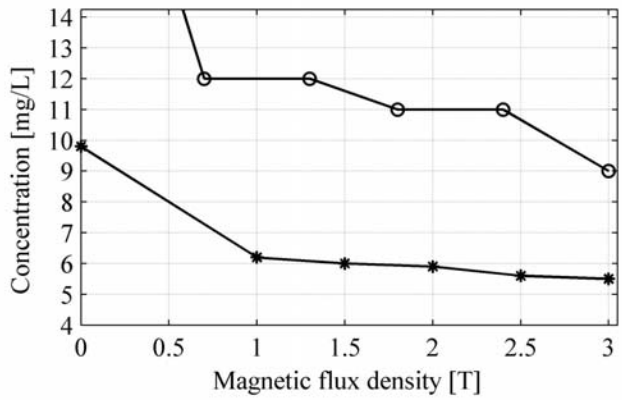

Fig. 3. Summary of first separation test results. Symbols * and o correspond to Mo and Cr. Initial concentrations were Cr: 25 mg/L and Mo: 9.8 mg/L.

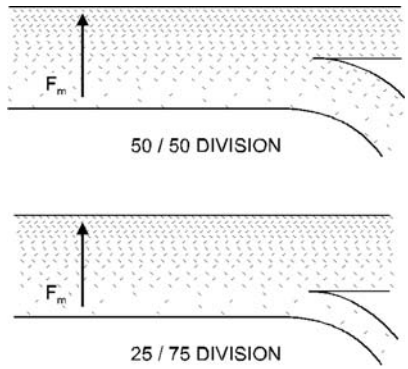

Fig. 4. Difference between pipe divisions 50/50 and 25/75. The catchment drops to half with 25/75, but cleaner samples are also expected because fewer particles should enter the lower pipe.

III. Results and Discussion

The Nb_3Sn superconducting wire has better current carrying characteristics than the NbTi. Although higher maximum magnetic flux density was expected with Nb_3Sn-magnet, just the opposite happened with these coils. NbTi-magnet reached 3.0 T, while the Nb_3Sn one performed well only up to 2.5 T, which was half of the expected value. Note, that this is the flux measured from the side of the separation pipe in the magnet bore; it is not the maximum magnetic flux density in the winding.

Poor performance was related to the problems in coil manufacturing. The first reason was poor quality of the winding process, which was outsourced to a local business winding conventional devices. Solenoid-shaped coils are easy to wind tight but racetracks, especially as large as these, would require experts to wind the coils. Also the used wax-based impregnation left the outermost layers of the coil too loose. At low temperatures even a slight movement of wire can release enough energy to raise the temperature over the critical temperature of the superconductor thereby quenching the magnet. Quenches were encountered at operating current of 321 A, corresponding to magnetic flux density of 2.5 T in the bore. Fig 5. presents the fall of current after the first three quenches. Attenuation was very fast and thus the temperature rise in the magnet due to quench was fortunately negligible.

Secondly, making of a magnet from Nb_3Sn requires a heat treatment that produces the superconducting phase in the wire. Heat treatment for the coil lasted about a month and temperature should have been kept all the time within ±1 °C from the set point. Even a slight variation from the predetermined heat treatment program can result in imperfect formation of the superconducting Nb_3Sn phase.

Thus in order to get a good performance with racetrack-shaped Nb_3Sn magnets, special attention should be paid in the winding process and in heat treatment conditions. In addition, impregnation substance should be epoxy-based rather than wax-based because epoxy-resin works as glue tying together the laps, whereas wax only fills the coil leaving outermost laps without support.

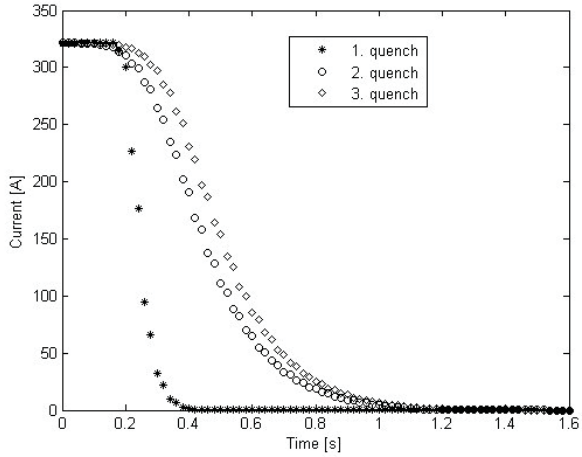

Fig. 5. Fall of current versus time during quenches. The first quench could have started from a different position of the magnet than the consecutive ones. Another possibility is that our power supply took the first one faster up.

Fig. 6. summarizes the results from the separation of Cr, Ni and Fe ions. The concentrations dropped to approximately 60% of the initial value already with the lowest magnetic flux density, 0.5 T. With increasing flux density, the separation results show linear improvement, except for Fe where concentration stays at 15 mg/L. The most probable reason for this behaviour is that the analytical grade chemicals used in building the network for ions and magnetite did contain trace amounts of Fe, and thus the atomic adsorption spectrophotometer detected it. Separation of Ni-ions was the most efficient. At the highest attained magnetic flux density, concentration of Ni dropped to 44% of the original. Concentration of Cr-ions dropped to 52% at the same magnetic field. As a comparison, with the firsts tests run by NbTi-magnet and 50/50 pipe division, the result at 2.5 T was 2 mg/L better for Cr. However, when comparing these with the results from Ni separation, one notifies that the result was exactly the same; concentration after separation was 11 mg/L for Ni-ions of this session and Cr-ions of the first session.

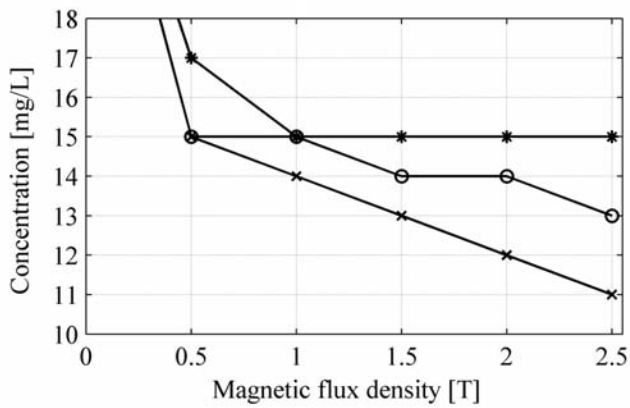

Fig. 6. Test results from the separation tests. Symbols * and o and x correspond to Fe, Cr and Ni, respectively. Initial concentrations were 25 mg/L for all heavy metals.

Interestingly, variation in flow velocity didn't have observable effect on separation results. These results were obtained with flow velocity of 3 L/min, while increasing the flow velocity to 6 L/min affected only the Fe concentrations by increasing results with one mg/L. Also, 50/50 division of the separation pipe seemed giving better results while the contrary was expected. Possibly the inhomogeneity in the volume distribution of magnetite particles caused them to behave unexpectedly under the turbulent conditions of the separation pipe.

The good results at low fields encouraged trying a permanent magnet separator as well. Results with that device appear in Table 1. The used wastewater was the one containing Ni-ions, which gave the best results with the superconducting device. The only controllable parameter was the flow velocity since the magnetic field was permanent. It is clear that further research is necessary because this time flow velocity did have effect on separation results – though the system was slightly different from the one used with superconducting magnets. However, this test showed that it is possible to construct a very simple and economical separator, which can remove up to 60% of dissolved metals.

IV. Conclusions

Magnetic separation of dissolved pollutants was demonstrated with a superconducting separator introducing magnetic seeding technique for wastewaters. Three wastewater samples containing 25 mg/L of dissolved Ni, Cr, and Fe, respectively were tested in magnetic flux densities up to 2.5 T. Results showed that already at 0.5 T, the concentration of heavy metals dropped to 60% of the original and by increasing flux density, linear decrease in concentration was detected. The information obtained from the superconducting device was exploited in construction of a plain permanent magnet separator. The system was tested with wastewater containing Ni-ions, and the concentration dropped down to 40% of the original. Tests showed that continuous removal of dissolved pollutants from fluid streams with magnetic separation is a promising alternative to conventional methods.

TABLE I
Results from permanent magnet separator for Ni-ions

Flow velocity [L/min]	Concentration [mg/L]
12	14
10	13
8	12
6	11
4	10

Original concentration of Ni was 25 mg/L.

References

[1] J. Svoboda, *Magnetic methods for the treatment of minerals*. Amsterdam: Elsevier, 1987, pp. 590–605.

[2] S. J. Lieberman and D. R. Kelland, "Magnetic Filtration of Aqueous Suspensions of Submicron Reactor Corrosion Products," *IEEE Trans. Magn.*, vol. 20(5), pp. 1195–1197, 1984.

[3] M. Myrmel, E. Rimstad, and Y. Wasteson, "Immunomagnetic Separation of a Norwalk-like Virus (Genogroup I) in Artificially Contaminated Environmental Water Samples," *Int. J. Food Microbiology*, vol. 62, pp. 17–26, 2000.

[4] H. Okada, Y. Kudo, H. Nakazawa, A. Chiba, K. Mitsuhashi, T. Ohara and H. Wada, "Removal System of Arsenic From Geothermal Water by High Gradient Magnetic Separation-HGMS Reciprocal Filter," *IEEE Trans. Appl. Supercond*, vol. 14(2), pp. 1576–1579, 2004.

[5] M. Franzreb and W. H. Höll, "Phosphate Removal by High-gradient Magnetic Filtration Using Permanent Magnets, " *IEEE Trans. Appl. Supercond.*, vol. 10(1), pp. 923–926, 2000.

[6] G. Gillet and F. Diot, "Removal of Heavy Metal Ions by Superconducting Magnetic Separation," *Separation Sci. Technol.*, vol. 34(10), pp. 2023–2037, 1999.

[7] M. Ahoranta, J. Lehtonen and R. Mikkonen, "Magnet Design for Superconducting Open Gradient Magnetic Separator," *Physica C*, vol. 386, pp. 398–402, 2003.

[8] B. Seeber, *Handbook of Applied Superconductivity*. London: IoP Publishing, 1998.

[9] T. Hartikainen, J.-P. Nikkanen and R. Mikkonen, "Magnetic Separation of Industrial Waste Waters as an Environmental Application of Superconductivity," *IEEE Trans. Appl. Supercond.*, vol. 15, pp. 2336–2339, 2005.

[10] J. Tuisku, M. Ahoranta, A. Korpela, J. Lehtonen and R. Mikkonen, " Cryogenic Design of an Isodynamic Magnetic Separator," *IEEE Trans. Appl. Supercond.*, vol. 14(2) pp. 1580–1583, 2003.

Tampereen teknillinen yliopisto
PL 527
33101 Tampere

Tampere University of Technology
P.O. Box 527
FIN-33101 Tampere, Finland